UNIVERSITY OF CALIFORNIA, SAN DIEGO

Early events in phytochrome signaling in *Arabidopsis*

A dissertation submitted in partial satisfaction of the
requirements for the degree Doctor of Philosophy

in

Biology

by

Brian Timothy Burger

Committee in charge:

Professor Joanne Chory, Chair
Professor Joseph Ecker
Professor Larry Goldstein
Professor Julian Schroeder
Professor Yunde Zhao

2008

The Dissertation of Brian Timothy Burger is approved and it is acceptable in quality and form for publication on microfilm and electronically:

_____

_____

_____

_____

_____

Chair

University of California, San Diego

2008

DEDICATION

To my parents.

EPIGRAPH

‘Cause what a difference, what a difference, what a difference

A little difference would make.

“Blueprint”, Fugazi

TABLE OF CONTENTS

LIST OF FIGURES AND TABLES

ACKNOWLEDGEMENTS

Thanks to the administrative assistants, past and present, who keep tabs on my boss, reserve rooms and parking spots, find forms, and the answers to countless questions, and just generally make my life easier: Kim Emerson, Nancy Benson, and Lynn Artale. Thanks also to the underappreciated few, past and present, that keep the department stocked and running smoothly: Tsegaye Dabi, Jack Bolado, Derek Hyman, Jason Lim, and Dionne Vafeados.

Thanks to the post-docs, too numerous to name individually, who have taken the time to advise and mentor me through these years. Special thanks to Jennifer Nemhauser, in particular, who always looked out for me and who served as my day-to-day mentor, sounding board, and sometimes ride to work. Thanks to those post-docs that I had the good fortune to collaborate with: Meng Chen, Yi Tao, Todd Michael, Todd Mockler, and Olivier Loudet. Thanks also to those post-docs that I enjoyed a beer or a surf with over the years: Greg Vert, Niko Geldner, Olivier Loudet, Ajit Nott, Chris Schwartz, Todd Michael, and Jennifer Nemhauser, to name a few.

Thanks to Jack Bolado and Jane Bugea for their help with the bHLH antibodies. I leaned heavily on you, and you both came through for me. Special thanks to Jane Bugea for her help on all my projects, those that worked and those that didn't. Thanks for sharing your bench and freezer space with me, for letting me borrow whatever I couldn't find on my own bench, and for never giving up on me for weekday social outings.

Thanks to Jeff Long for making the department a fun place to work. I imagine walking the line between friend and professor is tough, but you manage it well. Oh, and thanks for the toaster—bagels never tasted so good.

Thanks to my committee members for your time and patience: Joe Ecker, Julian Schroeder, Yunde Zhao, and Larry Goldstein. Your input was always appreciated.

Special thanks to my advisor, Joanne Chory. You provide a wonderful environment in which to do science. I'm thankful for your generosity and your patience. I've learned a lot in your lab, both scientifically and personally, and for that I'm very grateful.

Thanks to my fellow graduate students for the good times and the commiseration. A special thanks to Heidi Szemenyei, Mike Hannon, and Joe Pearson.

Special thanks to my family and non-science friends for providing support over the years, both financial and emotional. Thanks for the yearly snowboard trips, Jay. And for the music that keeps me sane, Manning. Thanks to my Mom, Dad, and sister for always believing in me even when they weren't quite sure what I was up to.

The most special of thanks to my wife-to-be, Michele Auldridge. You talked me down from many ledges, thankfully all of them figurative. You were always the glass half-full, and I'm not sure I would have made it without you. I look forward to our next chapter together.

Thanks to all the above, and anyone I may have missed, for making these past years an enjoyable and most memorable experience.

Chapter 5, in full, consists of the following manuscript in press at *Proceedings of the National Academy of Sciences*.

Loudet, Olivier; Michael, Todd P; Burger, Brian T; Le Metté, Claire, Mockler Todd C; Weigel, Detlef; Chory, Joanne. "A zinc knuckle protein that negatively controls morning-specific growth in *Arabidopsis thaliana*".

VITA

EDUCATION

2008	Ph.D., Biology, University of California San Diego
2001	M.S., Plant Molecular and Cellular Biology, University of Florida
1998	B.S., Botany, University of Florida

TEACHING EXPERIENCE

2005	University of California San Diego, Teaching Assistant, Metabolic Biochemistry (BIBC102)
2004	University of California San Diego, Teaching Assistant, Metabolic Biochemistry (BIBC102)
2003	University of California San Diego, Teaching Assistant, Plant Molecular Genetics and Biotechnology Lab (BICD123)

UNDERGRADUATE SUPERVISION:

2005-2008	Supervisor to Vicki Jane Bugea

COMMUNITY OUTREACH

2007	Salk High School Science Day
2007	Salk Mobile Science Lab

RESEARCH

Publications:

Loudet, O., Michael, T.P., **Burger, B. T**., Le Metté, C., Mockler, T.C., Weigel, D. and Chory, J. **(2008)** A zinc knuckle protein that negatively controls morning-specific growth in *Arabidopsis thaliana*. PNAS, *in press*.

Burger, B.T., Cross, J.M., Shaw, J.R., Caren, J.R., Greene, T.W., Okita, T.W., and Hannah, L.C. (**2003**). Relative turnover numbers of maize endosperm and potato tuber ADP-glucose pyrophosphorylases in the absence and presence of 3-PGA. Planta 217: 449-456.

Patents:

Co-inventor, US Patent 6,969,783. Heat stable mutants of starch biosynthesis enzymes.

Conference, Meeting, or Symposium Presentations:

BT Burger, M Chen, J Bugea, T Elich, & J Chory. (poster) *PIK* is a positive regulator of phytochrome signaling. Joint Annual Meeting of the American Society of Plant Biologists and the Canadian Society of Plant Physiologists; Boston, MA. August 5-9, **2006**.

BT Burger, M Chen, & J Chory. (poster) *PIK1 (PHYTOCHROME INTERACTOR WITH KELCH REPEATS 1*) is a positive acting component of light signaling. 16th International Conference on Arabidopsis Research; Madison, WI. June 15-19, **2005**.

BT Burger, M Chen, & J Chory. (poster) Understanding early events in phytochrome signal transduction. 14th International Conference on Arabidopsis Research; Madison, WI. June 20-24, **2003**.

BT Burger, JMF Cross, & LC Hannah. (poster) Differences in 3-PGA activation between potato tuber and maize endosperm ADP-glucose pyrophosphorylase. 43rd Maize Genetics Conference; Lake Geneva, WI. March 15-18, **2001**.

BT Burger, TW Greene, & LC Hannah. (poster) Temperature sensitive mutants of maize endosperm ADP-glucose pyrophosphorylase. 43rd Maize Genetics Conference; Lake Geneva, WI. March 15-18, **2001**.

BT Burger, TW Greene, & LC Hannah. (talk) Temperature sensitive mutants of maize endosperm ADP-glucose pyrophosphorylase. Plant Molecular and Cellular Biology Workshop. **2001, 1999, 1998**.

ABSTRACT OF THE DISSERTATION

Early events in phytochrome signaling in *Arabidopsis*

by

Brian Timothy Burger

Doctor of Philosophy in Biology

University of California, San Diego, 2008

Professor, Joanne Chory, Chair

Plants monitor their light environment with a sophisticated set of photoreceptors that includes the red/far-red light absorbing phytochromes. To better understand the early steps of phytochrome signaling, we performed a yeast two-hybrid screen and identified PIK (Phytochrome Interactor with Kelch Motifs) as a new phytochrome interactor. PIK interacts with phyA and phyB, and morphological phenotypes of a *PIK* mutant (*pik-1*) suggest that *PIK* acts as a positive regulator of phytochrome signaling. Downregulation of phyA is an important event in phytochrome signaling and occurs transcriptionally and post-translationally. We show that PIK downregulates *PHYA* transcription in response to light, and that *pik-1* phenotypes result from persistent phyA. We propose that PIK acts as an adaptor between phytochromes and transcriptional machinery to ensure proper light regulation of *PHYA*.

Inside the nucleus, phytochromes form subnuclear foci called nuclear bodies (NBs). We recovered two hypersensitive alleles of phyB in a mutant screen to identify factors involved in NB formation. These alleles exhibit hypersensitivity in terms of NB formation and inhibition of hypocotyl elongation by light. Mutations in *phyB-501* and *phyB-502* result in reduced intramolecular interactions, which may account for an impaired response to end-of-day far-red treatments. *phyB-501* and *phyB-502* also exhibit reduced affinity towards a downstream signaling factor. These mutations identify residues that are important for intra- and intermolecular interactions, and provide further evidence that NBs play a positive role in phytochrome signaling.

Genetic evidence implicates the PIF/PIL subfamily of bHLH transcription factors as important players in phytochrome signaling. However, the field lacks the tools to address their function biochemically. To that end, we generated antibodies against six members of this subfamily. We also identified T-DNA insertion alleles in five of the six genes encoding these proteins. Together, this represents a powerful set of tools for studying the role of these bHLH proteins in phytochrome signaling.

Lastly, we have identified a novel zinc knuckle/PLUS3 domain protein that directly regulates expression of key growth genes in a time-of-day fashion. Identification of TZP highlights the importance of daily synchronization of growth pathways, and underscores the utility of natural variation approaches to identifying new genes in light signaling.

Chapter 1

Introduction

Plants are one of the great evolutionary experiments in multicellularity. Their inability to move has many consequences. Plants must rely on insects, animals, or the elements for pollen and seed dispersal. They must defend themselves from predators in the absence of a "flight" response, instead relying on chemical defenses or physical barriers. But the defining characteristic of plants is their ability to convert light energy into chemical energy through the process of photosynthesis. This reliance on the sun has led to the development of a sophisticated suite of photoreceptors that ensures optimization of photosynthesis and proper timing of key developmental events. Plants track the position of the sun and also monitor light intensity and light quality, including shade from competing neighbors. They accomplish these feats, in part, through the action of phytochromes.

The Phytochrome Photoreceptor Family

Phytochromes are a family of red/far-red light absorbing photoreceptors first discovered in plants, but now widely recognized in cyanobacteria, purple and nonphotosynthetic bacteria, and fungi [1]. Due to their common ancestry, phytochromes share a common architecture and can be roughly divided into an N-terminal photosensory core and a C-terminal regulatory region. The N-terminal photosensory core can be further divided into PAS (P2), GAF (P3), and PHY (P4) domains. The GAF domain of plant phytochromes contains the bilin lyase activity responsible for covalent attachment of the bilin chromophore to a conserved cysteine residue [2]. The C-terminus (HKRD) of phytochromes contains homology to bacterial histidine kinases, though plant phytochromes have been shown to be atypical

serine/threonine kinases [3]. Plant phytochromes contain several additional domains, including a small N-terminal extension and two PAS-related domains preceding the HKRD. The hallmark of plant phytochromes, however, is their R/FR photoreversibility. It was this photoreversibility that first connected phytochrome preparations to the action spectrum of many plant responses. Phytochrome is synthesized in a red (R) light-absorbing form (Pr), with maximum absorption at 660 nm (Figure 1.1). The Pr form can be photoconverted with red light to a far-red (FR) light-absorbing form (Pfr). Because red light activates many plant responses, the Pfr form is considered the active form. Irradiation of Pfr with far-red light converts it back to Pr. The absorption maximum for Pfr is 730 nm, although there is significant overlap between the Pr and Pfr spectra. Thus in natural light conditions, phytochromes monitor changes in light quality as changes in the R to FR ratio (R/FR), which manifest in the plant as changes in the amount of total phytochrome in the Pfr form (% Pfr). Changes in the R/FR can be quite dramatic, ranging from 1.19 in full sunlight, to 0.96 at sunset, to as low as 0.13 in shade conditions [4]. Light absorption in phytochromes is made possible by a bilin chromophore derived from the oxidative metabolism of heme. In plant phytochromes the chromophore is known as phytochromobilin (PϕB). Upon light absorption, bilin chromophores undergo a Z to E isomerization about the C15-C16 double bond between the C- and D- tetrapyrrole rings [4]. The recently solved structure of the chromophore binding domain of phytochrome from *Deinococcus radiodurans* (DrBphP) provided a snapshot of the chromophore microenvironment of a phytochrome in the Pr state [5]. Surprisingly, the chromophore is buried deep within the GAF domain, which together with the PAS

domain forms a trefoil knot. This unusual structure may serve to stabilize domain-domain interactions, or to limit flexibility of the molecule during photoisomerization of the chromophore. A high degree of conservation of key amino acid residues in the structure suggests that this structure is likely common to all members of the phytochrome family.

Phytochromes in *Arabidopsis*

The phytochrome family in *Arabidopsis* is encoded by five genes, *PHYA-PHYE*. Plant phytochromes have been traditionally characterized as type I (light labile) or type II (light stable). In *Arabidopsis*, type I phytochromes are represented by phyA, while phyB-E constitute type II phytochromes. As a type I phytochrome, phyA is abundant in dark grown tissue but its levels drop rapidly in response to light. This decrease occurs due to the combined effects of *PHYA* mRNA instability, a light-mediated decrease in *PHYA* transcription, and the proteasome-mediated degradation of phyA in the Pfr form [4]. Type II phytochromes predominate in light grown plants. Phytochrome-mediated responses can be divided into three modes of action, distinguished by the amount of light required. Low fluence responses (LFRs) are the typical red/far-red reversible responses attributed to phytochromes. Very low fluence responses (VLFRs) occur at much lower fluence rates, are sensitive to a broad spectrum of light, and lack red/far-red reversibility. High irradiance responses (HIRs) require high fluence rates and also lack reversibility. Analysis of *phy* mutants has shown that phyA mediates the VLFR and far-red HIR, while the LFR and red HIR are predominantly mediated by phyB [4]. Stated more simply, phyA is the photoreceptor

mediating low fluence and far-red light responses, while phyB is the pre-dominant photoreceptor mediating responses to red light. phyC, phyD, and phyE play relatively minor, overlapping roles with phyB. For this reason, the remainder of this introduction will be restricted to discussion of phyA and phyB. The Pfr-mediated degradation of phyA in the Pfr form is likely the reason that phyA mediates responses to far-red light. Photoconversion to Pr by far-red light allows escape from Pfr-mediated degradation, thus allowing a higher pool of total phytochrome.

Owing to their wavelength and fluence rate requirements, phyA and phyB have both distinct and overlapping roles in plant growth and development. Both have positive roles in seed germination, seedling de-etiolation, and transition to flowering, while shade avoidance is largely mediated by phyB [4]. De-etiolation, the transition from heterotrophic growth in the dark to photoautotrophic growth in the light, is a vivid example of the effect of light on plant growth and development. Seedlings grown in the dark exhibit an etiolated phenotype characterized by a long hypocotyl (embryonic stem), an apical hook, and unopened cotyledons (embryonic leaves). This body plan is best suited to growth underneath soil, as the cotyledons are protected as the hypocotyl elongates through the soil in search of light. Upon sufficient light perception, hypocotyl growth is inhibited and cotyledons expand in anticipation of photosynthesis. Under natural light conditions, this process of de-etiolation is mediated by phyA and phyB. There is also evidence that antagonism exists between the phyA- and phyB-mediated signaling pathways. A powerful illustration of this antagonism is the stronger response to red light seen in *phyA* mutants as compared to wild-type seedlings [6].

Nuclear Localization of Phytochromes

Arguably the single most significant breakthrough in phytochrome signal transduction research in the last two decades was the discovery that phytochromes move to the nucleus in response to light. Placement of phytochromes in the nucleus was a revolution for the field and the discovery continues to impact phytochrome signaling today. Nuclear localization of phytochromes was first shown using COOH-terminal fragments of *Arabidopsis* phyB fused to GUS and expressed in *Arabidopsis* under control of the constitutive 35S promoter [7]. The authors found phyB in the nuclei of protoplasts isolated from hypocotyls of light grown seedlings. This work was extended with phyB:GFP fusion proteins that could be visualized in living tissue [8]. The authors make three key observations in this paper: nuclear localization occurs in the light but not in the dark, phyB nuclear localization follows a relatively slow time course (on the order of hours), and phyB:GFP forms sub-nuclear foci that increase in size but decrease in number in response to light. This latter observation is the first reference to speckles, now referred to as nuclear bodies (NBs).

The light-dependency of nuclear localization quickly led the field to ask if the nucleus, and not the cytoplasm as had long been believed, was the site of signal transduction. The identification of several bHLH transcription factors that interact physically with phytochromes provided anecdotal evidence that this might be the case [9-11]. The most direct evidence implicating the nucleus as the site of signal transduction came from work by the Quail lab [12]. In this paper, the authors show that rescue of a *phyB* mutant by a phyB:glucocorticoid receptor fusion occurs only in the presence of light and the steroid dexamethasone (Dex). This finding showed

unequivocally that the nucleus is the site of biological function, at least in the case of phyB-mediated photomorphogenesis. Further, mutants defective in phyA nuclear retention exhibit *phyA* seedling phenotypes under FRc, while a constitutively nuclear-localized phyA rescues a *phyA* mutant [13, 14]. This is not to say that no signaling occurs in the cytoplasm as there are many examples of phytochrome-mediated events which occur too rapidly to involve translocation to the nucleus, including photoreversible adhesion of barley root tips to glass [15], cytoplasmic streaming in *Vallisneria* [16], and electric potential changes in oat seedlings [17], among others. A recent paper demonstrates a cytoplasmic function for *Arabidopsis* phyA in abrogation of negative gravitropism in blue (B) light and in R-enhanced phototropism [18]. However, from a photomorphogenic standpoint, it is apparent that the overwhelming majority of phytochrome-mediated signaling events occur in the nucleus.

Once nuclear localization had been shown for phyB, the other phytochromes were investigated in a series of papers by the Schafer and Nagy labs [19-21]. These papers demonstrate differences in the light requirements and kinetics of nuclear import for the five *Arabidopsis* phytochromes. Importantly, all five *Arabidopsis* phytochromes are imported into the nucleus and form NBs in a light dependent manner. phyA and phyB exhibit several important differences. In etiolated seedlings phyA is localized exclusively in the cytoplasm while phyB exhibits both cytoplasmic and diffuse nuclear localization. phyA is transported into the nucleus within 10 minutes, while phyB import is greater than an order of magnitude slower. Consistent with phyA mediating HIR and VLFR responses, phyA nuclear import and NB formation is promoted by continuous far-red light (FRc) and brief pulses of light

irrespective of wavelength. phyB nuclear import and NB formation was induced only by continuous white light (WLc) and continuous red light (Rc), and to a lesser extent by continuous blue light (Bc). Consistent with its Pfr-mediated degradation, phyA NBs were short-lived in WLc and Rc, and long-lived, though slower to form, in FRc.

It remains to be seen if the mechanism by which phyA and phyB translocate to the nucleus is the same. Sequence analysis does not identify a NLS in either phytochrome. Accumulation of phyA in the nucleus requires the presence of FHY1 and the closely related FHL, as double loss of function results in cytoplasmic accumulation of phyA:GFP [13]. These small, plant-specific proteins contain both a functional NLS and a NES, and interact preferentially with phyA in the Pfr form [13, 22]. They are present in both the nucleus and the cytoplasm in etiolated seedlings, but colocalize with phyA in NBs upon light treatment [13, 23]. This data supports two non-mutually exclusive models for FHY1/FHL function in phyA nuclear accumulation: phyA is imported into the nucleus with FHY1/FHL through their NLSs, or phyA is retained in the nucleus by FHY1/FHL following import. Unlike phyA, no external factors for phyB nuclear accumulation have been defined. Several groups have shown that the C-terminus of phyB is transported into the nucleus and forms NBs regardless of light condition, though it fails to complement *phyB* mutants [7, 24]. This suggests that the C-terminus contains a cryptic NLS or an interacting domain through which phyB is brought to the nucleus. Since full-length phyB movement into the nucleus is conformation dependent, one parsimonious model would be that the N-terminus blocks these signals in the C-terminus in a light dependent manner. Indeed, Chen *et al.* showed in yeast two-hybrid experiments that interaction between the N-

and C-terminus of phyB was reduced in the light [25]. Whether this unmasking of the C-terminus results in contact with an accessory protein or exposure of a cryptic NLS is undetermined.

Though the function of NBs is still unclear, a growing body of evidence suggests that NBs play a positive role in phytochrome signaling. In the case of phyB, formation of NBs is correlated with increasing fluence rate, and maximum inhibition of hypocotyl elongation is accompanied by NB formation [26]. Further, *phyA* and *phyB* alleles defective in phytochrome signaling are imported into the nucleus but fail to form NBs [21, 26], while *phyB* alleles which cause constitutively photomorphogenic (COP) phenotypes in the dark also form NBs in the dark [27]. Matsushita *et al.* showed that expression of the N-terminus of phyB, when fused to a NLS and dimerization domain, resulted in hypersensitivity to Rc in the absence of NB formation [24]. This finding suggests that NBs play a negative role and supports a model whereby NBs serve as storage sites for phytochrome rather than sites of signal transduction. The field eagerly awaits the cloning of the *dsf* (*Deficient in Speckle Formation*) mutants that are impaired in phyB signaling and fail to form the large NBs observed at high fluence rates of Rc [26].

Phytochrome-Mediated Changes in Gene Expression

Once inside the nucleus, phytochromes initiate a signaling cascade that ultimately leads to a reprogramming of the developmental plan. The first systematic study of the effect of light on gene expression used an EST-based array to query the expression profiles of etiolated *Arabidopsis* seedlings and those grown under

monochromatic light [28]. Not surprisingly, given the phenotypic differences between etiolated and de-etiolated seedlings, approximately one-third of the EST clones displayed differential expression between dark- and WLc-grown seedlings. Interestingly, seedlings grown under Rc, Bc, or FRc light exhibited similar expression profiles, suggesting that phytochrome- and cryptochrome-mediated signaling may converge on a similar set of target genes. Work by Tepperman *et al.* using the Affymetrix 8K array showed that approximately 10% of the genes in seedlings exposed to FRc for 24 hours are regulated in a phyA-dependent manner [29]. The authors define early response (within 1 h) and late response (3 to 24 h) genes, and show that genes encoding transcription-related proteins are overrepresented in the early response genes. This suggests that phyA-mediated FRc signaling occurs through establishment of a transcriptional network. Interestingly, it seems that phyA is also responsible for regulation of genes that respond to Rc [28, 30, 31]. In array experiments using the Affymetrix full genome ATH1 microarray, Tepperman *et al.* demonstrate that phyA is largely responsible for transducing the Rc signal to the early response genes, with phyB playing a minimal role in the presence of phyA [31]. While this finding is somewhat counterintuitive based on phenotypes of *phyA* and *phyB* mutants under FRc and Rc, phyA has been shown to mediate the early hours of Rc signaling based on kinetic analysis of inhibition of hypocotyl elongation in *phy* mutants [32].

Genetic screens and yeast two-hybrid experiments have identified a wealth of components involved in the phytochrome signal transduction pathway. While a comprehensive review of phytochrome signaling is beyond the scope of this

introduction, I will highlight the core components and overarching themes of the pathway, especially as it pertains to my thesis work.

Regulated Protein Turnover in Phytochrome Signaling

Early genetic screens identified a number of recessive mutants, the so-called *cop*/*det*/*fus* mutants, which exhibit light grown phenotypes in the dark [33]. Interpretation of these phenotypes suggests that de-etiolation is repressed in the dark by the action of these genes, and analysis of the COP/*DET/FUS* gene products has established post-translational regulation and protein turnover as the mechanisms by which this repression occurs. With the exception of *COP1, COP10,* and *DET1*, the remaining *COP*/*DET*/*FUS* gene products comprise the eight individual components of the COP9 signalosome (CSN), an entity related to the lid subcomplex of the 26S proteasome and, more distantly, to the eIF3 complex. The initial correspondence between the subunits of the CSN and those of the lid subcomplex of the 19S regulatory particle of the 26S proteasome led to speculation that the CSN plays a role in ubiquitin-mediated degradation. Evidence for CSN function came from interaction of the CSN with SCF ubiquitin ligase subunits CUL1 from NIH 3T3 cells [34] and SCF^{TIR1} from *Arabidopsis* [35]. Further, a reduction in CSN5 activity in *Arabidopsis* resulted in accumulation of an SCF^{TIR1} target, suggesting that the CSN plays a positive role in E3 ubiquitin ligase-mediated protein degradation [35]. Work from several groups has established that deneddylation activity attributed to CSN5 is important in regulating SCF activity towards target substrates. Additionally, kinase and de-ubiquitination activities have also been associated with the CSN [36]. Together, data

suggests that the CSN supports the activity of cullin-containing E3 ubiquitin ligase complexes.

Phenotypes of *det1* and *cop1* mutants suggest that DET1 and COP1 play a role similar to CSN in regulating photomorphogenesis. Indeed, DET1 forms a complex with the *Arabidopsis* homolog of UV-Damaged DNA-Binding Protein 1 (DDB1) [37]. This complex has been shown to interact with the ubiquitin-conjugating enzyme variant COP10 and *Arabidopsis* CUL4 [38-40]. COP1 encodes an E3 ubiquitin ligase that has been shown to target a number of photomorphogenesis-promoting transcription factors for degradation in the dark, including the bZIP transcription factors HY5 and HYH, myb transcription factor LAF1, and bHLH transcription factor HFR1 [41-47]. Additionally, COP1 ubiquitinates the phyA photoreceptor and COP1 itself [44, 48]. COP1 ubiquitin ligase activity is modulated by members of the SPA family of WD-repeat proteins [44, 49-55]. Based on evidence showing translocation of COP1 from the nucleus to the cytoplasm in response to light [56, 57], the prevailing model for COP1 function is the ubiquitination of positive acting transcription factors in the dark, followed by translocation to the cytoplasm and subsequent de-repression of transcription factors in the light. The direct interaction with photoreceptors (including cryptochromes and phyB) provides an attractive mechanism whereby activated photoreceptors modulate localization or activity of COP1 [57-59].

As stated above, as both targets of phytochrome action and targets of protein degradation, transcription factors play a major role in phytochrome signaling. The identification of the bHLH transcription factor PIF3 in a yeast two-hybrid screen with phyB was an important event in phytochrome signaling in that it brought a new family

of transcription factors to the pathway [10]. For a thorough review of the role of PIF3 and related bHLH transcription factors in phytochrome signaling see Chapter 6.

Perhaps not surprising given the importance of light to plant development, the phytochrome signaling pathway interacts with other light signaling pathways and with hormone signal transduction pathways. While much progress has been made on understanding the structure/function relationship of phytochromes and on phytochrome signal transduction, many questions remain. The work presented here makes several advances in our understanding of phytochrome signaling and presents new tools with which to study the role of the PIF/PIL subfamily of bHLH transcription factors. Chapter 2 presents the identification and characterization of a new phytochrome-interacting partner implicated in regulating *PHYA* mRNA. Chapter 3 presents identification of hypersensitive alleles of phyB, with implications for signaling and NB formation as they pertain to phytochrome structure. Chapter 4 presents a set of antibodies directed against the PIF/PIL/HFR1 subfamily of bHLH transcription factors. Finally, chapter 5 presents the identification and characterization of novel gene involved in light-regulated growth in *Arabidopsis* using a natural variation approach.

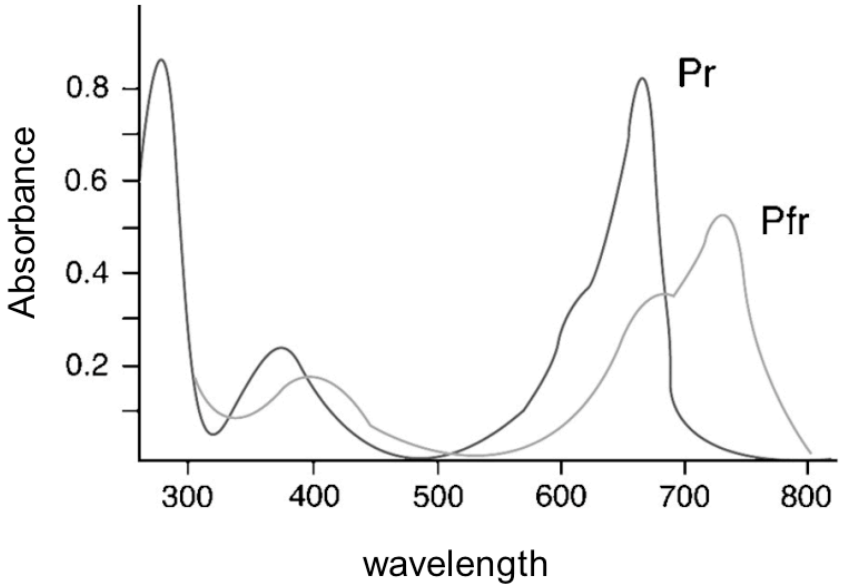

Figure 1.1. The absorption spectra for Pr and Pfr forms of phytochrome. Pr exhibits an absorption maximum at 660 nm. Pfr exhibits an absorption maximum at 730 nm. Note that there is overlap between the Pr and Pfr spectra. Figure from Chen *et al.* [60].

References

1. Montgomery, B., and Lagarias, J. (2002). Phytochrome ancestry: sensors of bilins and light. Trends Plant Sci *7*, 357.

2. Elich, T.D., and Lagarias, J.C. (1989). Formation of a photoreversible phycocyanobilin-apophytochrome adduct *in vitro*. J. Biol. Chem. *264*, 12902-12908.

3. Yeh, K.C., and Lagarias, J.C. (1998). Eukaryotic phytochromes: light-regulated serine/threonine protein kinases with histidine kinase ancestry. Proceedings of the National Academy of Sciences of the United States of America *95*, 13976-13981.

4. Taiz, L.Z., E. (1998). Plant Physiology, Second Edition, (Sunderland, MA: Sinauer Associates, Inc.).

5. Wagner, J.R., Brunzelle, J.S., Forest, K.T., and Vierstra, R.D. (2005). A light-sensing knot revealed by the structure of the chromophore-binding domain of phytochrome. Nature *438*, 325-331.

6. Mazzella, M.A., Alconada Magliano, T.M., and Casal, J.J. (1997). Dual effect of phytochrome A on hypocotyl growth under continuous red light. Plant, Cell and Environment *20*, 261-267.

7. Sakamoto, K., and Nagatani, A. (1996). Nuclear localization activity of phytochrome B. Plant J. *10*, 859-868.

8. Yamaguchi, R., Nakamura, M., Mochizuki, N., Kay, S.A., and Nagatani, A. (1999). Light-dependent Translocation of a Phytochrome B-GFP Fusion Protein to the Nucleus in Transgenic Arabidopsis. J Cell Biol *145*, 437-445.

9. Huq, E., Al-Sady, B., Hudson, M., Kim, C., Apel, K., and Quail, P.H. (2004). Phytochrome-interacting factor 1 is a critical bHLH regulator of chlorophyll biosynthesis. Science *305*, 1937-1941.

10. Ni, M., Tepperman, J.M., and Quail, P.H. (1998). PIF3, a phytochrome-interacting factor necessary for normal photoinduced signal transduction, is a novel basic helix-loop-helix protein. Cell *95*, 657-667.

11. Huq, E., and Quail, P.H. (2002). PIF4, a phytochrome-interacting bHLH factor, functions as a negative regulator of phytochrome B signaling in Arabidopsis. Embo J *21*, 2441-2450.

12. Huq, E., Al-Sady, B., and Quail, P.H. (2003). Nuclear translocation of the photoreceptor phytochrome B is necessary for its biological function in seedling photomorphogenesis. Plant J *35*, 660-664.

13. Hiltbrunner, A., Tscheuschler, A., Viczian, A., Kunkel, T., Kircher, S., and Schafer, E. (2006). FHY1 and FHL act together to mediate nuclear accumulation of the phytochrome A photoreceptor. Plant & cell physiology *47*, 1023-1034.

14. Genoud, T., Schweizer, F., Tscheuschler, A., Debrieux, D., Casal, J.J., Schafer, E., Hiltbrunner, A., and Fankhauser, C. (2008). FHY1 mediates nuclear import of the light-activated phytochrome A photoreceptor. PLoS genetics *4*, e1000143.

15. Tanada, T. (1968). A Rapid Photoreversible Response of Barley Root Tips in the Presence of 3-Indoleacetic Acid. Proceedings of the National Academy of Sciences of the United States of America *59*, 376-380.

16. Takagi, S., Kong, S.G., Mineyuki, Y., and Furuya, M. (2003). Regulation of actin-dependent cytoplasmic motility by type II phytochrome occurs within seconds in Vallisneria gigantea epidermal cells. The Plant cell *15*, 331-345.

17. Newman, I.A., and Briggs, W.R. (1972). Phytochrome-mediated Electric Potential Changes in Oat Seedlings. Plant physiology *50*, 687-693.

18. Rosler, J., Klein, I., and Zeidler, M. (2007). Arabidopsis fhl/fhy1 double mutant reveals a distinct cytoplasmic action of phytochrome A. Proceedings of the National Academy of Sciences of the United States of America *104*, 10737-10742.

19. Kircher, S., Kozma-Bognar, L., Kim, L., Adam, E., Harter, K., Schafer, E., and Nagy, F. (1999). Light quality-dependent nuclear import of the plant photoreceptors phytochrome A and B. The Plant cell *11*, 1445-1456.

20. Kim, L., Kircher, S., Toth, R., Adam, E., Schafer, E., and Nagy, F. (2000). Light-induced nuclear import of phytochrome-A:GFP fusion proteins is differentially regulated in transgenic tobacco and Arabidopsis. Plant J *22*, 125-133.

21. Kircher, S., Gil, P., Kozma-Bognar, L., Fejes, E., Speth, V., Husselstein-Muller, T., Bauer, D., Adam, E., Schafer, E., and Nagy, F. (2002). Nucleocytoplasmic partitioning of the plant photoreceptors phytochrome A, B, C, D, and E is regulated differentially by light and exhibits a diurnal rhythm. The Plant cell *14*, 1541-1555.

22. Hiltbrunner, A., Viczian, A., Bury, E., Tscheuschler, A., Kircher, S., Toth, R., Honsberger, A., Nagy, F., Fankhauser, C., and Schafer, E. (2005). Nuclear accumulation of the phytochrome A photoreceptor requires FHY1. Curr Biol *15*, 2125-2130.

23. Zeidler, M., Zhou, Q., Sarda, X., Yau, C.P., and Chua, N.H. (2004). The nuclear localization signal and the C-terminal region of FHY1 are required for transmission of phytochrome A signals. Plant J *40*, 355-365.

24. Matsushita, T., Mochizuki, N., and Nagatani, A. (2003). Dimers of the N-terminal domain of phytochrome B are functional in the nucleus. Nature *424*, 571-574.

25. Chen, M., Tao, Y., Lim, J., Shaw, A., and Chory, J. (2005). Regulation of phytochrome B nuclear localization through light-dependent unmasking of nuclear-localization signals. Curr Biol *15*, 637-642.

26. Chen, M., Schwab, R., and Chory, J. (2003). Characterization of the requirements for localization of phytochrome B to nuclear bodies. Proceedings of the National Academy of Sciences of the United States of America *100*, 14493-14498.

27. Su, Y.S., and Lagarias, J.C. (2007). Light-independent phytochrome signaling mediated by dominant GAF domain tyrosine mutants of Arabidopsis phytochromes in transgenic plants. The Plant cell *19*, 2124-2139.

28. Ma, L., Li, J., Qu, L., Hager, J., Chen, Z., Zhao, H., and Deng, X.W. (2001). Light control of Arabidopsis development entails coordinated regulation of genome expression and cellular pathways. The Plant cell *13*, 2589-2607.

29. Tepperman, J.M., Zhu, T., Chang, H.S., Wang, X., and Quail, P.H. (2001). Multiple transcription-factor genes are early targets of phytochrome A signaling. Proceedings of the National Academy of Sciences of the United States of America *98*, 9437-9442.

30. Tepperman, J.M., Hudson, M.E., Khanna, R., Zhu, T., Chang, S.H., Wang, X., and Quail, P.H. (2004). Expression profiling of phyB mutant demonstrates substantial contribution of other phytochromes to red-light-regulated gene expression during seedling de-etiolation. Plant J *38*, 725-739.

31. Tepperman, J.M., Hwang, Y.S., and Quail, P.H. (2006). phyA dominates in transduction of red-light signals to rapidly responding genes at the initiation of Arabidopsis seedling de-etiolation. Plant J *48*, 728-742.

32. Parks, B.M., and Spalding, E.P. (1999). Sequential and coordinated action of phytochromes A and B during Arabidopsis stem growth revealed by kinetic analysis. Proceedings of the National Academy of Sciences of the United States of America *96*, 14142-14146.

33. Fankhauser, C., and Chory, J. (1997). Light control of plant development. Annu Rev Cell Dev Biol *13*, 203-229.

34. Lyapina, S., Cope, G., Shevchenko, A., Serino, G., Tsuge, T., Zhou, C., Wolf, D.A., Wei, N., and Deshaies, R.J. (2001). Promotion of NEDD-CUL1 conjugate cleavage by COP9 signalosome. Science *292*, 1382-1385.

35. Schwechheimer, C., Serino, G., Callis, J., Crosby, W.L., Lyapina, S., Deshaies, R.J., Gray, W.M., Estelle, M., and Deng, X.W. (2001). Interactions of the COP9 signalosome with the E3 ubiquitin ligase SCFTIRI in mediating auxin response. Science *292*, 1379-1382.

36. Wei, N., and Deng, X.W. (2003). The COP9 signalosome. Annu. Rev. Cell Dev. Biol. *19*, 261-286.

37. Schroeder, D.F., Gahrtz, M., Maxwell, B.B., Cook, R.K., Kan, J.M., Alonso, J.M., Ecker, J.R., and Chory, J. (2002). De-etiolated 1 and Damaged DNA Binding Protein 1 interact to regulate *Arabidopsis* photomorphogenesis. Curr. Biol. *12*, 1462-1472.

38. Yanagawa, Y., Sullivan, J.A., Komatsu, S., Gusmaroli, G., Suzuki, G., Yin, J., Ishibashi, T., Saijo, Y., Rubio, V., Kimura, S., et al. (2004). Arabidopsis COP10 forms a complex with DDB1 and DET1 in vivo and enhances the activity of ubiquitin conjugating enzymes. Genes & development *18*, 2172-2181.

39. Chen, H., Shen, Y., Tang, X., Yu, L., Wang, J., Guo, L., Zhang, Y., Zhang, H., Feng, S., Strickland, E., et al. (2006). Arabidopsis CULLIN4 Forms an E3 Ubiquitin Ligase with RBX1 and the CDD Complex in Mediating Light Control of Development. The Plant cell *18*, 1991-2004.

40. Bernhardt, A., Lechner, E., Hano, P., Schade, V., Dieterle, M., Anders, M., Dubin, M.J., Benvenuto, G., Bowler, C., Genschik, P., et al. (2006). CUL4 associates with DDB1 and DET1 and its downregulation affects diverse aspects of development in Arabidopsis thaliana. Plant J *47*, 591-603.

41. Osterlund, M.T., Hardtke, C.S., Wei, N., and Deng, X.W. (2000). Targeted destabilization of HY5 during light-regulated development of Arabidopsis. Nature *405*, 462-466.

42. Hardtke, C.S., Gohda, K., Osterlund, M.T., Oyama, T., Okada, K., and Deng, X.W. (2000). HY5 stability and activity in arabidopsis is regulated by phosphorylation in its COP1 binding domain. Embo J *19*, 4997-5006.

43. Holm, M., Ma, L.G., Qu, L.J., and Deng, X.W. (2002). Two interacting bZIP proteins are direct targets of COP1-mediated control of light-dependent gene expression in Arabidopsis. Genes & development *16*, 1247-1259.

44. Seo, H.S., Yang, J.Y., Ishikawa, M., Bolle, C., Ballesteros, M.L., and Chua, N.H. (2003). LAF1 ubiquitination by COP1 controls photomorphogenesis and is stimulated by SPA1. Nature *424*, 995-999.

45. Duek, P.D., Elmer, M.V., van Oosten, V.R., and Fankhauser, C. (2004). The degradation of HFR1, a putative bHLH class transcription factor involved in light signaling, is regulated by phosphorylation and requires COP1. Curr Biol *14*, 2296-2301.

46. Yang, J., Lin, R., Sullivan, J., Hoecker, U., Liu, B., Xu, L., Deng, X.W., and Wang, H. (2005). Light regulates COP1-mediated degradation of HFR1, a transcription factor essential for light signaling in Arabidopsis. The Plant cell *17*, 804-821.

47. Jang, I.C., Yang, J.Y., Seo, H.S., and Chua, N.H. (2005). HFR1 is targeted by COP1 E3 ligase for post-translational proteolysis during phytochrome A signaling. Genes & development *19*, 593-602.

48. Seo, H.S., Watanabe, E., Tokutomi, S., Nagatani, A., and Chua, N.H. (2004). Photoreceptor ubiquitination by COP1 E3 ligase desensitizes phytochrome A signaling. Genes & development *18*, 617-622.

49. Hoecker, U., and Quail, P.H. (2001). The phytochrome A-specific signaling intermediate SPA1 interacts directly with COP1, a constitutive repressor of light signaling in Arabidopsis. J Biol Chem *276*, 38173-38178.

50. Hoecker, U., Tepperman, J.M., and Quail, P.H. (1999). SPA1, a WD-repeat protein specific to phytochrome A signal transduction. Science *284*, 496-499.

51. Hoecker, U., Xu, Y., and Quail, P.H. (1998). SPA1: a new genetic locus involved in phytochrome A-specific signal transduction. The Plant cell *10*, 19-33.

52. Laubinger, S., Fittinghoff, K., and Hoecker, U. (2004). The SPA quartet: a family of WD-repeat proteins with a central role in suppression of photomorphogenesis in arabidopsis. The Plant cell *16*, 2293-2306.

53. Laubinger, S., and Hoecker, U. (2003). The SPA1-like proteins SPA3 and SPA4 repress photomorphogenesis in the light. Plant J *35*, 373-385.

54. Saijo, Y., Sullivan, J.A., Wang, H., Yang, J., Shen, Y., Rubio, V., Ma, L., Hoecker, U., and Deng, X.W. (2003). The COP1-SPA1 interaction defines a critical step in phytochrome A-mediated regulation of HY5 activity. Genes & development *17*, 2642-2647.

55. Yang, J., Lin, R., Hoecker, U., Liu, B., Xu, L., and Wang, H. (2005). Repression of light signaling by Arabidopsis SPA1 involves post-translational regulation of HFR1 protein accumulation. Plant J *43*, 131-141.

56. von Arnim, A.G., and Deng, X.-W. (1994). Light inactivation of Arabidopsis photomorphogenic repressor COP1 involves a cell-specific regulation of its nucleocytoplasmic partitioning. Cell *79*, 1035-1045.

57. Osterlund, M.T., and Deng, X.W. (1998). Multiple photoreceptors mediate the light-induced reduction of GUS-COP1 from Arabidopsis hypocotyl nuclei. Plant J *16*, 201-208.

58. Wang, H., Ma, L.G., Li, J.M., Zhao, H.Y., and Deng, X.W. (2001). Direct interaction of Arabidopsis cryptochromes with COP1 in light control development. Science *294*, 154-158.

59. Yang, H.Q., Tang, R.H., and Cashmore, A.R. (2001). The signaling mechanism of Arabidopsis CRY1 involves direct interaction with COP1. The Plant cell *13*, 2573-2587.

60. Chen, M., Chory, J., and Fankhauser, C. (2004). Light signal transduction in higher plants. Annual review of genetics *38*, 87-117.

Chapter 2

Characterization of Phytochrome Interactor with Kelch Repeats (PIK)

Introduction

Plants utilize light not only as their energy source, but also as an environmental cue affecting time-keeping mechanisms and developmental decisions. Survival and reproductive success depend on execution of developmental plans at appropriate times. For examples, seedlings growing in the soil remain etiolated until a light cue signifies that they are above soil. De-etiolation beneath the soil would have a devastating effect on survival. Phytochromes play an important role in plant development as monitors of light quality. Their red/far-red photoreversibility suits them perfectly in this capacity. Yet despite intense study, the signaling pathway through which phytochromes convert changes in light quality to changes in growth and development is unknown. We performed a yeast two-hybrid experiment with the C-terminus of phyB in hopes of identifying new players in the signaling pathway. Here, we present characterization of one such component.

Results

phyA and phyB Interact With a Kelch Repeat Domain-Containing Protein

We used the C-terminus of phyB in a yeast two-hybrid screen to identify interacting proteins. Yeast two-hybrid screens have been successful in identifying phytochrome signal transduction components, including PIF3, PKS1, and NDPK2, among others [1-3]. Several interacting proteins were identified and PIK (Phytochrome Interactor with Kelch motifs), presented here, was selected for further study. We demonstrated that PIK also interacts with phyA in a yeast two-hybrid assay (Figure 2.1A). We confirmed the interaction between PIK and phytochromes with pull

down assays using recombinant GST-tagged phytochromes, and *in vitro* transcribed and translated PIK (Figure 2.1B). PIK interaction with both phyA and phyB is conformation and chromophore independent, as no interaction differences are observed with phytochromes in Pr or Pfr conformation, or with phytochrome apo-proteins.

PIK (At1g54040) encodes a 342 amino acid protein with five Kelch motifs (Figure 2.2A). A Kelch motif is typically 44-56 amino acids long and occurs in a series of four to seven repeats, which together form a four- to seven-bladed β-propeller kelch repeat domain [4]. Kelch repeat domains are found in a wide range of species, have varied cellular distribution, and participate in a wide range of activities. The three-dimensional organization of the β-propeller provides many potential protein-protein interaction sites. There are no other recognizable sequence motifs or signals for subcellular targeting in PIK. Evidence for a smaller cDNA exists on the RIKEN *Arabidopsis* full-length CDNA database (http://rarge.gsc.riken.jp/cdna/). This splice site variant encodes a 262 amino acid protein, the significance of which is unknown. *PIK* is a member of a seven-member gene family in *Arabidopsis*. All family members contain the Kelch repeat domain, and four of the members contain one or two NH2-terminal jacalin-related lectin domains (Figure 2.2A). Lectins are carbohydrate-binding proteins, with jacalins having specificity for galactose. The seven family members exhibit a high degree of identity at the amino acid level (Figure 2.2B), surprising given that Kelch repeat proteins often share little sequence similarity [4]. A keyword search in The Arabidopsis Information Resource (TAIR) database (http://www.arabidopsis.org) returns 228 gene matches, suggesting that proteins

containing Kelch repeat domains are widespread in *Arabidopsis*. The role of the family members in phytochrome signal transduction is currently underway (see Discussion). PIK has been identified previously as an epithiospecifier protein (ESP), a protein that non-enzymatically alters the hydrolysis products of glucosinolates, sulfur-rich secondary metabolites commonly involved in plant defense [5, 6]. More recently PIK was identified as an interactor of WRKY53, a transcription factor involved in leaf senescence [7].

Overexpression of a PIK:CFP fusion protein driven by the Cauliflower mosaic virus 35S (35S) promoter shows nuclear and endoplasmic reticulum localization (Figure 2.3A). Nuclear localization for PIK has been published recently [7]. Northern analysis shows that *PIK* is expressed strongest in whole flowers compared to cotyledons, leaves, cauline leaves, roots, and floral stems (Figure 2.3B). This expression pattern is confirmed by data from Genevestigator (www.genevestigator.ethz.ch), which shows strongest expression in sepals followed by that in cotyledons. Transcriptional and translational GUS fusions showed no staining (data not shown), likely due to the low expression of *PIK* in the Col-0 ecotype, where expression is approximately 100-fold lower than in the Ler ecotype (Figure 2.10B).

PIK is a Positive Factor in Phytochrome Signaling

Hypocotyls (the stem-like structure bearing the embryonic leaves) are extremely sensitive to light and provide a direct read-out of the activity of the phytochrome signal transduction pathway. For example, in seedlings grown in low

light conditions (or in seedlings where phytochrome signaling is impaired), hypocotyl elongation is less inhibited than in seedlings grown in high light conditions (or in wild-type seedlings). The resulting hypocotyl is longer and the seedling is said to be hyposensitive. To study the role of *PIK* in phytochrome signaling we isolated a T-DNA insertion in *PIK* (*pik-1*) and generated *35S*::*PIK* overexpression lines in Col-0. qPCR analysis indicates that *pik-1* is an RNA null (Figure 2.11). *pik-1* seedlings are hyposensitive in both Rc (Figure 2.4A) and FRc (Figure 2.4B). No phenotypes were observed in *pik-1* seedlings grown in Bc or WLc (data not shown). Additionally, no phenotypes were observed in the *35S*::*PIK* (Col-0) overexpression lines under any light condition (data not shown). We tested the VLFR response of *pik-1* in seedlings given three minute FR pulses (FRp) hourly for four days. FRp were less effective in inhibiting hypocotyl elongation in *pik-1* than wild-type (Figure 2.4C D).

The light environment regulates the transition from vegetative to reproductive growth, in part, through the action of phytochromes. As a result, an impaired phytochrome signal transduction pathway results in a variation from normal flowering time. We observed that flowering time is affected in *pik-1* (Figure 2.4E). Time to flower (in days) was measured for Col-0, *phyB-9*, *pik-1*, *phyA-211*, and PIK OX *phyA-211* under LD conditions, with *pik-1* flowering earlier than Col-0 but later than the *phyB* null allele, *phyB-9*. *pik-1* does not flower as early as *phyB-9*, consistent with the relatively weak hypocotyl phenotype compared to *phyB-9* (data not shown). Together, the above data suggest that PIK is a positive factor in phytochrome signaling.

As mentioned above, PIK/ESP is involved in glucosinolate catabolism, which can be linked to the auxin biosynthetic pathway (see below). Because increased auxin

concentrations result in hypocotyl elongation and early flowering [8], we investigated this link as the potential cause of the *pik-1* phenotype. Glucosinolates are sulfur-rich secondary metabolites found mostly in plants from the order Capparales, whose hydrolysis products are important to plants as both defense compounds and attractants [9]. Glucosinolate hydrolysis by myrosinases leads to the formation of glucose and an unstable aglycone, which rearranges to form products that depend on the structure of its side chain and the presence of additional cofactors and proteins. One such protein is the epithiospecifier protein (ESP), whose presence during hydrolysis results in the formation of nitriles and epithionitriles despite any catalytic ability by ESP alone. Tryptophan serves as the precursor for both indolic glucosinolates and the plant phytohormone auxin, and data suggest that the indolic glucosinolate biosynthetic pathway functions in maintaining auxin homeostasis. Mutations in genes encoding the first three steps in indolic glucosinolate biosynthesis from indole-3-acetaldoxime (IAOx) lead to auxin accumulation and high-auxin phenotypes [10-18]. Further, hydrolysis of indolic glucosinolates in the presence of ESP leads to indole acteonitrile (IAN), which can be hydrolyzed by nitrilases to auxin (indole-3-acetic acid; IAA). In collaboration with Dr. Dan Kliebenstein (UC Davis) we measured total glucosinolates in Col-0 and *pik-1* seedlings grown for four days in Rc (Figure 2.5). Total glucosinolates are increased more than two-fold in *pik-1* compared to Col-0. This finding suggests that ESP plays a role in turnover of glucosinolates in the absence of herbivory, perhaps to provide pools for indole and methionine. Despite the absence of high-auxin phenotypes (increased secondary root formation, epinastic leaves, etc.) in *pik-1*, the above data raise the possibility that ESP affects auxin homeostasis. To test

this directly, we measured free auxin in seedlings grown for four days in Rc (in collaboration with Dr. Karin Ljung, Umea Plant Science Center). There were no significant differences in free auxin between Col-0, *pik-1*, *phyA-211* and *PIK OX phyA-211* (Figure 2.6). The data presented here suggest that while PIK/ESP shapes the outcome of glucosinolate hydrolysis, and may play a role in glucosinolate cycling outside plant defense, the phenotypes observed in *pik-1* are not the result of increased auxin.

PIK1 functions to repress *PHYA* transcription

To test if the observed phenotypes were the result of altered photoreceptor levels, we measured phyA and phyB levels in *pik-1* and Col-0 seedlings grown for four days in continuous dark and then transferred to Rc for 24 hours. While phyB levels in *pik-1* appear more or less the same as Col-0 (Figure 2.7A), phyA degradation is delayed (Figure 2.7B). The rapid, proteasome-mediated degradation of phyA upon conversion to Pfr classifies it as a light labile (type I) phytochrome, in contrast to the light stable (type II) phyB-E isoforms. To ensure that a functional phyB signal transduction pathway is not required for phyA degradation, we tested phyA degradation in *phyB-9* and observed no difference with Col-0 (Figure 2.7C). phyA is also regulated at the transcriptional level, where *PHYA* mRNA decreases rapidly, in a phy-dependent manner, upon light exposure [19]. In an effort to determine at which level *PIK* is functioning, we performed the above experiments in the presence and absence of the translational inhibitor, cycloheximide (CHX). The results of this experiment show that CHX abrogates the effect of *pik-1* on phyA degradation (Figure

2.8A-2.8E). This demonstrates that protein synthesis is required, and suggests that *PIK* functions at the level of transcriptional regulation. To verify this, we performed qPCR analysis on seedlings grown in the same conditions as for the western blots above (Figure 2.9). As expected, *PHYA* mRNA decreases in wild type seedlings upon light exposure. In *pik-1,* however, we observe a delay in the reduction of *PHYA* mRNA that correlates with the delay observed in phyA protein degradation.

phyA regulates *PIK* expression

We investigated regulation of *PIK* mRNA using DIURNAL (http://diurnal.cgrb.oregonstate.edu/), a searchable database of diurnal and circadian microarray data [20]. *PIK* transcript levels cycle under intermediate day conditions (12 h light:12 h dark) but remain fairly constant under continuous light (Figure 2.10A), suggesting that *PIK* is controlled by light but not by the circadian clock. Under SD conditions *PIK* transcripts accumulate during daylight hours with a peak at dusk, while under LD conditions *PIK* transcripts experience a peak that is shifted eight hours, suggesting that *PIK* transcript levels reflect how much light a plant experiences (Figure 2.10B and C). We confirmed the SD data by qPCR in a time course experiment where seedlings were grown in SD conditions for seven days and then sampled every four hours over the course of a day, beginning at dawn. As expected, *PIK* mRNA in Col-0 (CLT; Col-0 *toc1::LUC*) increased steadily during the light period with a peak at dusk and then declined during the dark period (Figure 2.11). Interestingly, *PIK* mRNA levels were increased in *phyA-211*, although the pattern remained the same. No change was observed in *phyB-9*. The above data suggests that

PIK is regulated by light (but not the circadian clock), that *PIK* transcript accumulation reflects daylength, and that phyA represses *PIK* expression.

To further investigate the finding that phyA regulates *PIK* expression we generated 35S::*PIK* overexpression lines in *phyA-211*. *PIK* mRNA and protein accumulation is higher in the *phyA-211* background than in Col-0 or *phyB-9* (Figure 2.12). Interestingly, in the *phyA-211* background *PIK* overexpression results in hypersensitivity to Rc (Figure 2.13), WLc (data not shown), and Bc (data not shown). Overexpression of *PIK* in a *phyB-9* background resulted in no hypersensitive phenotype (data not shown).

The reciprocal regulation between PIK and phyA led us to check for a genetic interaction between the two. We generated the *pik-1 phyA-211* double mutant and tested for defects in inhibition of hypocotyl elongation. As reported previously, *phyA-211* exhibits shorter hypocotyls than Col-0 when grown under Rc [21]. While *pik-1* has long hypocotyls under Rc, *pik-1 phyA-211* double mutants exhibit hypocotyls that resemble *phyA-211* (Figure 2.14). This suggests *phyA-211* is epistatic to *pik-1*, and that a functional phyA is required for the *pik-1* phenotype.

Discussion

We have shown that PIK interacts with phytochrome, is a positive regulator of phytochrome signaling, and is involved with regulation of *PHYA* mRNA. We considered several possibilities for PIK function in phytochrome signaling. First, PIK may be involved in nuclear retention of, at least, phyA. It has been shown directly that nuclear localization is required for phyB function [22] and there is reason to believe

this is the case for phyA, as mutants that affect phyA nuclear retention are impaired in the phyA-mediated phytochrome response [23]. If PIK functions in nuclear retention, loss of PIK function would manifest itself as hyposensitivity in seedlings. This model could also explain the delay in reduction of *PHYA* mRNA in *pik-1*, as phyA and phyB are required for downregulation of *PHYA* mRNA [19]. The relatively weak phenotype of *pik-1*, in terms of both inhibition of hypocotyl elongation and *PHYA* mRNA reduction, suggests that additional factors play a role in phytochrome import and retention. In the case of phyA, FHY1 and FHL are required for nuclear accumulation of phyA [23]. To test this model, we crossed *pik-1* to a *phyA-211 phyA::phyA:GFP* line [24] to generate a *pik-1 phyA-211* double mutant containing a phyA:GFP fusion protein under control of its own promoter. Using this line, we observed that the *pik-1* mutation does not affect the ability of phyA:GFP to form NBs under FRc (data not shown). We are currently investigating whether the kinetics of phyA NB formation or disappearance are affected in *pik-1*. We are also generating a *pik-1 phyB-9 phyB::phyB:GFP* line to study the effect of *pik-1* on phyB nuclear import and NB formation. This work is in progress.

A second model for PIK function centers around direct regulation of *PHY* mRNA. We have shown that the reduction of *PHYA* mRNA is delayed in *pik-1* seedlings exposed to light. It is not intuitive why an impairment in *PHYA* mRNA reduction would manifest itself as hyposensitivity in *pik-1* seedlings exposed to Rc and FRc. However, it has been shown that antagonism exists between the phyA and phyB signaling pathways [21]. phyA has been shown to mediate the early stages of phy-mediated Rc signaling [25]. PIK is involved in the downregulation of *PHYA*

mRNA (Figure 2.9) and in its absence phyA is present during the time when Rc signaling transitions from phyA- to phyB-mediated (Figure 2.7). Presence of phyA at this time may impair phyB signaling due to competition for shared signaling components. It is also not intuitive why persistence of phyA would also impair phyA-mediated FRc signaling, though it is interesting to note that *PHYA* mRNA is reduced upon exposure to both FRc and Rc [19]. Further, while FRc is more effective than hourly FR pulses (FRp) in initiating cotyledon unfolding in etiolated seedlings, phyA levels are reduced significantly more under FRc than by hourly FRp [26]. Finally, the FRc-hyposensitive *Arabidopsis* Lm-2 accession contains a *PHYA* allele with a single amino acid polymorphism relative to Col-0, the result of which is enhanced stability of phyA in the light [27]. Together, these data suggest that degradation of phyA may be required for its activity.

PIK is a member of a seven-member gene family in *Arabidopsis*. As mentioned above, the seven family members exhibit a high degree of identity at the amino acid level. That *pik-1* has a subtle phenotype suggests that it is involved in fine-tuning a process rather than having a major role in phytochrome signaling. It is also possible that family members are partially functionally redundant. We have observed no defects in inhibition of hypocotyl elongation in individual family members. Interestingly, PKR2 was identified in a proteomic screen for phyB protein complexes in etiolated *Arabidopsis* seedlings, though it did not retest as a direct phyB interactor in co-immunoprecipitation experiments in tobacco (K. Nito and J. Chory, unpublished data). We also have data showing that PKR1, PKR3, and PKR5 localize to the nucleus in *Arabidopsis* as YFP fusion proteins under control of a constitutive UBQ10

promoter (Figure 2.18). *PKR3*, *PKR4*, and *PKR6* appear to have arisen due to a gene duplication event(s) on chromosome 3. This arrangement makes generation of the septuple mutant to test redundancy unfeasible. Therefore, in an effort to assess functional redundancy among the family members, we employed artificial microRNA (amiRNA) technology to simultaneously knock down expression of several family members [28]. We have generated three different lines: two lines (amiRNA8 and amiRNA11) use different amiRNAs to target *PKR3* and *PKR4*, while the third line (amiRNAD) targets *PKR1*, *PKR3*, *PKR4*, *PKR5*, and *PKR6*. Together with a collection of T-DNA insertion mutants in remaining family members, plants expressing amiRNAs should allow us to address the role of *PIK* family members, and functional redundancy within the family, in phy signaling. Preliminary results suggest that transcript levels of targeted genes are reduced (Figure 2.19). However, no phenotypes were observed in T1 plants grown on plates under BASTA selection, or in T2 plants grown on soil. We are still awaiting one T-DNA insertion line from the GABI-Kat collection (http://www.gabi-kat.de/) that would be necessary to generate the "septuple mutant".

We performed a yeast two-hybrid screen with PIK to identify interacting proteins in hopes of gaining insight into PIK function. We identified six putative interacting proteins: At1g75440, UBIQUITIN CONJUGATING ENZYME 16; At1g71020, U-box domain containing protein; At1g17360, COP1-interacting protein-related; At2g38470, WRKY33 transcription factor; At2g44100, GDP DISSOCIATION INHIBITOR 1; and At1g10170, homologue of the human transcriptional repressor NF-X1 (Table 2.1). Only At1g10170 retested positive as a

full-length protein in yeast two-hybrid experiments with PIK (Figure 2.15). This protein has been identified as an *Arabidopsis* homolog of the human transcriptional repressor NF-X1 [29]. NF-X1 binds to the conserved X-box motif of class II MHC genes and in co-transfection experiments reduces transcription of a reporter construct containing an X-box binding site [30]. Mutations in the homologous gene in *Drosophila* (*shuttle craft*; *stc*) are embryo lethal, as mutant embryos lack the peristaltic muscle contractions required to hatch from the egg case [31]. In yeast, the NF-X1 homologue FAP1 binds the rapamycin target FKBP12, competing with rapamycin for FKBP12 binding [32]. In *Arabidopsis*, *AtNFXL1* is required for growth under both salt stress [29] and heat stress [33]. More recently, *AtNFXL1* was shown to be a negative regulator of the SA-dependent defense response to trichothecene phytotoxins [34].

The presence of a RING motif in AtNFXL1 as predicted by the SMART domain prediction program (http://smart.embl-heidelberg.de/) suggests that AtNFXL1 could possess E3 ubiquitin ligase activity, with PIK potentially functioning as an adaptor. Indeed, a Kelch repeat-containing protein has been shown to act as an adaptor between a transcription factor and its cognate E3 [35]. However, it should be noted that the RING domain of AtNFXL1 has also been classified as a PHD domain, a zinc-binding domain with structural similarity to RING domains [36]. PHD domains are commonly found in nuclear proteins that interact with chromatin, and have not been found to possess E3 ligase activity. Additionally, no ubiquitin E3 ligase activity has been attributed to NF-X1 or its homologs in *Drosophila*, yeast or *Arabidopsis*. While AtNFXL1 does contain the aromatic residue two amino acids before metal ligand 7 and amino acid spacing between metal ligands 4 and 5 that are characteristic of PHD

domains, the spacing between metal ligands 6 and 7 is more similar to that of the defined RING variant domain than the PHD (Figure 2.16). Further experiments are needed to address possible AtNFXL1 ubiquitination activity.

We tested whether AtNFXL1 could function as a transcriptional repressor using a yeast repression assay where proteins are fused to LexA and tested for their ability to repress expression of *lacZ* fused downstream of LexA operators [37]. While preliminary experiments showed that AtNFXL1 possessed transcriptional repression activity, subsequent experiments showed no significant repression activity (data not shown). While these results suggest that AtNFXL1 is not a transcriptional repressor, lack of repression activity could be attributable to any one of a number of problems with in vitro assays: fusion to LexA, lack of required cofactor, or absence of plant-specific post-translational modification.

An *AtNFXL1* KO line exhibited no defects in inhibition of hypocotyl elongation in Rc. We also tested phyA degradation in the *AtNFXL1* KO line. Compared to Col-0, phyA degradation is unchanged in the *AtNFXL1* KO line. AtNFXL1 has a closely related family member that may provide functional redundancy in the absence of AtNFXL1, thus leaving open the possibility that AtNFXL1 functions in phytochrome signaling.

Nonetheless, as a putative transcriptional repressor, AtNFXL1 fits the role that would be required in a repressor model where PIK regulates *PHYA* mRNA (Figure 2.17). In the dark, phyA is localized in the cytoplasm and phyA protein levels and *PHYA* mRNA levels are high. Upon light absorption, phyA translocates to the nucleus where it interacts with PIK, located constitutively in the nucleus. *PHYA* transcription

is reduced through the activity of a transcriptional repressor, whose activity is modulated by interaction with a PIK/phyA complex. As phyA is degraded and phyB enters the nucleus, phyB assumes the role of phyA in the complex. A similar model involves removal of a transcriptional activator by a PIK/phyA complex in response to light. PIK was recently identified in a yeast two-hybrid screen with a senescence-specific transcription factor, WRKY53 [7]. PIK reduces the ability of WRKY53 to bind DNA in vitro, demonstrating that PIK is able to modulate DNA-binding capacity and suggesting that WRKY53 is a candidate for the transcription factor in the activator model. We are currently investigating the role of WRKY53 in phytochrome signaling. Both of these models provide testable hypotheses. From a biochemical perspective, one could test whether AtNFXL1 or WRKY53 bind the *PHYA* promoter, and whether PIK can modulate this binding. AtNFXL1 or WRKY53 might also be expected to interact with phyA, and could be targets of phytochrome kinase activity. The absence of a phenotype in Col-0 seedlings overexpressing *PIK* is consistent with this model, as phyA levels in dark grown tissue are sufficiently high to compensate for high PIK levels. However, why *PIK* overexpression in *phyA-211* results in hypersensitivity is unclear. Perhaps in the absence of phyA, PIK is free to interact with phyB outside the context of transcriptional regulation of *PHYA*.

Materials and Methods

Yeast two-hybrid assays Yeast two-hybrid assays were performed using the MATCHMAKER LexA Two-Hybrid System (Clontech) according to manufacturer instructions. Primers used for cloning are as follows: At2g44100: 5080 (5'-gcaattccatATGGATGAAGAGTACGAAG-3') and 5081 (5'-ggaattcTCATTCCTCCTCTGCAGCAC-3'); At1g10170: 5102 (5'-gcaattccatATGAGCTTTCAAGTCAGGCG-3') and 5103 (5'-tcccccgggTCACTCACATACCTTCTC-3'); At2g38470: 5104 (5'-gcaattccatATGGCTGCTTCTTTTCTTAC-3') and 5105 (5'-ggaattcTCAGGGCATAAACGAATCG-3'); At1g75440: 5082 (5'-gcaattccatATGTCAAGTTCTGGTGCTCC-3') and 5083 (5'-ggaattcTTATACTTTATCGTCGTGG-3'); At1g71020: 5084 (5'-gcaattccatATGGCTGGTGGAGCTATCAC-3') and 5085 (5'-ggaattcTTAGAGTGAACCTAATTTTCG-3'); At1g17360: 5100 (5'-gcaattccatATGAAGGCTGATACTGTTC-3') and 5101 (5'-cgggatccCTAAGACCCTAATGAAGCTG-3'); At1g54040: 5091 (5'-gcaattccatATGGCTCCGACTTTGCAAGGCC-3') and 5090 (5'-ggaattcTTAAGCTGAATTGACCGCATAG-3'); At1g09570: 8629 (5'-ccatggACAAGGAGTTTACCTTG-3') and 8630 (5'-ctcgagCTACTTGTTTGCTGCAGC-3').

In vitro pull down assay Expression and induction of phytochromes was performed as described [38]. PIK was amplified with primers LS119 (5'-ACTTATATTGATATCATGGCTCCGACTTTGCAAGGCCAG-3') and LS120 (5'-

ACACAAATCTTGACTCGAGTTAAGCTGAATTGACCG-3') and cloned into the *in vitro* transcription and translation vector pCMX-PL1 (a gift from Dr. Ron Evans) as an EcoRV/XhoI fragment. Proteins were separated on 4-20% 1.0 mm Novex Tris-glycine gels (Invitrogen). Gels were fixed, and incubated with Enlightning (Perkin-Elmer) for 15-30 minutes prior to drying. Gels were dried using a Bio-Rad gel dryer (model) and developed on a Fuji phosphorimager.

PIK overexpression and CFP lines An RGS-His tag was added to the PIK coding region by PCR. PIK-RGS-His was subcloned into binary vector pCHF3 [39]. For nuclear localization, PIK coding region was subcloned into pCHF3 containing the CFP coding region.

Seed Sterilization *Arabidopsis* seeds were sterilized by washing 10 min with 1 mL 70% EtOH containing 0.05% [v/v] Triton X-100, followed by washing 5 min with 1 mL 95% EtOH. Seeds were dried on Whatman filter paper, plated on 1/2 x Linsmaier and Skoog (Caisson Laboratories, Inc.) plates containing 0.8% agar and stratified in the dark for 3 to 4 d at 4°C.

Microscopy Confocal microscopy was performed using a Leica TCS SP2 AOBS confocal laser scanning microscope and a HCX PL APO 63X 1.2-numerical-aperture water-immersion objective lens (Leica Microsystems, Mannheim, Germany). 4-day old seedlings were mounted in water. GFP fluorescence was monitored using a 460 nm - 480 nm band pass emission and 488 nm excitation line of an Ar laser.

T-DNA Genotyping Genomic DNA was extracted using Edwards Buffer [40]. *pik-1* T-DNA lines was genotyped using T-DNA primer LB18 (5'-GGCAATCAGCTGTTGCCCGTCTCACTGGTG-3') and the following gene-specific

primers: 5339 (5'-AAATATTTTAGTCGTTGCGGGA-3') and 5340 (5'-ATGTTATATTTGTTGGTAAACAT-3').

Hypocotyl Measurements Seeds were surface sterilized as above, plated on 1/2 x Linsmaier and Skoog (Caisson Laboratories, Inc.) plates containing 0.8% agar, and stratified in the dark for 3 to 4 d at 4°C. Germination was induced by 3 hr of WLc. For hypocotyl measurements, seedlings were grown at 22°C in a light-emitting diode (LED) chamber (Percival Scientific) under indicated fluence rates for 4 d. Fluence rates were measured with a LiCor LI-1800 spectroradiometer (LiCor). Seedlings were scanned and hypocotyls measured using NIH Image (http://rsb.info.nih.gov/nih-image/) or ImageJ (http://rsbweb.nih.gov/ij/).

Flowering time experiments Seedlings were surface-sterilized using ethanol. Seedlings were imbibed in water and stratified for 4 days in the dark at 4°C. Seedlings were resuspended in 0.1% agarose and distributed on soil (Company). Seedlings were grown under short-day (SD) or long-day (LD) conditions. SD conditions consist of 8 h light:16 h dark with 79.75 μE light intensity. LD conditions consist of 16 h light:8 h dark with 72.04 μE light intensity. Plants were considered to have flowered in LD when the primary inflorescence reached 1 cm.

Western Blots Seeds were surface sterilized as above and plated directly plated on 1/2 x Linsmaier and Skoog (Caisson Laboratories, Inc.) plates containing 0.8% agar, and stratified in the dark for 3 to 4 d at 4°C. Germination was induced by 3 h WLc and seedlings were grown in light conditions as described in text. Seedlings were harvested, immediately frozen in liquid N_2 in 1.5 mL tubes containing three metal bearings, and stored at –70°C until protein extraction. Samples were disrupted by

shaking for 90 s at 29 vibrations s^{-1} in a MM 300 Mixer Mill (Retsch, Germany). 5X SDS sample buffer was added to each sample on a per weight basis. Tubes were vortexed, heated for 3 min at 95°C, and then spun at 14,000 rpm for 3 min in an Eppendorf 5417C centrifuge (Eppendorf). Proteins were resolved on 4-20% SDS-PAGE gels (Invitrogen) and transferred to nitrocellulose. Nitrocellulose membranes were blocked in blocking buffer (1X PBS, 5% [w/v] nonfat dry milk, .01% [v/v] Tween-20) for 30-60 min, and incubated overnight in blocking buffer containing antibodies. Membranes were washed three times in blocking buffer, 5 min each. Membranes were incubated in blocking buffer containing anti-mouse HRP secondary antibodies (BioRad) for 1-4 h, and washed in blocking buffer minus milk as above. Proteins were visualized using SuperSignal West Pico Chemiluminescent Substrate (Thermo Scientific).

Cycloheximide treatment Seedlings were grown for four days on 60 x 15 mm round plates (Fisher) in the dark. 90 min prior to light exposure, plates were flooded with 10 mL of either 0.5 μM cycloheximide or a mock water treatment.

qPCR Analysis qPCR was performed using RNA extracted from seedlings sterilized and stratified as above, and grown as indicated. Total RNA was isolated from using the Spectrum Plant Total RNA Kit (Sigma) according to manufacturer instructions. cDNA was synthesized from 5 μg total RNA using the Superscript III First Strand cDNA Synthesis Kit (Invitrogen) according to manufacturer instructions. qPCR was performed using SYBR Green and the iCycler iQ Real-Time PCR Detection System (Bio-Rad). A standard curve was constructed for each primer using an equal mixture of all cDNAs. PCR reactions were performed in triplicate. Primers were as follows:

At1g02340 (*PHYA*): 11389 (5'-GTCAGCTAACTGTTTCAGCTTCCC-3') and 11390 (5'-CAGAACGCCCGAGCTGAT-3'); At1g54040 (*PIK*): 11546 (5'-CAATCGCTCAACCCAAAGGA-3') and 11547 (5'-GCACGCCTAAGCAGGATACAGT-3'); At3g16400 (*PKR3*): 8541 (5'-TCATCCTATCGAAAAAAGACCTG-3') and 8542 (5'-CCCCAAGGGAGTGTAAAACATCT-3'); At5g15400 (*U-Box*) was used to normalize values: 3652 (5'-TGCGCTGCCAGATAATACACTATT-3') and 3653 (5'-TGCTGCCCAACATCAGGTT-3').

PIK family member subcellular localization We obtained ORF clones of PKR1, PKR3, and PKR5 from ABRC (http://www.biosci.ohio-state.edu/pcmb/Facilities/abrc/). These were recombined into pNIGEL7, a UBQ10 promoter-driven YFP plasmid (a gift from Dr. Niko Geldner; http://www.unil.ch/dbmv/page52928_en.html#2) using the Cre-lox system described by Liu et al. [41].

amiRNA cloning amiRNA constructs were generated according to Schwab et al [28] using the following primers: amiRNA8I (5'-gaTTAGTGTATTGAGTCGTGCGGtctctcttttgtattcc-3'), amiRNA8II (5'-gaCCGCACGACTCAATACACTAAtcaaagagaatcaatga-3'), amiRNA8III (5'-gaCCACACGACTCAAAACACTATtcacaggtcgtgatatg-3'), amiRNA8IV (5'-gaATAGTGTTTTGAGTCGTGTGGtctacatatatattcct-3'), amiRNA11I (5'-gaTAAAGACATAGAGGGTCGACCtctctcttttgtattcc-3'), amiRNA11II (5'-gaGGTCGACCCTCTATGTCTTTAtcaaagagaatcaatga-3'), amiRNA11III (5'-gaGGCCGACCCTCTAAGTCTTTTtcacaggtcgtgatatg-3'), amiRNA11IV (5'-

gaAAAAGACTTAGAGGGTCGGCCtctacatatatattcct-3'), amiRNADI (5'-gaTTGTTTCCCAATAGGCGCACTtctctctttgtattcc-3'), amiRNADII (5'-gaAGTGCGCCTATTGGGAAACAAtcaaagagaatcaatga-3'), amiRNADIII (5'-gaAGCGCGCCTATTGCGAAACATtcacaggtcgtgatatg-3'), and amiRNADIV; (5'-gaATGTTTCGCAATAGGCGCGCTtctacatatatattcct-3'). PCR products were cloned into pCR-Blunt II-TOPO (Invitrogen) according to manufacturer instructions, sequence verified, and subcloned into pBJ36-35S (a gift from Dr. Jeff Long), placing the amiRNA precursor downstream of the constitutive 35S promoter. A NotI fragment containing the 35S promoter and amiRNA precursor was then subcloned into the binary vector pMLBART (a gift from Dr. Jeff Long). *pik-1* plants were used in *Agrobacterium*-mediated transformation.

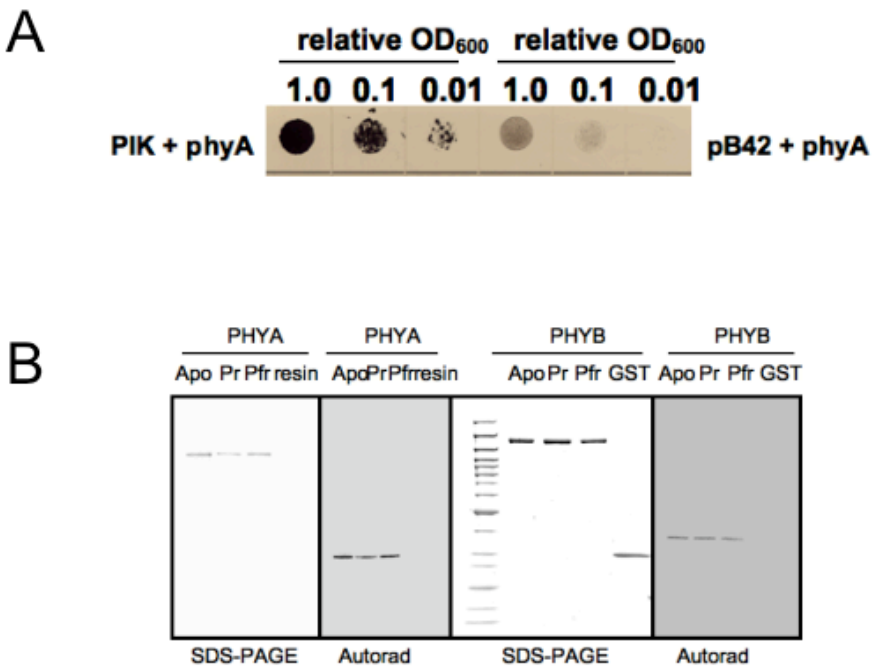

Figure 2.1. PIK interacts with phyA and phyB.
(**A**) Yeast two-hybrid experiment showing interaction between PIK and the C-terminus of phyA. Interaction is scored as the ability to grow on dropout media. Empty vector controls are shown at right. (**B**) phyA and phyB purified from yeast as GST fusion proteins were used to pull down *in vitro* transcribed and translated PIK. Pull-downs were performed with phytochrome minus chromophore (apo-protein, apo) or with phytochrome in Pr or Pfr conformation.

A

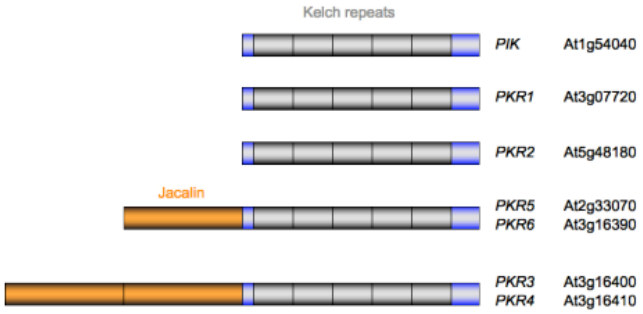

B

	PIK	PKR1	PKR2	PKR3	PKR4	PKR5	PKR6
PIK	*	*	*	*	*	*	*
PKR1	47.3	*	*	*	*	*	*
PKR2	48.7	54.5	*	*	*	*	*
PKR3	40.5	37	37.4	*	*	*	*
PKR4	30.1	27.2	27.8	70.9	*	*	*
PKR5	40.2	37.5	36.7	81.1	61	*	*
PKR6	40.7	35.5	35.8	89.6	65.1	78.8	*

Figure 2.2. PIK is a Kelch repeat protein.
(**A**) PIK contains 5 Kelch repeats and is a member of a seven gene family. (**B**) Amino acid identity among PIK and PIK family members.

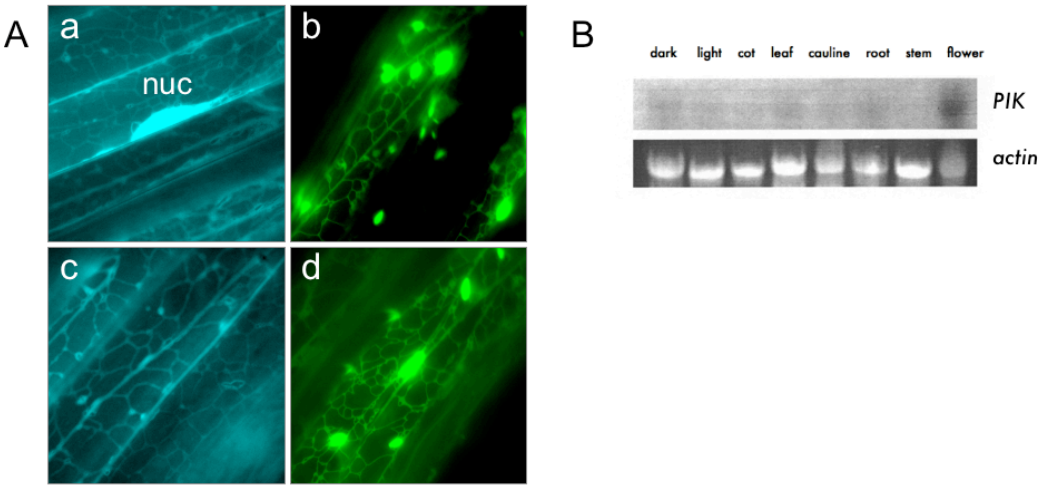

Figure 2.3. PIK is localized to the nucleus and ER.
(**A**) PIK is localized to the nucleus and ER. PIK:CFP proteins were overexpressed in *Arabidopsis* using the 35S promoter (a and c). ER-GFP control (b and d). nuc, nucleus. (**B**) Northern blot showing *PIK* expression in tissues indicated.

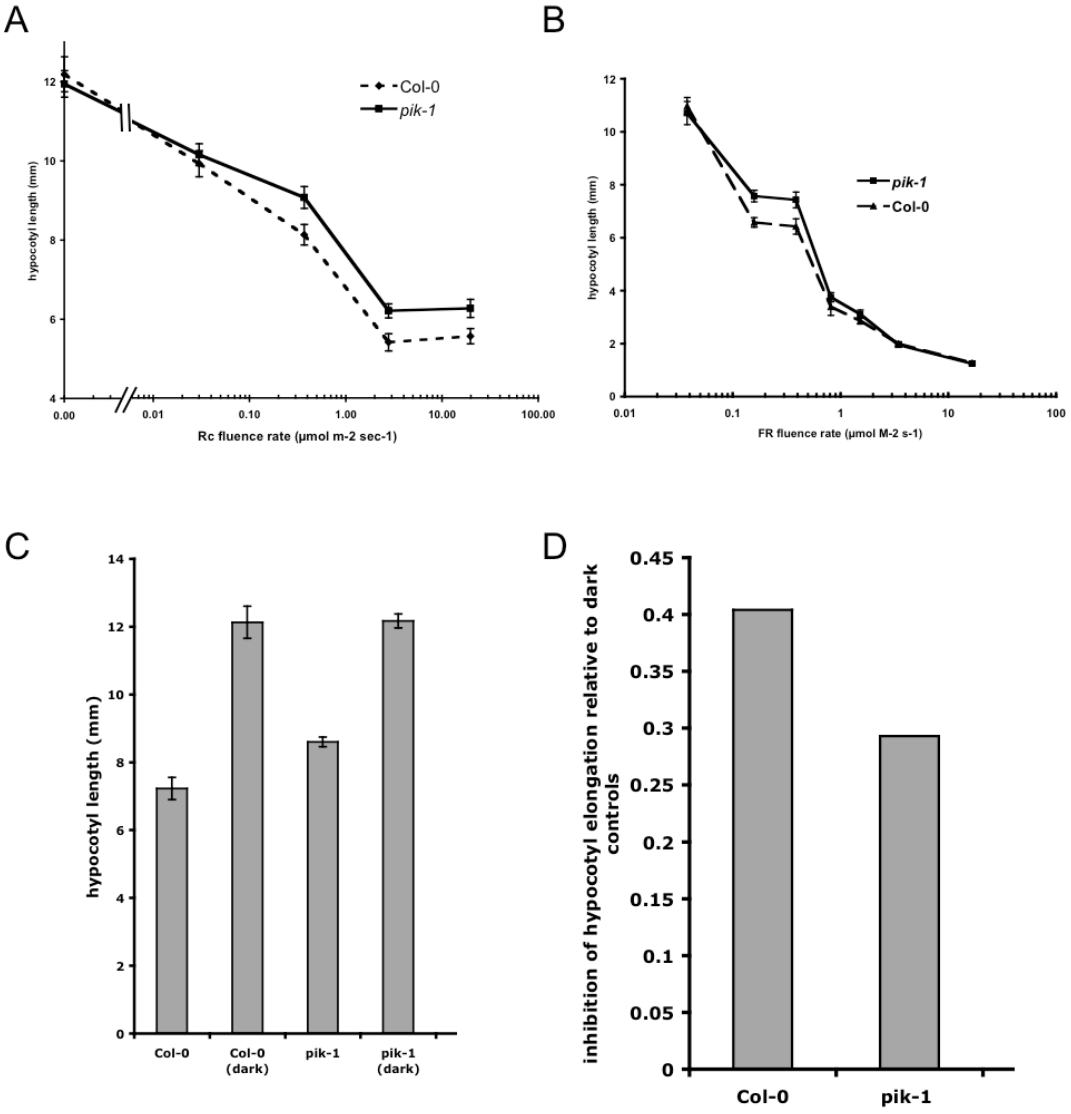

Figure 2.4. Phenotypes of *pik-1*.
Seedlings were grown for 4 days in either Rc (**A**) or FRc (**B**) at the fluence rates shown. Error bars represent standard error of the mean. (**C**) Seedlings were grown for 4 days with 3 min hourly FRp. Error bars represent standard error of the mean. Data plotted relative to dark controls (**D**). (**E**)Flowering time in days. Plants were grown in LD conditions and flowering was measured at onset of bolting.

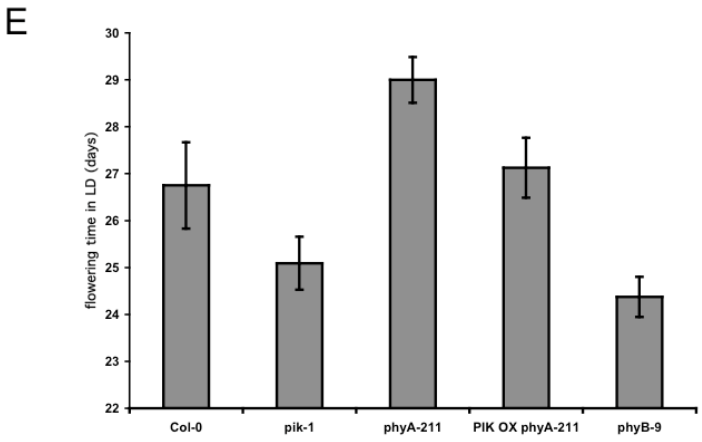

Figure 2.4. continued.

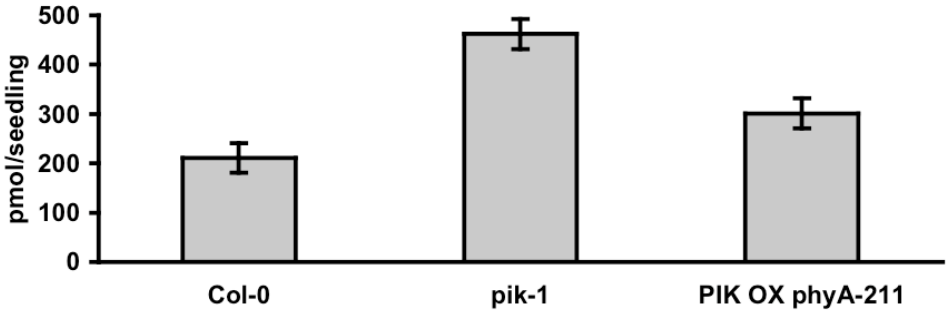

Figure 2.5. Total glucosinolate levels in Rc-grown seedlings.
Seedlings of the genotype indicated were grown for 4 days in Rc. Total glucosinolates were measure by LC-MS as described in Kliebenstein *et al.* [42]. Error bars represent standard error of the mean.

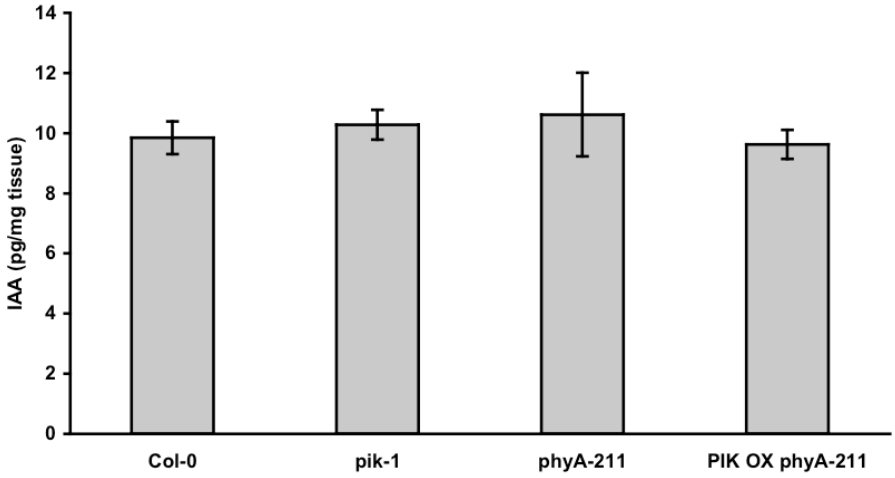

Figure 2.6. Free auxin concentration in Rc-grown seedlings.
Seedlings of the genotype indicated were grown for 4 days in 1 μE Rc. Free auxin (IAA) was measured as described in Ljung *et al*. [43]. Error bars represent standard error of the mean.

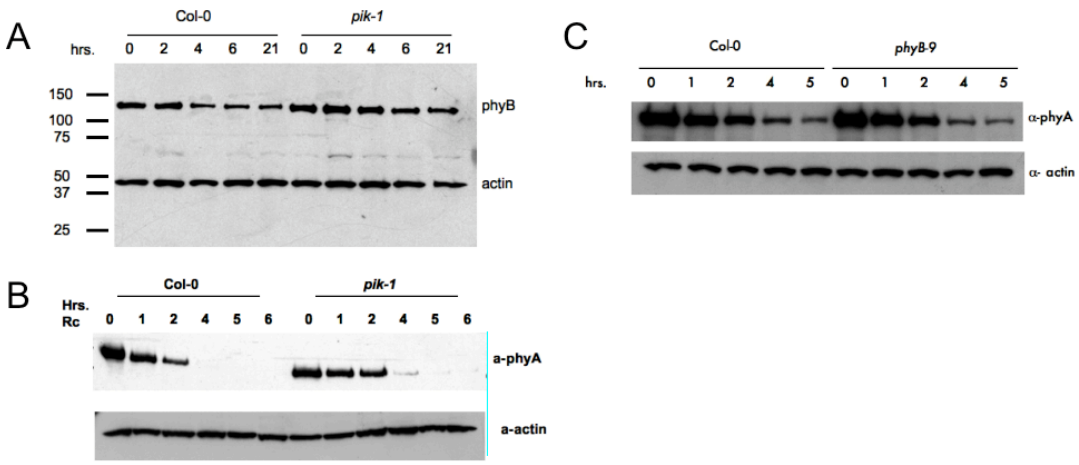

Figure 2.7. *pik-1* mutation results in an increase in phyA levels.
Col-0 and *pik-1* seedlings were germinated and grown for 4 days in the dark before being transferred to 1µE Rc. Seedlings were harvested at times indicated, and proteins were extracted and separated by SDS-PAGE. (**A**) (**B**) Western blots were performed with phyB (**A**) and phyA (**B**) antibodies (gifts from Drs. Peter Quail and Akira Nagatani). Blots were stripped and probed with actin for loading control. (**B**) (**C**) phyA western blot was performed with Col-0 and *phyB-9* seedlings as described above.

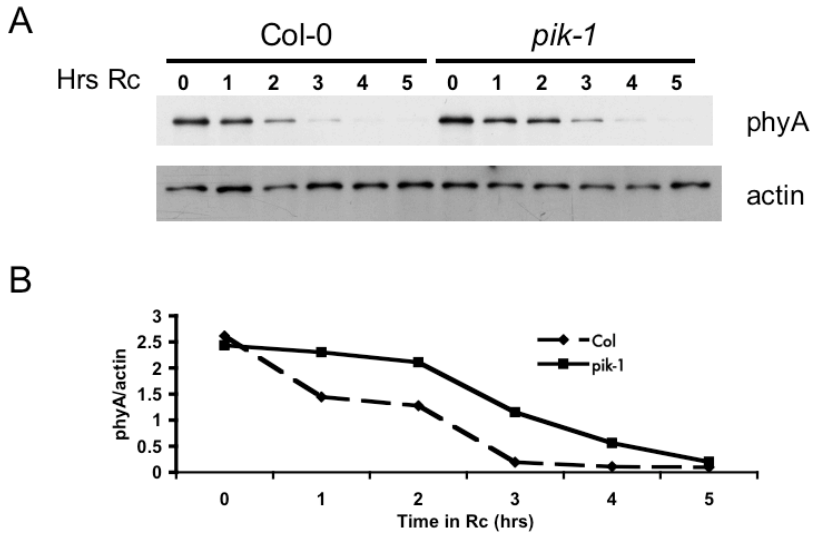

Figure 2.8 Treatment with cycloheximide abrogates the effect of *pik-1* on phyA levels (**A**) phyA western blot was performed, as in Figure 2.7, in the absence of cycloheximide (CHX). (**B**) Quantification of western blot in (A). (**C**) phyA western blot was performed, as in Figure 2.7, in the presence of CHX. Seedlings were treated with 0.5 μM CHX 1.5 hr prior to Rc exposure. (**D**) Quantification of western blot in (C). (**E**) Graph showing the effect of CHX in *pik-1* on phyA levels. Plotted are quantification of phyA levels in Col-0 minus CHX, and *pik-1* in the presence and absence of CHX. Treatment of *pik-1* seedlings with CHX shifts the phyA degradation profile towards that of Col-0 minus CHX.

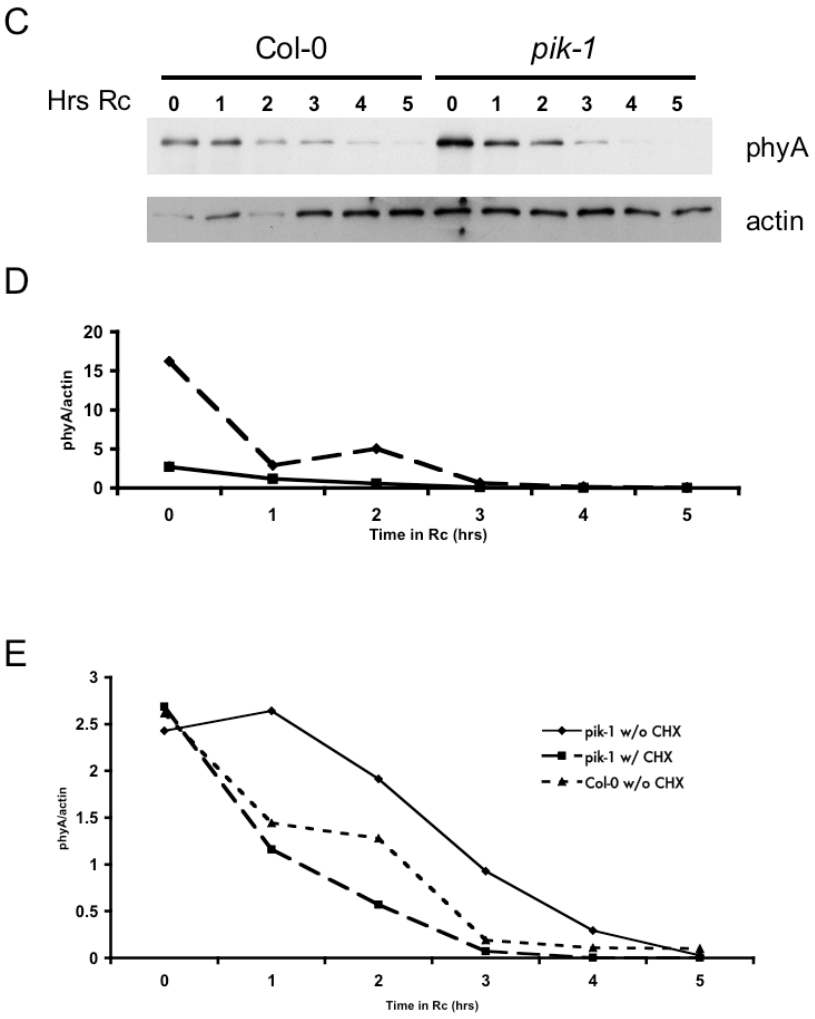

Figure 2.8 continued.

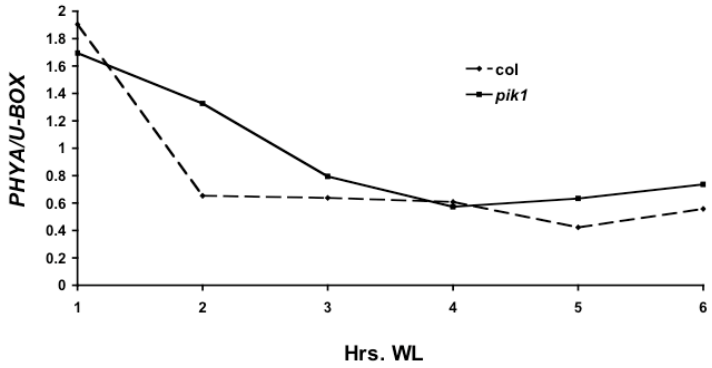

Figure 2.9. Increased phyA levels in *pik-1* result from delayed *PHYA* repression. qPCR was performed on RNA extracted from 7 day-old SD grown seedlings, at times indicated after dawn (lights on). PHYA transcript levels were normalized to a U-box control.

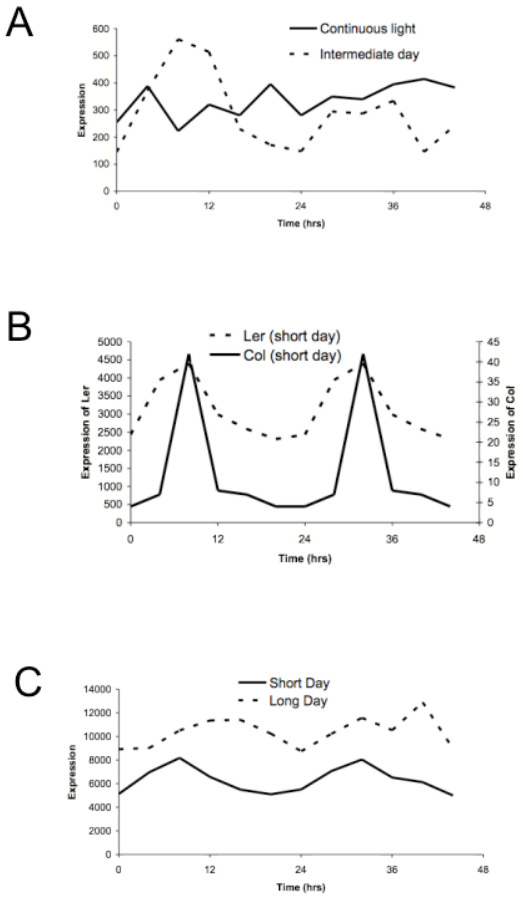

Figure 2.10. Data from DIURNAL microarray database.
(**A**) *PIK* expression in continuous light (solid line) and intermediate day conditions (broken line). (**B**) *PIK* expression in SD in Ler (broken line) and Col (solid line). Note difference in scale. (**C**) PIK expression in SD (solid line) and LD (broken line).

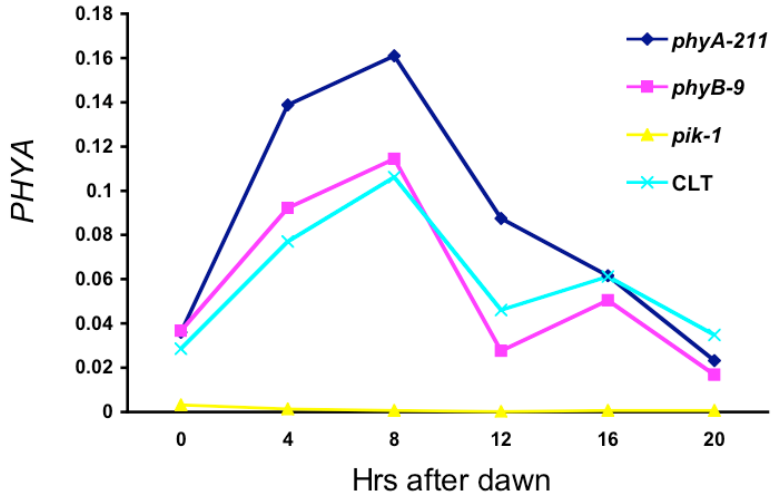

Figure 2.11. *PIK* mRNA is repressed by phyA.
Genotypes indicated were grown for seven days in SD conditions. Tissue was collected every four hours for one day, beginning at dawn (lights on). qPCR was performed on first strand cDNA made from total RNA. CLT (Col-0 *toc1::LUC*).

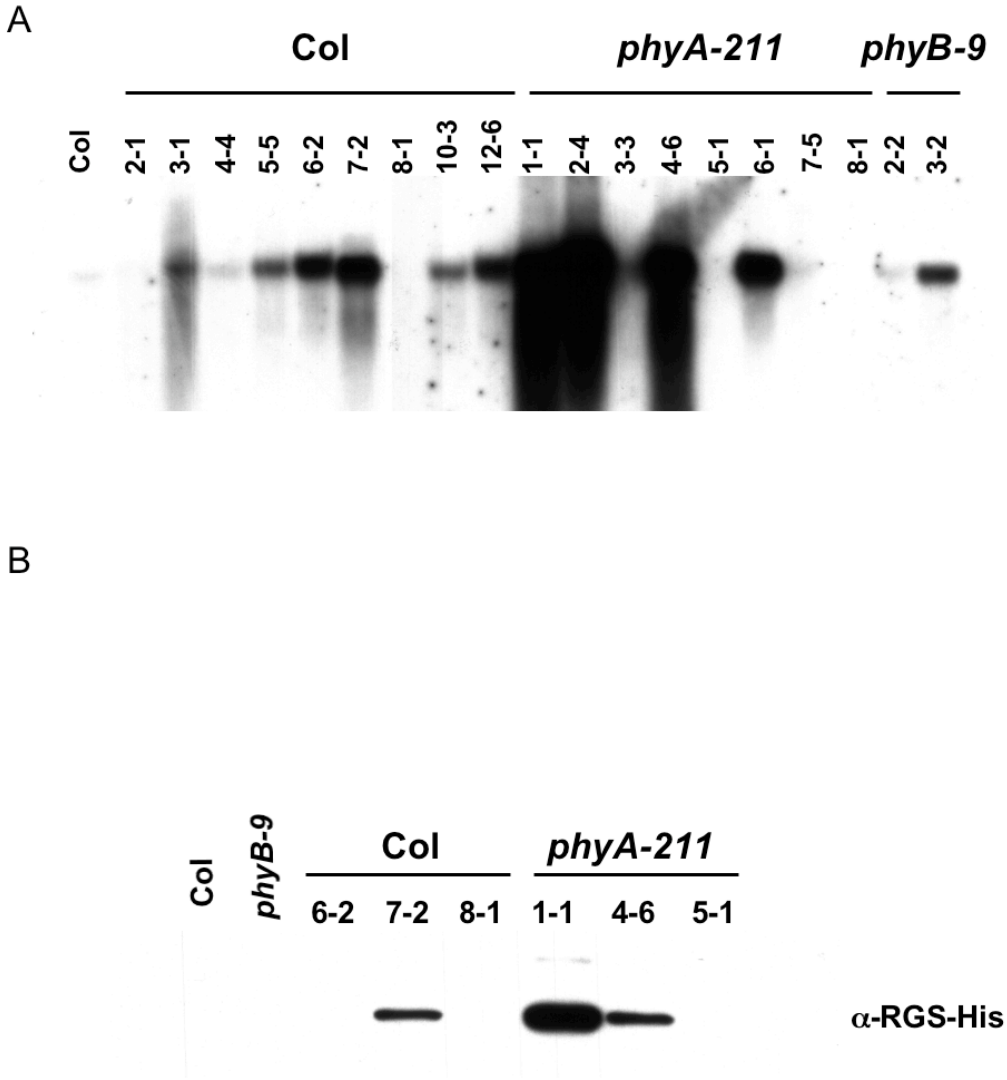

Figure 2.12. *PIK* mRNA and protein accumulation is repressed by phyA.
(**A**) *PIK* northern blot of seedlings expressing a *35S::PIK:RGS-His* transgene. Numbers represent individual lines. (**B**)Western blot of seedlings expressing a *35S::PIK:RGS-His* transgene using an RGS-His antibody (Qiagen).

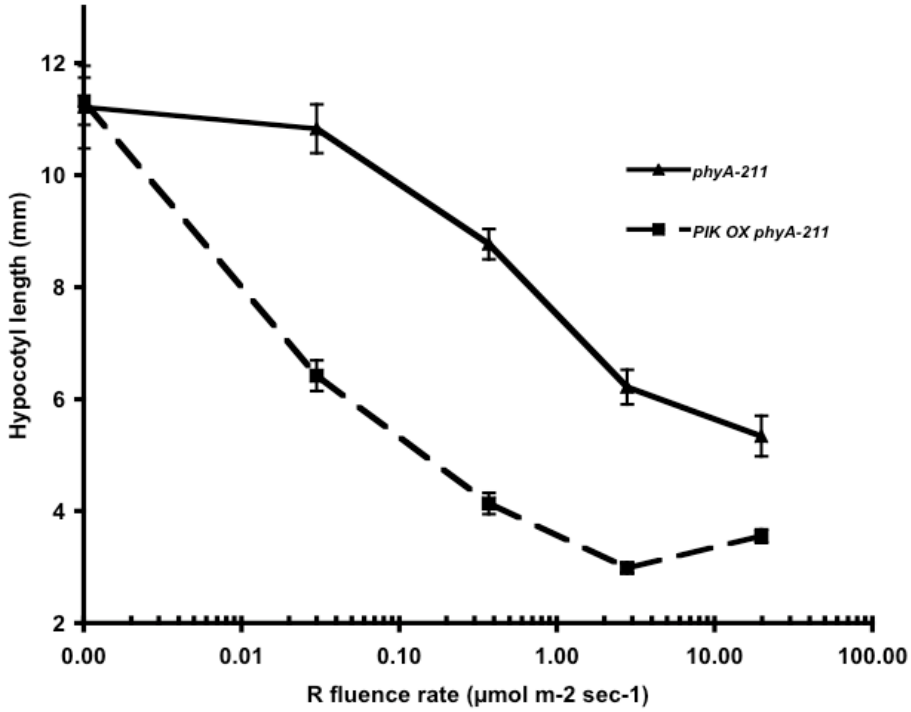

Figure 2.13. Overexpression of *PIK* in *phyA-211* results in hypersensitivity.
Seedlings were grown for four days in Rc at fluence rates indicated. Error bars represent standard error of the mean.

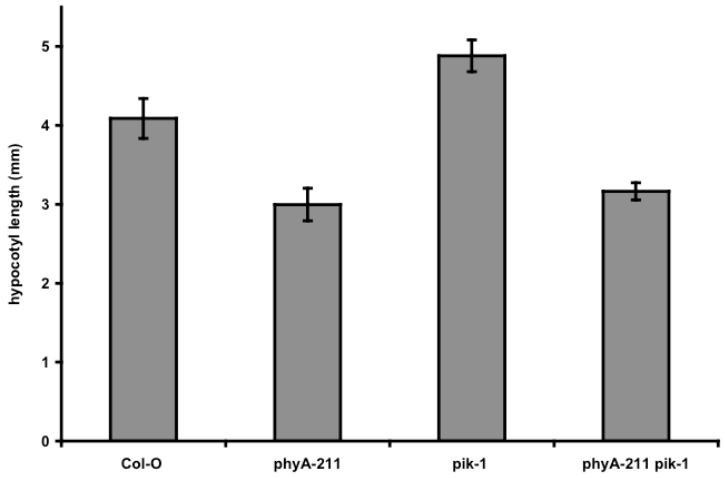

Figure 2.14. The *pik-1* phenotype requires a functional phyA.
Genotypes indicated were grown in 1μE Rc for four days. Error bars represent standard error of the mean.

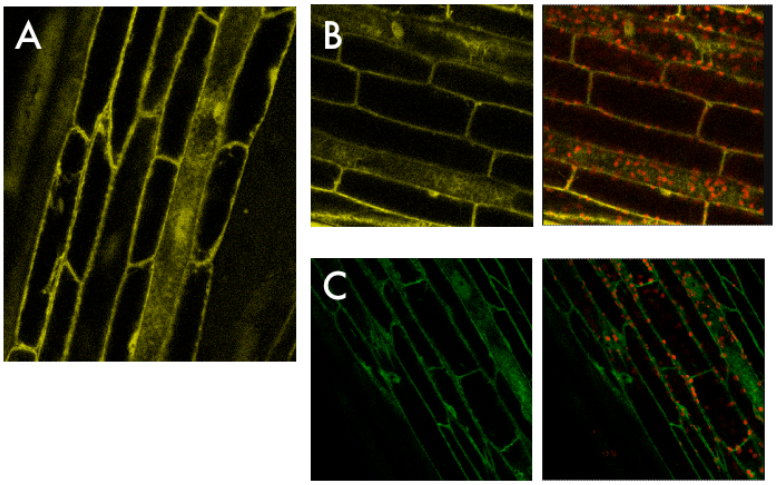

Figure 2.15. PIK family members localize to the nucleus.
Seedlings expressing (**A**) *UBQ10::PKR1:YFP* (**B**) *UBQ10::PKR3:YFP* and (**C**) *UBQ10::PKR5:YFP* were grown in WLc for seven days. Red color indicates chlorophyll autofluorescence.

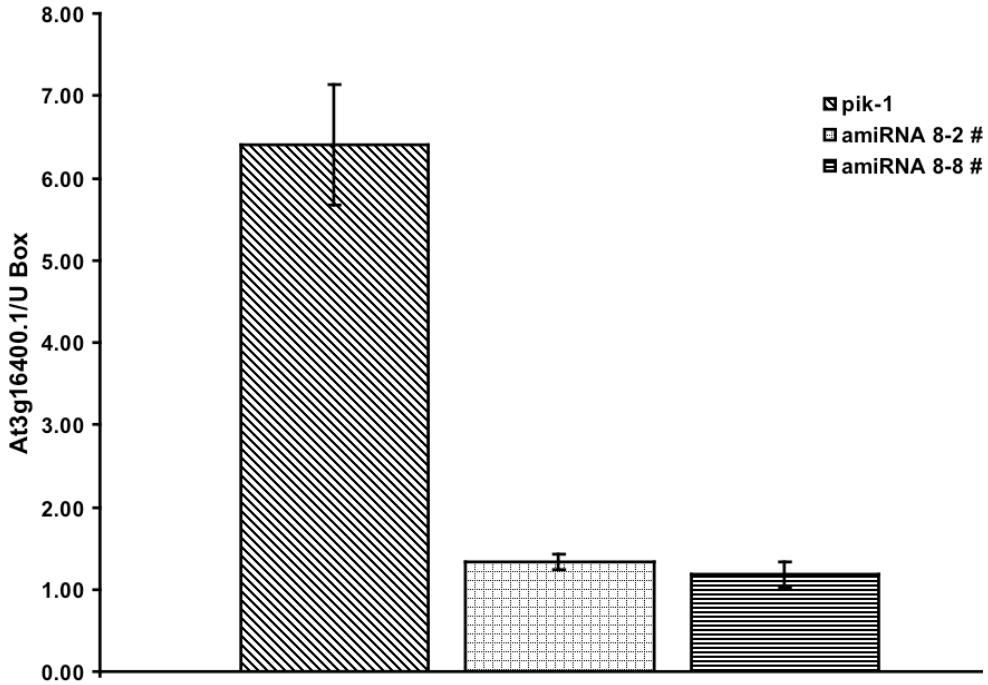

Figure 2.16. Effect of amiRNA8 on target gene expression.
qPCR analysis in seedlings of two lines expressing amiRNA8. At3g16400 is an amiRNA target. Expression is relative to U-box control. *pik-1* parental background is shown as control.

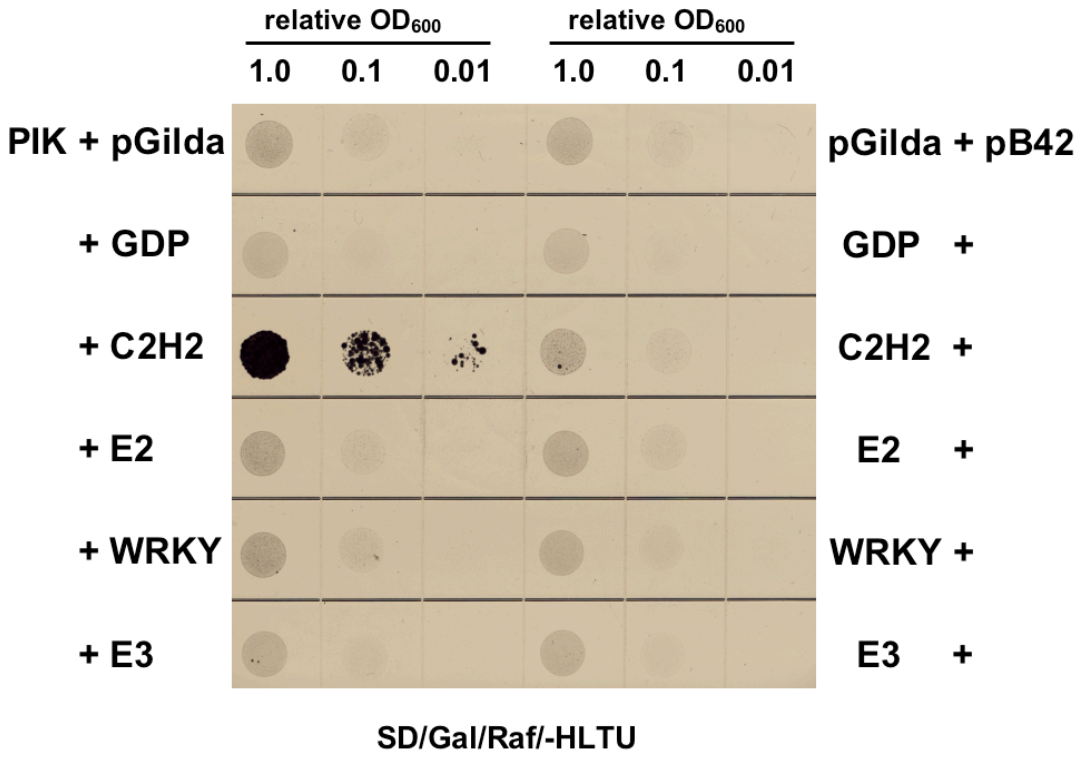

Figure 2.17. PIK interacts with AtNFXL1.
Yeast two-hybrid experiment showing interaction between PIK and full-length putative interactors. Interaction is scored as the ability to grow on dropout media. Empty vector controls are shown at right.

```
C-x(2)  -C-x(9-39) -C-x(1-3) -H-x(2-3) -C-x(2)-C-x(4-48) -C-x(2)-C  RING

C-x(2)  -C-x(10-45)-C-x(1)   -C-x(7)   -H-x(2)-C-x(11-25)-C-x(2)-C  RINGv

C-x(1-2)-C-x(7-13) -C-x(2-4) -C-x(4-5) -H-x(2)-C-x(10-21)-C-x(2)-C  PHD

CMICYDKVGRSANIWSCSSCYSIFHINCIKRWARAPTSVDLLAEKNQGDNWRCPGC            At1g10170

C-x(2)  -C-(12)    -C-x-(2) -C-x-(4)  -H-x-(2)-C-x-(24) -C-x-(2)-C
```

Figure 2.18. AtNFXL1 has features of both RING and PHD domains.
Domain signatures of RING, RING variant (RINGv) and PHD domains compared to AtNFXL1. Adapted from Kosarev *et al.*, 2002. Two features separate RING and PHD domains: the loop between metal ligands 4 and 5 can be up to five residues in PHD domains rather than only up to three in RING domains, in PHD domains the residue two positions in front of metal ligand 7 is an aromatic residue.

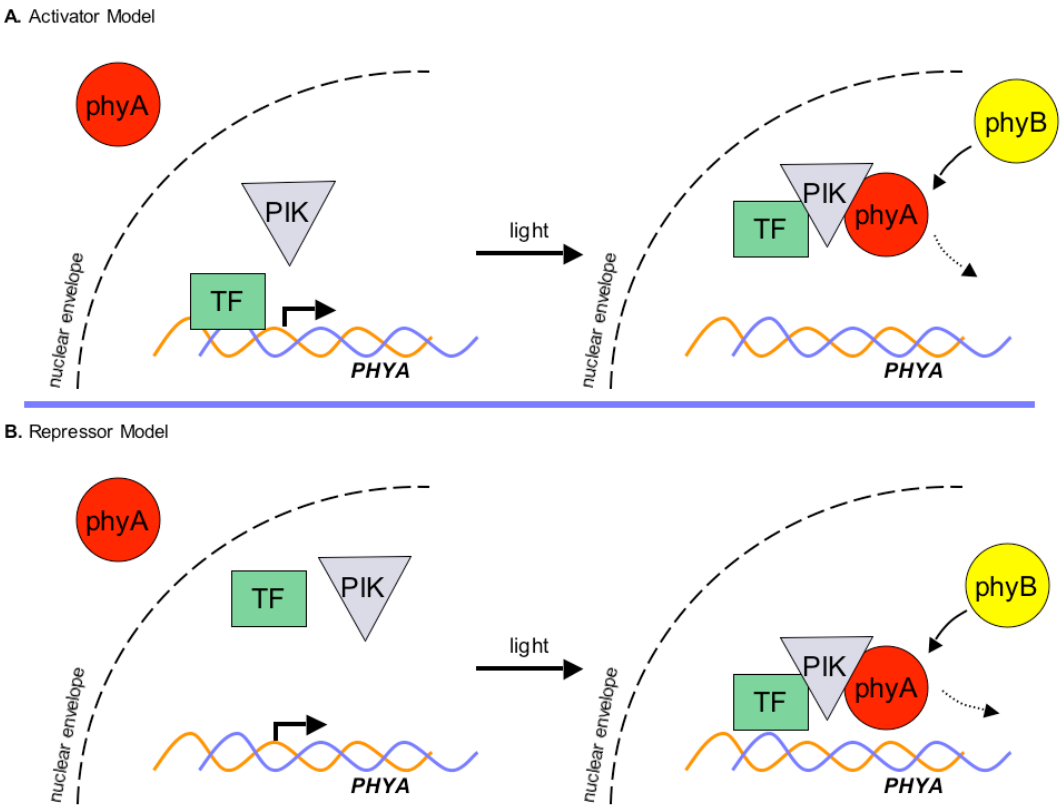

Figure 2.19. Models for PIK function in phytochrome signaling.
PIK can function as part of an activator (**A**) or repressor complex (**B**). PIK is localized constitutively in the nucleus. In the dark phyA is localized outside the nucleus. In (**A**) a transcriptional activator is bound to DNA and phyA mRNA is high in the dark. In (**B**) a transcriptional repressor is not bound to DNA in the dark. In either scenario, PIK may or may not be directly bound to the transcription factor. Upon light absorption phyA travels to the nucleus where it interacts with PIK. In (**A**) phyA/PIK interaction with the transcriptional activator causes release from DNA and termination of transcription. In (**B**) phyA/PIK interaction results in activation of the transcriptional repressor and *PHYA* transcription is repressed. In both (**A**) and (**B**) in the light, phyB replaces phyA upon phyA degradation to maintain activity.

References

1. Ni, M., Tepperman, J.M., and Quail, P.H. (1998). PIF3, a phytochrome-interacting factor necessary for normal photoinduced signal transduction, is a novel basic helix-loop-helix protein. Cell *95*, 657-667.

2. Fankhauser, C., Yeh, K.C., Lagarias, J.C., Zhang, H., Elich, T.D., and Chory, J. (1999). PKS1, a substrate phosphorylated by phytochrome that modulates light signaling in Arabidopsis. Science (New York, N.Y *284*, 1539-1541.

3. Choi, G., Yi, H., Lee, J., Kwon, Y.K., Soh, M.S., Shin, B., Luka, Z., Hahn, T.R., and Song, P.S. (1999). Phytochrome signalling is mediated through nucleoside diphosphate kinase 2. Nature *401*, 610-613.

4. Adams, J., Kelso, R., and Cooley, L. (2000). The kelch repeat superfamily of proteins: propellers of cell function. Trends in cell biology *10*, 17-24.

5. Jander, G., Cui, J., Nhan, B., Pierce, N.E., and Ausubel, F.M. (2001). The TASTY locus on chromosome 1 of Arabidopsis affects feeding of the insect herbivore Trichoplusia ni. Plant physiology *126*, 890-898.

6. Lambrix, V., Reichelt, M., Mitchell-Olds, T., Kliebenstein, D.J., and Gershenzon, J. (2001). The Arabidopsis epithiospecifier protein promotes the hydrolysis of glucosinolates to nitriles and influences Trichoplusia ni herbivory. The Plant cell *13*, 2793-2807.

7. Miao, Y., and Zentgraf, U. (2007). The antagonist function of Arabidopsis WRKY53 and ESR/ESP in leaf senescence is modulated by the jasmonic and salicylic acid equilibrium. The Plant cell *19*, 819-830.

8. Gray, W.M., Ostin, A., Sandberg, G., Romano, C.P., and Estelle, M. (1998). High temperature promotes auxin-mediated hypocotyl elongation in Arabidopsis. Proceedings of the National Academy of Sciences of the United States of America *95*, 7197-7202.

9. Halkier, B.A., and Gershenzon, J. (2006). Biology and biochemistry of glucosinolates. Annual review of plant biology *57*, 303-333.

10. Boerjan, W., Cervera, M.T., Delarue, M., Beeckman, T., Dewitte, W., Bellini, C., Caboche, M., Van Onckelen, H., Van Montagu, M., and Inze, D. (1995). Superroot, a recessive mutation in Arabidopsis, confers auxin overproduction. The Plant cell *7*, 1405-1419.

11. Bak, S., Tax, F.E., Feldmann, K.A., Galbraith, D.W., and Feyereisen, R. (2001). CYP83B1, a cytochrome P450 at the metabolic branch point in auxin

and indole glucosinolate biosynthesis in Arabidopsis. The Plant cell *13*, 101-111.

12. Mikkelsen, M.D., Naur, P., and Halkier, B.A. (2004). Arabidopsis mutants in the C-S lyase of glucosinolate biosynthesis establish a critical role for indole-3-acetaldoxime in auxin homeostasis. Plant J *37*, 770-777.

13. Barlier, I., Kowalczyk, M., Marchant, A., Ljung, K., Bhalerao, R., Bennett, M., Sandberg, G., and Bellini, C. (2000). The SUR2 gene of Arabidopsis thaliana encodes the cytochrome P450 CYP83B1, a modulator of auxin homeostasis. Proceedings of the National Academy of Sciences of the United States of America *97*, 14819-14824.

14. Celenza, J.L., Jr., Grisafi, P.L., and Fink, G.R. (1995). A pathway for lateral root formation in Arabidopsis thaliana. Genes & development *9*, 2131-2142.

15. Delarue, M., Prinsen, E., Onckelen, H.V., Caboche, M., and Bellini, C. (1998). Sur2 mutations of Arabidopsis thaliana define a new locus involved in the control of auxin homeostasis. Plant J *14*, 603-611.

16. Grubb, C.D., Zipp, B.J., Ludwig-Muller, J., Masuno, M.N., Molinski, T.F., and Abel, S. (2004). Arabidopsis glucosyltransferase UGT74B1 functions in glucosinolate biosynthesis and auxin homeostasis. Plant J *40*, 893-908.

17. King, J.J., Stimart, D.P., Fisher, R.H., and Bleecker, A.B. (1995). A Mutation Altering Auxin Homeostasis and Plant Morphology in Arabidopsis. The Plant cell *7*, 2023-2037.

18. Smolen, G., and Bender, J. (2002). Arabidopsis cytochrome P450 cyp83B1 mutations activate the tryptophan biosynthetic pathway. Genetics *160*, 323-332.

19. Canton, F.R., and Quail, P.H. (1999). Both phyA and phyB mediate light-imposed repression of PHYA gene expression in Arabidopsis. Plant physiology *121*, 1207-1216.

20. Michael, T.P., Mockler, T.C., Breton, G., McEntee, C., Byer, A., Trout, J.D., Hazen, S.P., Shen, R., Priest, H.D., Sullivan, C.M., et al. (2008). Network discovery pipeline elucidates conserved time-of-day-specific cis-regulatory modules. PLoS genetics *4*, e14.

21. Mazzella, M.A., Alconada Magliano, T.M., and Casal, J.J. (1997). Dual effect of phytochrome A on hypocotyl growth under continuous red light. Plant, Cell and Environment *20*, 261-267.

22. Huq, E., Al-Sady, B., and Quail, P.H. (2003). Nuclear translocation of the photoreceptor phytochrome B is necessary for its biological function in seedling photomorphogenesis. Plant J *35*, 660-664.

23. Hiltbrunner, A., Tscheuschler, A., Viczian, A., Kunkel, T., Kircher, S., and Schafer, E. (2006). FHY1 and FHL act together to mediate nuclear accumulation of the phytochrome A photoreceptor. Plant & cell physiology *47*, 1023-1034.

24. Hiltbrunner, A., Viczian, A., Bury, E., Tscheuschler, A., Kircher, S., Toth, R., Honsberger, A., Nagy, F., Fankhauser, C., and Schafer, E. (2005). Nuclear accumulation of the phytochrome A photoreceptor requires FHY1. Curr Biol *15*, 2125-2130.

25. Parks, B.M., and Spalding, E.P. (1999). Sequential and coordinated action of phytochromes A and B during Arabidopsis stem growth revealed by kinetic analysis. Proceedings of the National Academy of Sciences of the United States of America *96*, 14142-14146.

26. Casal, J.J., Yanovsky, M.J., and Luppi, J.P. (2000). Two photobiological pathways of phytochrome A activity, only one of which shows dominant negative suppression by phytochrome B. Photochem Photobiol *71*, 481-486.

27. Maloof, J.N., Borevitz, J.O., Dabi, T., Lutes, J., Nehring, R.B., Redfern, J.L., Trainer, G.T., Wilson, J.M., Asami, T., Berry, C.C., et al. (2001). Natural variation in light sensitivity of Arabidopsis. Nat Genet *29*, 441-446.

28. Schwab, R., Ossowski, S., Riester, M., Warthmann, N., and Weigel, D. (2006). Highly specific gene silencing by artificial microRNAs in Arabidopsis. The Plant cell *18*, 1121-1133.

29. Lisso, J., Altmann, T., and Mussig, C. (2006). The AtNFXL1 gene encodes a NF-X1 type zinc finger protein required for growth under salt stress. FEBS letters *580*, 4851-4856.

30. Song, Z., Krishna, S., Thanos, D., Strominger, J.L., and Ono, S.J. (1994). A novel cysteine-rich sequence-specific DNA-binding protein interacts with the conserved X-box motif of the human major histocompatibility complex class II genes via a repeated Cys-His domain and functions as a transcriptional repressor. The Journal of experimental medicine *180*, 1763-1774.

31. Stroumbakis, N.D., Li, Z., and Tolias, P.P. (1996). A homolog of human transcription factor NF-X1 encoded by the Drosophila shuttle craft gene is required in the embryonic central nervous system. Molecular and cellular biology *16*, 192-201.

32. Kunz, J., Loeschmann, A., Deuter-Reinhard, M., and Hall, M.N. (2000). FAP1, a homologue of human transcription factor NF-X1, competes with rapamycin for binding to FKBP12 in yeast. Molecular microbiology *37*, 1480-1493.

33. Larkindale, J., and Vierling, E. (2008). Core genome responses involved in acclimation to high temperature. Plant physiology *146*, 748-761.

34. Asano, T., Masuda, D., Yasuda, M., Nakashita, H., Kudo, T., Kimura, M., Yamaguchi, K., and Nishiuchi, T. (2008). AtNFXL1, an Arabidopsis homologue of the human transcription factor NF-X1, functions as a negative regulator of the trichothecene phytotoxin-induced defense response. Plant J *53*, 450-464.

35. Furukawa, M., and Xiong, Y. (2005). BTB protein Keap1 targets antioxidant transcription factor Nrf2 for ubiquitination by the Cullin 3-Roc1 ligase. Molecular and cellular biology *25*, 162-171.

36. Kosarev, P., Mayer, K.F., and Hardtke, C.S. (2002). Evaluation and classification of RING-finger domains encoded by the Arabidopsis genome. Genome Biol *3*, RESEARCH0016.

37. Keleher, C.A., Redd, M.J., Schultz, J., Carlson, M., and Johnson, A.D. (1992). Ssn6-Tup1 is a general repressor of transcription in yeast. Cell *68*, 709-719.

38. Elich, T.D., and Chory, J. (1997). Biochemical characterization of Arabidopsis wild-type and mutant phytochrome B holoproteins. The Plant cell *9*, 2271-2280.

39. Borevitz, J.O., Xia, Y., Blount, J., Dixon, R.A., and Lamb, C. (2000). Activation tagging identifies a conserved MYB regulator of phenylpropanoid biosynthesis. The Plant cell *12*, 2383-2394.

40. Edwards, K., Johnstone, C., and Thompson, C. (1991). A simple and rapid method for the preparation of plant genomic DNA for PCR analysis. Nucleic acids research *19*, 1349.

41. Liu, Q., Li, M.Z., Leibham, D., Cortez, D., and Elledge, S.J. (1998). The univector plasmid-fusion system, a method for rapid construction of recombinant DNA without restriction enzymes. Curr Biol *8*, 1300-1309.

42. Kliebenstein, D.J., Lambrix, V.M., Reichelt, M., Gershenzon, J., and Mitchell-Olds, T. (2001). Gene duplication in the diversification of secondary metabolism: tandem 2-oxoglutarate-dependent dioxygenases control glucosinolate biosynthesis in Arabidopsis. The Plant cell *13*, 681-693.

43. Ljung, K., Hull, A.K., Celenza, J., Yamada, M., Estelle, M., Normanly, J., and Sandberg, G. (2005). Sites and regulation of auxin biosynthesis in Arabidopsis roots. The Plant cell *17*, 1090-1104.

Chapter 3

Isolation and characterization of *phyB-501* and *phyB-502* hypersensitive alleles

Introduction

On the heels of the discovery that phytochromes translocate to the nucleus in response to light came the observation that phytochromes form sub-nuclear foci, now called nuclear bodies (NBs) [1-3]. Mounting evidence suggests that phytochrome signaling and NB formation are intimately linked, though some data suggests that NB formation is not required for phytochrome signaling [4]. Despite a strong interest in NB function, the role of NBs is still unknown. No purification of NBs has been published, likely due to the large number of phytochrome interactions which make identification of discrete complexes difficult (Kazu Nito and Joanne Chory, unpublished data). In an attempt to define factors required for NB formation, we performed a forward mutagenesis screen using the *35S::phyB:GFP* (PBG) background [5]. This screen identified seedlings with impaired response to continuous red light (Rc) and impaired NB formation. The responsible lesions comprised two classes: intragenic phyB mutations defining residues important for proper phy signaling and NB targeting or formation, and extragenic components that may define factors required for NB formation. In addition to these previously described mutations, we isolated the two hypersensitive alleles presented here. These alleles not only provide further evidence that NBs and phy signaling are closely tied, but the corresponding mutations define residues that couple light perception to signal transduction.

Results

Isolation of *phyB-501* and *phyB-502*

To identify hypersensitive mutants we screened for seedlings with short hypocotyls relative to PBG when grown under dim red light. Seedlings meeting this initial criteria were then analyzed by confocal microscopy for phyB:GFP nuclear localization patterns under the same light conditions as above. We isolated two hypersensitive mutants, both of which exhibited increased phyB:GFP NB formation relative to PBG (Figure 3.1A). Whereas phyB:GFP is evenly distributed in the nucleus (stage I) at this fluence rate, hypersensitive mutants exhibited a small number of phyB:GFP NBs (stage III to stage IV). The stages exhibited by the hypersensitive mutants are typically seen in seedlings exposed to higher fluence rates of red light, when % Pfr is estimated to be higher [5].

We sequenced the *phyB:GFP* transgene in these mutants to distinguish intragenic *phyB* mutations from second-site mutations. One mutant contained a proline to serine conversion at amino acid 189 in the P2 domain. The second mutant contained an arginine to histidine conversion at amino acid 272 of the GAF domain. These new alleles of *phyB* were renamed *phyB*-501and *phyB-502*, respectively (Figure 3.1B). Sequence alignments indicate that P189 is conserved among the plant phytochromes and Cph1 from *Synechocystis*, while R272 is conserved among all phytochromes, excluding PHY1 from *Selaginella* but including BphP from *Deinococcus radiodurans* [6].

We performed a more rigorous analysis of the hypersensitivity of these alleles by measuring hypocotyl length across a variety of fluence rates of Rc (Figure 3.1C).

These results demonstrate that the hypocotyl lengths of *phyB-501* and *phyB-502* are not different from that of PBG when grown in the dark. This suggests that absorption of light is required for the hypersensitive phenotype. This contrasts with the so-called Y^{GAF} mutant alleles that exhibit light-independent photomorphogenesis [7]. However, at low fluence rates of Rc, *phyB-501* and *phyB-502* are clearly hypersensitive compared to the parental PBG line.

***phyB-501* and *phyB-502* exhibit reduced N- and C-terminal interactions**

We initially considered two hypotheses for the cause of the hypersensitive phenotypes observed in *phyB-501* and *phyB-502* seedlings: an increase in phyB protein levels relative to PBG or a reduced interaction between the N- and C- termini of mutant phyB. To investigate the first possibility, we performed α-GFP western blots of the phyB:GFP transgene in PBG, *phyB-501*, and *phyB-502* (Figure 3.2A and B). We observe no differences in phyB protein level between these lines in etiolated seedlings, while in Rc grown seedlings phyB:GFP levels are increased in *phyB-501* and *phyB-502* relative to PBG (1.4 and 2.6 fold, respectively). However, overexpression of phyB three- to four-fold that of endogenous phyB is sufficient to saturate the inhibition of hypocotyl elongation [8]. As *phyB-501* and *phyB-502* are in the PBG background (i.e., under control of the constitutive 35S promoter) it seems unlikely that further increasing the phyB:GFP level would result in increased inhibition of hypocotyl elongation. The second hypothesis relates to the relative affinity of the phyB N- and C- termini. Previously, we showed that phyB N- and C-termini interact in a light dependent manner [9]. A model was proposed whereby

absorption of red light by phyB converts the molecule from the Pr (inactive) to the Pfr (active) form, and concomitantly reduces phyB N- and C- termini interaction resulting in the unmasking of a cryptic nuclear localization signal. We reasoned that a reduction in N- and C- termini interaction would result in hypersensitivity as the molecule would be less likely to exist in the Pr state. To investigate this possibility we employed a yeast two-hybrid assay that was used previously to demonstrate intramolecular interactions between the N- and C-termini of phyB [9] (Figure 3.3A). The results demonstrate that mutations in *phyB-501* and *phyB-502* reduce the ability of the N- and C- termini to interact in the dark 9.2 and 9.8 fold, respectively (Figure 3.3B)

phyB-501 **and** ***phyB-502*** **have reduced response to end-of-day far-red treatment**

Arabidopsis seedlings grown in light and dark cycles exhibit growth at a specific time of day. In short day (SD; 8 h light, 16 h dark) grown seedlings, growth occurs at dawn [10]. Nozue *et al.* proposed a model whereby light inhibits growth, in part by degrading the growth-promoting transcription factors PIF4 and PIF5. The circadian clock maintains growth inhibition during the first half of the night by repressing *PIF4* and *PIF5* transcription. Repression wanes as the night progresses, with growth promotion occurring at dawn as PIF4 and PIF5 accumulate. The cycle continues with degradation of PIF4 and PIF5 by light. This model incorporates both circadian (internal) and light (external) cues in an example of an external coincidence model. During the day, light stable phytochromes are converted to the active Pfr form, resulting in a high percentage of Pfr at dusk. During the night, Pfr is slowly converted to the inactive Pr form via a thermal process known as dark reversion [11]. End-of-day

far-red (EODFR) treatments rapidly shift active Pfr phytochrome to the inactive Pr isoform, the result of which is an increase in hypocotyl elongation relative to non-treated controls. We performed EODFR experiments with Ler, PBG, *phyB-501* and *phyB-502* seedlings under intermediate day (10 h light, 14 h dark) and SD conditions (Figure 3.4A and B, respectively). The results in intermediate day conditions demonstrate that while PBG retains an EODFR response, the EODFR response in *phyB-501* and *phyB-502* is impaired, with both mutants having shorter hypocotyls than PBG after EODFR treatment (Figure 3.4A). Interestingly, in SD conditions, *phyB-501* and PBG exhibit a similar EODFR response, while the EODFR response for *phyB-502* is greatly impaired (Figure 3.4B). These findings are consistent with *phyB-501* and *phyB-502* being impaired in their ability to convert fully to the Pr form.

phyB-501 and _phyB-502_ have reduced interaction with PIF3

phyB exhibits Pfr-preferential interactions with many of its interacting partners, including PIF3 [12]. To test whether this interaction is affected in *phyB-501* and *phyB-502* we employed an *in vitro* pull-down experiment using *in vitro* transcribed and translated, full-length, HA-tagged phyB, and *in vitro* transcribed and translated GST-tagged PIF3 under both R and FR light (Figure 3.5A and 3.5B). Using wild-type phyB we confirmed the Pfr preferential interaction with PIF3. However, using *phyB-501* and *phyB-502* we observed a dramatic reduction in the ability of these mutants to interact with PIF3 under both R and FR light. This result was most dramatic for *phyB-501*, which showed only a 1.5-fold stronger preference for PIF3 under R light compared to FR light. *phyB-502*, like wild-type phyB, showed a greater

than 3-fold preference for PIF3 under R light compared to FR light, although overall *phyB-502* interaction with PIF3 under R light was nearly seven-fold less than wild-type phyB.

Discussion

We initiated a screen to identify components of the NB in *Arabidopsis*. This screen has yielded mutants that support a positive role for NBs in phy signaling and has identified amino acids that link proper Pr to Pfr photoconversion to faithful phytochrome signaling. We have identified two alleles of phyB that exhibit a hypersensitive phenotype not only in terms of hypocotyl elongation, but NB formation as well (Figure 3.1). We have shown that mutations in *phyB-501* and *phyB-502* affect the ability of the N- and C-termini to interact in yeast two-hybrid assays (Figure 3.3). According to the model proposed by Chen *et al.*, whereby intramolecular interactions between the N- and C-termini in the Pr form mask a cryptic nuclear localization signal, we predicted that *phyB-501* and *phyB-502* would exhibit defects in the EODFR response as far-red light would be ineffective in conversion of Pfr to Pr. Indeed, these mutants respond less to the far-red light treatment than PBG, suggesting that far-red light is less effective in conversion to Pr in the mutants (Figure 3.4). The mutants do retain some response to EODFR treatments, but this is not surprising considering the increased inhibition of hypocotyl elongation phenotype observed under Rc is light dependent. *phyB-502* was less sensitive to EODFR treatments than *phyB-501*. This difference may stem from the fact that the mutations in *phyB-501* and *phyB-502* lie in different domains of the phytochrome molecule and, thus may have different effects

on phytochrome signaling. Based on results from the yeast two-hybrid and EODFR experiments, we predicted that *phyB-501* and *phyB-502* would exhibit a less marked Pfr preference for PIF3 in pull-down experiments. Surprisingly, we found that *phyB-501* and *phyB-502* interaction with GST:PIF3 was greatly reduced under both Rc and FRc compared to GST alone. Despite this overall reduction in the ability to interact with PIF3, *phyB-502* maintained a Pfr preference similar to wild-type. This was not the case for *phyB-501*, however, as the interaction with PIF3 under Rc was only twice that under FRc. This, too, suggests that despite both being hypersensitive, the underlying cause might be slightly different. Spectral analysis of the mutants might help to resolve this point and is planned in the future.

The publication of the crystal structure of the chromophore-binding domain of *Deinococcus radiodurans* phytochrome was a pivotal event in phytochrome signaling [13]. The structure, with bound chromophore, revealed that the interface between the PAS and GAF domains forms a deep trefoil knot that may function in stabilizing the interaction between these domains. Further, the structure showed that essential residues that form the PAS and GAF domains, bind the bilin, and create the trefoil knot are highly conserved amongst all phytochrome members, suggesting that this topology is common to all red/far-red photochromic phytochromes. This conservation gives us some confidence when mapping the residues mutated in *phyB-501* and *phyB-502* onto the *Deinococcus* structure (Figure 3.6). As stated above, the P189S mutation in *phyB-501* occurs in a residue in the PAS domain that is conserved among plant phytochromes and *Cph1* from *Synechocystis* but is not conserved in *Deinococcus radiodurans*. The corresponding residue in *Deinococcus* BphP lies at the interface

between the PAS and GAF domains (Figure 3.6A and B). While it is not clear from the structure why mutation of this residue in phyB results in hypersensitivity, it is possible that this mutation de-stabilizes interactions between the PAS and GAF domains, or between the PAS domain and an as-yet unresolved part of the full-length phytochrome molecule. Elucidation of the structure of full-length phytochrome will likely provide the experimental evidence for the role of this residue. The R272H mutation in *phyB-502* occurs in a residue in the GAF domain that is conserved among all phytochromes, excluding PHY1 from *Selaginalla* but including BphP from *Deinococcus radiodurans*. This residue lines the chromophore-binding pocket, though at a distance of 7.5 Å is unlikely to have direct contact with the chromophore (Figure 3.6C). Instead, R272 is a second tier residue, likely forming a hydrogen bond with a residue (H403) in direct contact with the chromophore. Disruption of this hydrogen bonding network apparently results in alterations in the chromophore environment. Mutation of residues in the chromophore binding pocket can have dramatic effects on the photoreceptor, as has been shown for a conserved tyrosine residue in *Synechocystis* Cph1 and *Arabidopsis* phyB [7, 14, 15]. Expression of a *phyB* transgene containing a mutation in this tyrosine residue in *Arabidopsis* can result in plants with constitutive photomorphogenic (COP) phenotypes in the dark, meaning these mutant photoreceptors mimic light activated photoreceptors. Interestingly, the phenotypic effect of mutation of this tyrosine residue is dependent on the substituted amino acid. Whereas replacement of the tyrosine with histidine or glutamine yields COP phenotypes, replacement with isoleucine or arginine does not [7]. It would be interesting to know if saturation mutagenesis of R272 would yield similar results.

Despite widespread interest, the role of nuclear bodies (NBs) in phytochrome signaling is unknown. Two models have been proposed for their function: storage as a means to downregulate phytochrome signaling and the site of phytochrome signaling itself. Evidence for the storage model comes mostly from data showing that *phyB* plants expressing the N-terminus of phyB fused to GFP, GUS (to promote dimerization) and a nuclear localization signal (NLS) are hypersensitive to Rc yet do not form NBs [16]. This suggests that NBs are not required for, and may play a negative role in, phytochrome signaling. Further, work by Chen *et al.* [5] showed that at low fluence rates of Rc, inhibition of hypocotyl elongation occurs in the absence of NB formation. However, in the same paper the authors show that increases in the fluence rate of Rc result in NB formation and further inhibition of hypocotyl elongation. The authors also identify new hyposensitive alleles of *phyB* that do not form NBs. Kircher *et al.* had shown previously that mutations in phyA and phyB that impair phytochrome signaling also impair NB formation [17]. Identification of the Y^{GAF} *phyB* alleles also suggests that NBs may function in phytochrome signaling as these mutants exhibit NB formation and constitutively photomorphogenic phenotypes in the dark [7]. Similar to the Y^{GAF} *phyB* alleles, the two hypersensitive alleles presented here provide further evidence that NB formation is required for phytochrome signaling. And while mounting evidence suggests that NB formation and phytochrome signaling are intimately linked, definite evidence that NBs are the site of signaling is still lacking. A promising resolution of this question may come from a mutant screen performed by Chen *et al.* [5]. In this screen the authors identify Rc hyposensitive mutants with lesions outside the *PHYB* coding region. These so-called

dsf (*Defective in Speckle Formation*) mutants should provide unique insight into the make-up of the NB.

Material and Methods

Plant Material PBG seeds were mutagenized with ethylmethanesulfonate as described previously [5] and screened for seedlings with short hypocotyls compared to PBG under 0.4 μmol·m^{-2} s^{-1} red (R) light. A secondary screen was performed by examining phyB:GFP nuclear localization patterns of seedlings grown under 0.4 μmol m^{-2} s^{-1} of R for 4 days. Seedlings with distinct phyB:GFP nuclear bodies compared to the evenly distributed phyB:GFP nuclear localization seen in the parental PBG line were selected. The *phyB:GFP* transgene in these lines was sequenced.

Microscopy Confocal microscopy was performed using a Leica TCS SP2 AOBS confocal laser scanning microscope and a HCX PL APO 63X 1.2-numerical-aperture water-immersion objective lens (Leica Microsystems, Mannheim, Germany). 4-day old seedlings were mounted in water. GFP fluorescence was monitored using a 460 nm - 480 nm band pass emission and 488 nm excitation line of an Ar laser.

Hypocotyl Measurements Seeds were surface sterilized in 75% ethanol with 0.05% Triton-X 100, followed by 10 min in 95% ethanol. After sterilization seeds were suspended in 0.1% agar and plated on 0.5x MS (Gibco-BRL) with 0.7% agar plates. Seeds were stratified in the dark at 4°C for 4 d. Germination was induced by 2 hr of R light and followed by a 1 d incubation in the dark. For hypocotyl measurements, seedling were grown at 22°C in a light-emitting diode (LED) chamber (Percival Scientific) under indicated fluence rates for 4 d. Fluence rates were measured with a LiCor LI-1800 spectroradiometer (LiCor). Seedlings were scanned and hypocotyls measured using NIH Image (http://rsb.info.nih.gov/nih-image/).

GFP Western Blot Seeds were surface sterilized as above and plated directly on 0.5x MS plates with 0.7% agar. Seeds were stratified in the dark at 4°C for 3 d. Germination was induced by 3 h WLc and seedlings were grown in light conditions as described in text. Seedlings were harvested, immediately frozen in liquid N_2 in 1.5 mL tubes containing three metal bearings, and stored at –70°C until protein extraction. Samples were disrupted by shaking for 90 s at 29 vibrations s^{-1} in a MM 300 Mixer Mill (Retsch). 5X SDS sample buffer was added to each sample on a per weight basis. Tubes were vortexed, heated for 3 min at 95°C, and then spun at 14,000 rpm for 3 min in an Eppendorf 5417C centrifuge (Eppendorf).

Yeast Two-hybrid Assay phyB constructs carrying the R272H or P189S point mutation were generated using the QuikChange XL Site-Directed Mutagenesis Kit (Stratagene, La Jolla, CA). Primers used to generate the R272H mutation were MC427 (5'-CTTGACTGGTTATGATCaTGTTATGGTTTATA-3') and MC428 (5'-TATAAACCATAACAtGATCATAACCAGTCAAG-3'). Primers used to generate the P189S mutation were MC425 (5'-GATTACCTTGTTAAATtCGGTTTGGATCCATT-3') and MC426 (5'-AATGGATCCAAACCGaATTTAACAAGGTAATC-3'). The wild-type phyB construct and protocols for the β-galactosidase liquid assays and yeast western blots were described previously [9].

In vitro pull-down assays Wild-type and hypersensitive alleles were cloned into Gateway entry vector pDONR221 according to manufacturer instructions (Invitrogen). Clones were then recombined into an expression vector consisting of a modified pTNT vector (Promega) with an HA tag (a kind gift from Dr. Kazu Nito). GST and

GST:PIF3 were gifts from Dr. Kazu Nito. All proteins were expressed in the SP6 High-Yield Protein Expression System (Promega) according to manufacturer's instructions. Glutathione Sepharose 4B (GE Healthcare) previously equilibrated in binding buffer (50 mM NaPO4, pH 7.4, 150 mM NaCL, and 1 mM DTT) was incubated with GST and GST:PIF3 proteins for one hour in binding buffer at 4°C on a rotisserie shaker. phyB apoproteins were diluted in binding buffer and incubated with PCB chromophore (10 μM final concentration) in darkness for one hour on ice. GST and GST:PIF3 bound to Glutathione Sepharose 4B was washed three times with 400 μL binding buffer. After PCB binding, phyB holoproteins were incubated with washed GST or GST:PIF3 for two hours with rotation on a rotisserie shaker at 10°C in an LED (Percival) with either R or FR light. GST bound proteins were washed with binding buffer. An equal volume of 5X SDS sample buffer was added to each sample. Tubes were vortexed, heated for 3 min at 95°C, and then spun at 14,000 rpm for 3 min in an Eppendorf 5417C centrifuge (Eppendorf). Proteins were visualized by western blot with HA and GST antibodies.

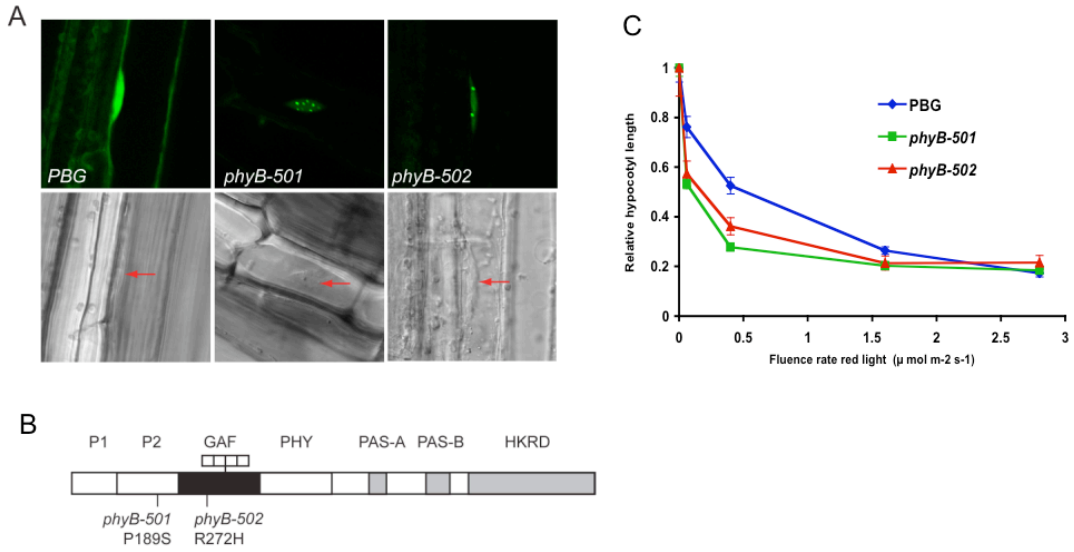

Figure 3.1. Phenotypes of *phyB-501* and *phyB-502* hypersensitive mutants.
(**A**) *phyB-501* and *phyB-502* exhibit phyB:GFP nuclear bodies at 0.4 μmol m^{-2} s^{-1} red light compared to diffuse phyB:GFP accumulation in the PBG parental line. Confocal microscopy performed by Meng Chen. (**B**) Schematic illustration of the mutations in *phyB-501* and *phyB-502*. (**C**) Hypocotyl length of PBG, *phyB-501*, and *phyB-502* grown in continuous red light at fluence rates indicated. Hypocotyl measurements performed by Meng Chen.

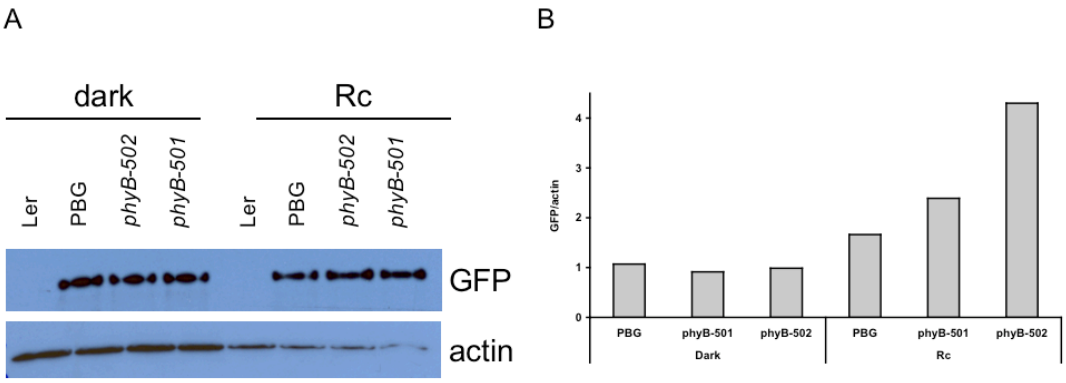

Figure 3.2. phyB:GFP transgene levels in PBG, *phyB-501* and *phyB-502*.
(**A**) Anti-GFP western blot (top panel) in Ler, PBG, *phyB-501* and *phyB-502* seedlings. Seedlings were either grown in dark or 0.4 μmol m^{-2} s^{-1} red light (Rc) for four days. Actin loading control (bottom panel). (**B**) Quantification of phyB:GFP signal using western blots from (A).

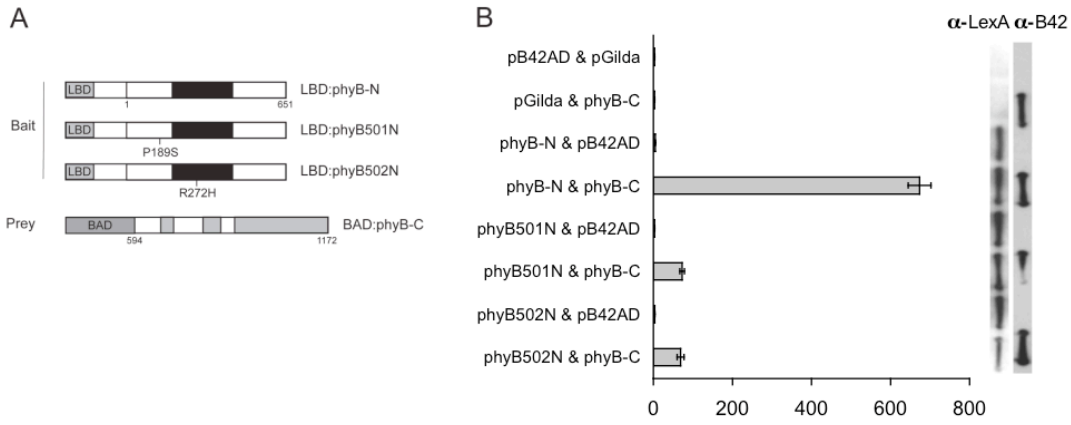

Figure 3.3. *phyB-501* and *phyB-502* exhibit reduced N- and C-terminal interactions. (**A**) Schematic illustration of constructs used in the yeast two-hybrid assay. The phyB N-terminus (amino acids 1-651) was fused to the LexA DNA binding-domain (LBD:phyB-N). The phyB C-terminus (amino acids 594-1172) was fused to the B42 activation domain (BAD:phyB-C). *phyB-501* and *phyB-502* mutations are indicated. (**B**) Yeast two-hybrid liquid β-galactosidase activity assay between LBD:phyB-N and BAD:phyB-C in dark. Activity is shown in Miller units. Western blot shows the protein levels of the bait (anti-LexA) and prey (anti-B42) proteins. Yeast two-hybrid assays performed by Yi Tao.

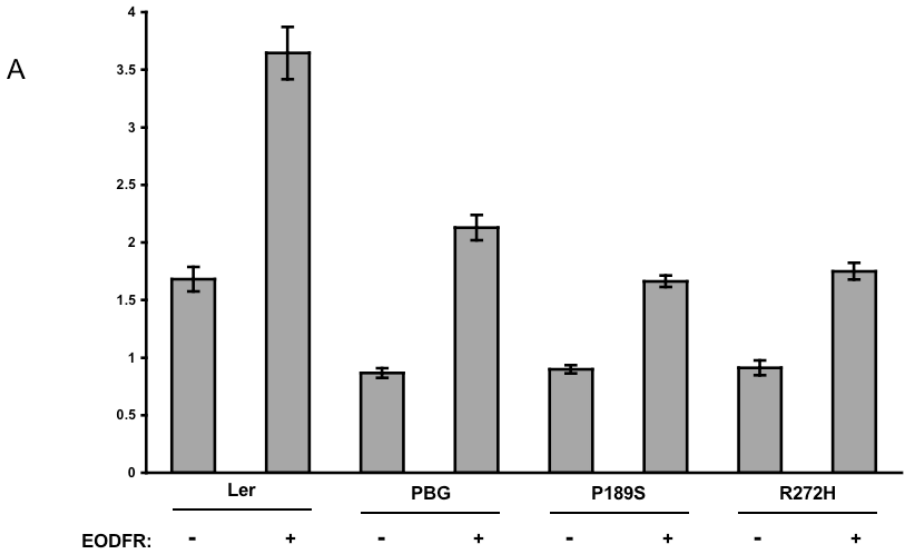

Figure 3.4. *phyB-501* and *phyB-502* exhibit reduced response to end-of-day far-red treatment.
(**A**) Seedlings were grown for 4 days in intermediate conditions (10 h/14 h light-dark cycles). Seedlings receiving the end-of-day far-red (EODFR) treatment were given 15 minutes of far-red light (80 μE) prior to dark. Error bars represent standard error of the mean. (**B**) Seedlings were grown for 4 days in SD conditions (8 h/16 h light-dark cycles). Seedlings receiving the end-of-day far-red (EODFR) treatment were given 15 minutes of far-red light (80 μE) prior to dark. Error bars represent standard error of the mean.

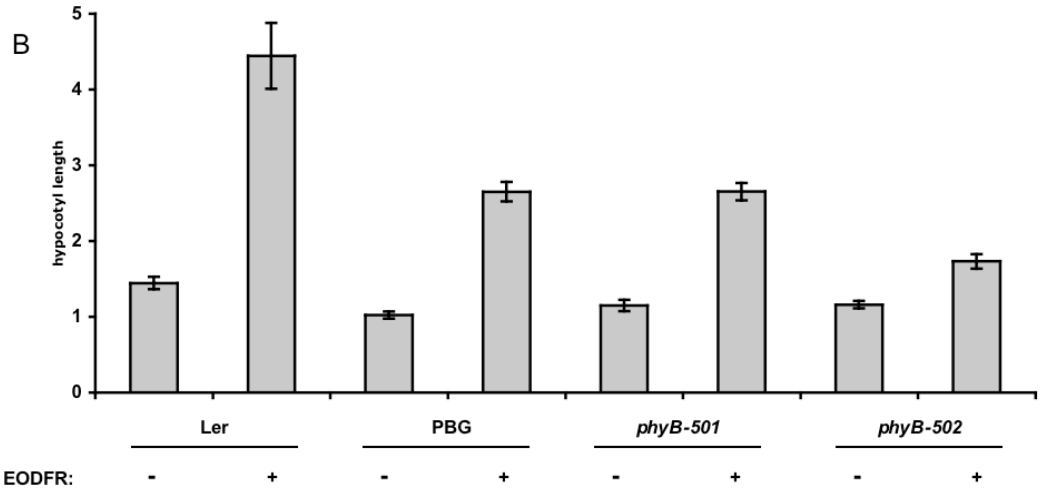

Figure 3.4. continued.

A

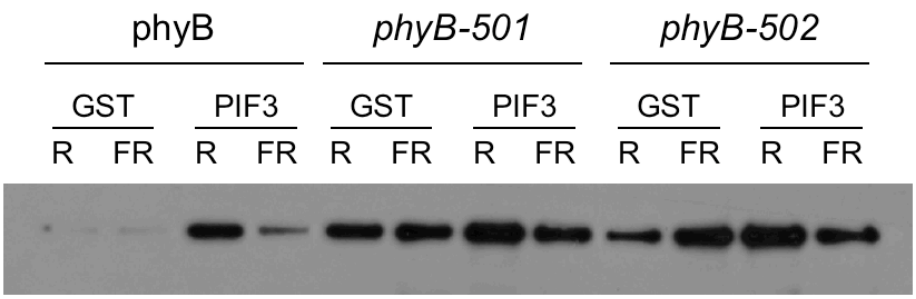

Figure 3.5. *phyB-501* and *phyB-502* exhibit reduced interaction with PIF3
(**A**) HA-tagged phyB (wild-type or containing the *phyB-501* or *phyB-502* mutations) was expressed in vitro and incubated with glutathione-agarose bound in vitro produced GST or GST:PIF3 under Rc or FRc. Beads were washed and bound proteins were solubilized in SDS loading buffer. Proteins were resolved by SDS-PAGE and subjected to anti-HA western blot. (**B**) Quantification of western blot in (A). Bands were quantified using ImageJ. Values shown are the ratio of phyB bound to GST:PIF3 versus GST alone.

B

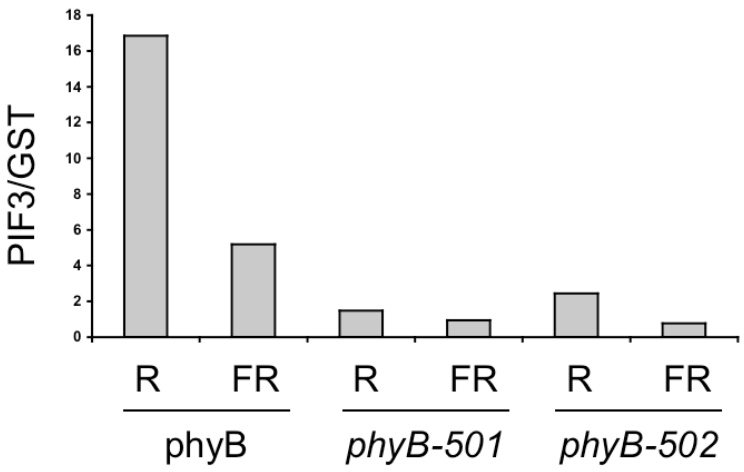

Figure 3.5. continued.

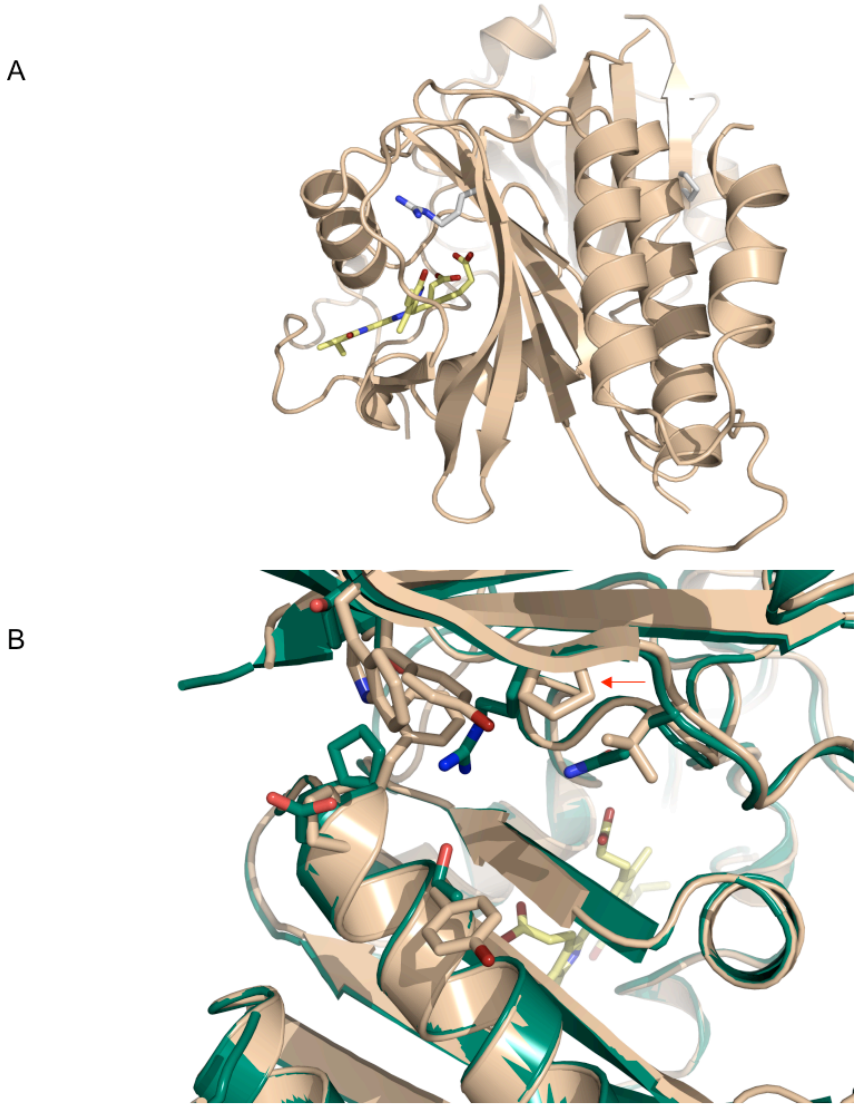

Figure 3.6. Model of N-terminus of *Arabidopsis* phyB using the crystal structure of *Deinococcus radiodurans* BphP as template. Model done in collaboration with Michele Auldridge, Salk Institute.
(**A**) Overall view of the chromophore binding domain of *Arabidopsis* phyB. Residues corresponding to mutations in *phyB-501* and *phyB-502* are highlighted. Chromophore is shown in yellow. (**B**) Close-up view of the interface between the PAS and GAF domains. Chromophore is shown in yellow. *Deinococcus* BphP structure (green). *Arabidopsis* phyB (tan). Red arrow indicates the proline residue mutated in *phyB-501*. (**C**) View of the chromophore binding pocket in *Arabidopsis* phyB highlighting the position of R272. Chromophore is shown in yellow.

C

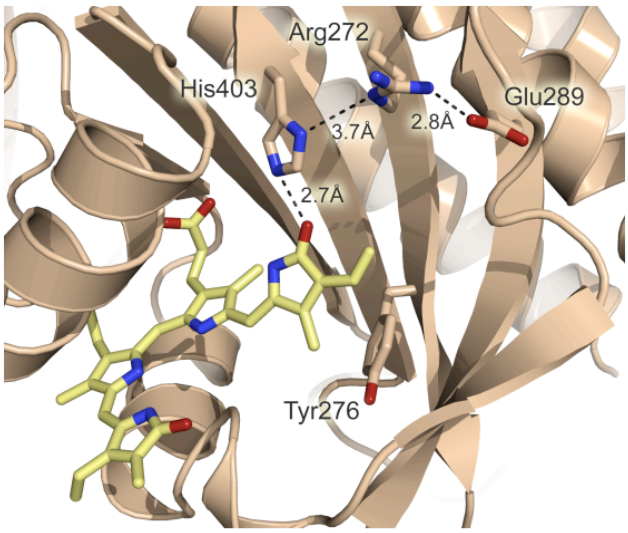

Figure 3.6. continued.

References

1. Sakamoto, K., and Nagatani, A. (1996). Nuclear localization activity of phytochrome B. Plant J. *10*, 859-868.

2. Yamaguchi, R., Nakamura, M., Mochizuki, N., Kay, S.A., and Nagatani, A. (1999). Light-dependent Translocation of a Phytochrome B-GFP Fusion Protein to the Nucleus in Transgenic Arabidopsis. J Cell Biol *145*, 437-445.

3. Kircher, S., Kozma-Bognar, L., Kim, L., Adam, E., Harter, K., Schafer, E., and Nagy, F. (1999). Light quality-dependent nuclear import of the plant photoreceptors phytochrome A and B. The Plant cell *11*, 1445-1456.

4. Chen, M. (2008). Phytochrome nuclear body: an emerging model to study interphase nuclear dynamics and signaling. Current opinion in plant biology.

5. Chen, M., Schwab, R., and Chory, J. (2003). Characterization of the requirements for localization of phytochrome B to nuclear bodies. Proceedings of the National Academy of Sciences of the United States of America *100*, 14493-14498.

6. Hughes, J., and Lamparter, T. (1999). Prokaryotes and phytochrome. The connection to chromophores and signaling. Plant physiology *121*, 1059-1068.

7. Su, Y.S., and Lagarias, J.C. (2007). Light-independent phytochrome signaling mediated by dominant GAF domain tyrosine mutants of Arabidopsis phytochromes in transgenic plants. The Plant cell *19*, 2124-2139.

8. Wagner, D., Koloszvari, M., and Quail, P.H. (1996b). Two small spatially distinct regions of Phytochrome B are required for efficient signaling rates. The Plant cell *8*, 859-871.

9. Chen, M., Tao, Y., Lim, J., Shaw, A., and Chory, J. (2005). Regulation of phytochrome B nuclear localization through light-dependent unmasking of nuclear-localization signals. Curr Biol *15*, 637-642.

10. Nozue, K., Covington, M.F., Duek, P.D., Lorrain, S., Fankhauser, C., Harmer, S.L., and Maloof, J.N. (2007). Rhythmic growth explained by coincidence between internal and external cues. Nature *448*, 358-361.

11. Taiz, L.Z., E. (1998). Plant Physiology, Second Edition, (Sunderland, MA: Sinauer Associates, Inc.).

12. Ni, M., Tepperman, J.M., and Quail, P.H. (1999). Binding of phytochrome B to its nuclear signalling partner PIF3 is reversibly induced by light. Nature *400*, 781-784.

13. Wagner, J.R., Brunzelle, J.S., Forest, K.T., and Vierstra, R.D. (2005). A light-sensing knot revealed by the structure of the chromophore-binding domain of phytochrome. Nature *438*, 325-331.

14. Fischer, A.J., and Lagarias, J.C. (2004). Harnessing phytochrome's glowing potential. Proceedings of the National Academy of Sciences of the United States of America *101*, 17334-17339.

15. Fischer, A.J., Rockwell, N.C., Jang, A.Y., Ernst, L.A., Waggoner, A.S., Duan, Y., Lei, H., and Lagarias, J.C. (2005). Multiple roles of a conserved GAF domain tyrosine residue in cyanobacterial and plant phytochromes. Biochemistry *44*, 15203-15215.

16. Matsushita, T., Mochizuki, N., and Nagatani, A. (2003). Dimers of the N-terminal domain of phytochrome B are functional in the nucleus. Nature *424*, 571-574.

17. Kircher, S., Gil, P., Kozma-Bognar, L., Fejes, E., Speth, V., Husselstein-Muller, T., Bauer, D., Adam, E., Schafer, E., and Nagy, F. (2002). Nucleocytoplasmic partitioning of the plant photoreceptors phytochrome A, B, C, D, and E is regulated differentially by light and exhibits a diurnal rhythm. The Plant cell *14*, 1541-1555.

Chapter 4

Generation of antibodies against a key subset of bHLH transcription factors in phytochrome signaling

Introduction

Biochemical experiments and genetic screens have been fruitful in identifying components of the phytochrome signal transduction pathway. In many cases, however, a detailed characterization of these components is lacking. What characterization is available too often relies on tagged proteins expressed under control of non-native promoters. While this type of approach can generate useful data, it is less than ideal. Specific antibodies allow use of any genetic background, and when competent for immunoprecipitations, are an extremely valuable tool. We chose to generate specific antibodies towards a subfamily of bHLH transcription factors that play a major role in phytochrome signaling, the PIF/PIL subfamily.

The identification of PIF3, the founding member of the PIF family, was an important event in the study of phytochrome signaling. From that time forward, characterization of PIF3 and closely-related proteins have come to dominate the phytochrome signaling field. Importantly, they have provided the fodder for many working models. Below is a detailed review of the role that each of these proteins plays in phytochrome signaling.

PIF3

PIF3 was first identified in a yeast two-hybrid screen with the COOH-terminus of *Arabidopsis* phyB as bait but was also shown to interact with the COOH-terminus of *Arabidopsis* phyA, suggesting that PIF3 could be a shared component between the phyA and phyB signal transduction pathways [1]. Accordingly, *PIF3* antisense lines exhibited hyposensitivity to Rc and FRc light, while *PIF3* sense lines showed a slight

hypersensitivity to Rc and FRc light. The strength of the phenotypes correlated roughly to the increase or decrease of *PIF3* mRNA in multiple sense or antisense lines, respectively. Additionally, the authors observed reduced rates of light-induced hook opening and cotyledon expansion in the *PIF3* antisense lines, consistent with their proposed classification of PIF3 as a positively acting signaling intermediate. A paper by the same lab [2] identified a Rc hypersensitive mutant (*poc1*) in a T-DNA screen, with the causative insertion 1 kB upstream of the *PIF3* start codon. qPCR analysis of the *poc1* mutant showed increased levels of *PIF3* but not of the gene upstream of the insertion in Rc, providing corroborative evidence that PIF3 is a positively acting phytochrome signaling intermediate.

Subsequent papers by the Quail lab showed in vitro that PIF3 binds preferentially to phyB in the Pfr form [3], and that Pfr phyB can interact with G-box bound PIF3 [4]. phyA also interacts with PIF3 in a Pfr-dependent manner, albeit with 10-fold less affinity than phyB [5]. Removal of a 37 amino acid NH-terminal extension from phyB (absent in phyA) reduces the PIF3 interaction with phyB to a level only 2-fold greater than phyA, suggesting that this extension is largely responsible for the difference in PIF3 binding between phyA and phyB. Together, these papers provided the experimental evidence for an attractive model whereby light sensing by phytochromes could be directly translated into changes in gene expression by interaction with DNA bound transcription factors.

A paper by the Choi lab [6] challenged the idea of PIF3 as a positive regulator of phytochrome signaling. Here, the authors revisit the role of PIF3 in phy signaling using a T-DNA insertion allele (*pif3-1*) rather than *PIF3* antisense lines, and full-

length *PIF3* overexpression lines rather than the NH-terminal truncated *PIF3* construct used in earlier reports. They conclude that PIF3 plays multiple roles that depend on light conditions. PIF3 functions as a positive regulator for both phyA- and phyB-mediated *CHS* induction, a negative regulator of both phyB- and phyA-induced cotyledon expansion and opening, and a negative regulator of phyB- but not phyA-mediated inhibition of hypocotyl elongation. These findings were subsequently corroborated by several groups [7, 8]. Further, the *poc1* mutant was shown to lack detectable levels of PIF3 [7]. The use of *PIF3* antisense lines in determining the role of PIF3 in flowering time also caused confusion in the literature. A report showing early flowering in *PIF3* antisense lines under LD and SD conditions [9] was later shown to be an artifact of the *PIF3* antisense lines as *pif3* T-DNA alleles and *PIF3* overexpression had no effect on flowering time [10].

While the role of PIF3 as either positive or negative regulator of phytochrome signal transduction was debated in the literature, much progress was made on its regulation. In a pivotal paper by Nagy and Schäfer's groups, PIF3 was shown to be degraded in response to light and to co-localize with phyA/B/D nuclear speckles, with degradation rapid (~ 10 min in Rc) and dependent upon phyA/B/D [7]. Interestingly, COP1 was shown to be necessary for the accumulation of PIF3 in the dark, but dispensable for its degradation. Degradation of PIF3 was, however, inhibited by proteasome inhibitors MG115 and MG132 [11]. Monte et al. showed that PIF3 protein levels undergo diurnal fluctuations, and that PIF3 protein levels declined to a steady state level in the light (~ 20% of dark levels) rather than declining to undetectable levels as reported earlier [8]. This report conflicts with that by Viczian et al. [10] who

show a low level of PIF3 accumulation during the night in plants grown under 12 h light/12 h D cycles, but rather an increase at the end of the light phase. This point remains unresolved. An important paper by the Quail lab showed that PIF3 is phosphorylated prior to degradation in a phyA/B dependent manner [12]. Previously, Khanna et al. defined the active phytochrome binding (APB) motif in PIF3 responsible for its interaction with phyB [13]. Here, Al-Sady et al. define the active phyA (APA) binding motif for PIF3/phyA binding and show that mutations within the APA and APB motifs of PIF3 result in loss of phosphorylation, speckle formation, and degradation [12]. Taken together, the above results led to a rethinking of the earlier model. While PIF3 has been shown to interact with phytochromes and bind DNA, the phosphorylation, speckle formation and rapid degradation in response to light suggests that the PIF3/phytochrome complex is not a stable or long-lived entity.

Two recent papers by the Quail lab have changed the way we think about PIF3 specifically, and the PIFs in general. In the first paper, the authors show that the mechanism of PIF3 function can be divided into two roles that are separated temporally [14]. The first role is one of transcriptional activator, requiring only the ability of PIF3 to bind DNA and not its ability to bind either phyA or phyB. The second role is control of hypocotyl elongation, which requires the APB motif of PIF3 but not the APA motif or the DNA-binding ability of the bHLH domain. Surprisingly, they show that PIF3 controls hypocotyl elongation through the ability to regulate phyB protein levels posttranscriptionally. The second paper expounds on the regulation of phyB protein levels by PIFs (including PIF4 and PIF7) [15]. This dual role offers a ready explanation for how PIF3 effects both the early (within hours) induction of

light-regulated genes and hypocotyl elongation, whose phenotype in *pif3-1* manifests itself over several days.

HFR1

HFR1/RSF1/REP1 was identified independently by several labs using forward genetic screens aimed at identifying long hypocotyl mutants under FRc light [16-18]. Phenotypic analysis by the three labs was mostly consistent, with defects in inhibition of hypocotyl elongation reported only in FRc [16-18] and Bc light [17]. Suppression of hypocotyl negative gravitropism was observed in *hfr1/rep1* mutants only under FRc [16, 18]. All three labs reported no difference in phyA levels in darkness or in phyA degradation kinetics in the *hfr1/rsf1/rep1* mutants [16-18]. However, some discrepancies amongst the labs were evident with regards to cotyledon expansion and anthocyanin accumulation in the *rsf1/rep1* mutants, with differences reported by some only under FRc [17, 18]. No defects were observed for flowering time, end-of-day far-red (EOD FR) response, FR block of greening, or FR-induced germination. Finally, induction of *CHS* and *FNR* by FR was normal in *rep1*, while *CAB* induction by FR was not [18]. Together, the data suggest that *HFR1* encodes a signaling component required in a discrete branch of the phyA signal transduction pathway. Later work showed that HFR1 is a positively acting component of the CRY1-mediated blue light signal transduction pathway as well [19]. And more recently, HFR1 has been implicated in the shade avoidance response as *HFR1* transcripts are upregulated in response to low R/FR and *hfr1* mutants exhibit an exaggerated response to shade conditions [20]. Interestingly, transcript levels of shade upregulated genes are higher

in *hfr1* mutants. Together, this suggests that HFR1 plays a negative role in the shade avoidance response and may function in preventing the plant from overcommitting to shade avoidance.

Cloning of the locus showed that *HFR1* encodes a bHLH protein related to PIF3 [16-18, 21]. As expected, HFR1 localizes to nuclei as a GUS fusion protein when transiently expressed in onion cells [16, 18]. Attributable to its lack of either an APA or APB motif, HFR1 does not bind phyA or phyB, but can bind PIF3 and subsequently interact with both phyA and phyB in a Pfr-dependent manner as a PIF3/HFR1 heterodimer [13, 16]. Fairchild et al. reported that *HFR1* mRNA is upregulated by FRc and downregulated by Rc compared to darkness [16]. This is in apparent contrast to the report by the Song lab that *HFR1* mRNA is upregulated by FRc and by Rc and WLc (data not shown) [18].

Work by Kim et al. showed that HFR1 mediates phyA-dependent inhibition of hypocotyl elongation independent of HY5 and acts downstream of COP1, as HFR1 is required for a subset of *cop1* phenotypes in the dark [22]. A series of papers by three labs showed that HFR1 interacts with, and is ubiquitinated by, COP1 in vitro and that COP1 is required for its degradation [23-25]. Degradation of HFR1 is preceded by phosphorylation and requires the N-terminus of HFR1, shown to interact with COP1 [23-25]. HFR1 protein levels were shown to be low in the dark, and rapidly and transiently increased upon light exposure [23, 24]. Together, the data suggest that degradation of HFR1 might be involved in suppression of photomorphogenesis in the dark and is supported by experiments showing that overexpression of a stabilized HFR1 lacking the N-terminus results in constitutive photomorphogenic phenotypes in

the dark [24-26]. SPA1, a protein structurally related to COP1, and LAF1 have also been shown to be involved in the post-translational regulation of HFR1 [27, 28]. Both have been shown to interact physically with HFR1, and while HFR1 levels are higher in *spa* mutants they are lower in *laf* mutants. Interaction of HFR1 with LAF1 prevents ubiquitination of both by COP1, thus stabilizing both proteins. And while HFR1 interaction with SPA1 likely leads to its degradation, the mechanism is unclear.

PIF4

PIF4 was originally identified as the Rc hypersensitive mutant *srl2* in a T-DNA screen from the Quail lab [29]. The authors show that the hypersensitive phenotype is Rc specific and phyB dependent, suggesting that PIF4 is a negative regulator of phyB signaling. Interestingly, they observe no difference in phyB protein levels in the mutant, though they would later provide evidence to the contrary [15]. PIF4 interacts preferentially with the Pfr form of phyB, and weakly with the Pfr form of phyA. As expected, PIF4 is localized to the nucleus and binds G-box motifs in a sequence-specific manner in vitro. However, unlike PIF3, PIF4 does not bind DNA and phytochromes simultaneously. There is no effect on *CAB*, *RBCS*, *CCA1*, or *LHY* mRNA levels in a *pif4* mutant.

Work by Julin Maloof's lab showed that *PIF4* (and *PIF5*) transcript levels are regulated by the circadian clock and that PIF4 (and PIF5) protein levels are light regulated, with degradation in response to light [30]. Thus, the circadian clock and light work together on PIF4 (and PIF5) to control diurnal hypocotyl growth, in an example of an external coincidence model. Work by Lorrain et al. [31] showed that

degradation of PIF4 (and PIF5) in response to Rc is preceded by phosphorylation and requires the APB domain. This suggests that PIF4 (and PIF5) are degraded upon interaction with light-activated phyB. Interestingly, *pif4* mutants are not complemented by expressing a *PIF4* transgene containing a mutation in the APB domain [13]. Recent work by two labs has furthered our understanding of the role that PIFs (including PIF3, PIF4, and PIF5) play in diurnal growth rhythms [32, 33]. Overlayed on light regulation of PIFs is modulation of PIF activity by the GA pathway. They showed that light-induced DELLA accumulation leads to DELLA/PIF interactions which block PIF transcriptional activity by occluding the DNA-binding domains. An increase in GA levels leads to DELLA turnover and release of PIFs.

PIL1

PIL1 (PHYTOCHROME INTERACTING FACTOR 3–LIKE 1) was originally identified in a yeast two-hybrid screen using APRR1 as bait [34]. The goal of the screen was to gain insight into the negative regulation of *APRR9* by *APRR1*. A subsequent study, however, showed that the light-induced expression of *APRR9* is unchanged in *pil1* mutants [35]. Moreover, no phenotypes were observed for *pil1* mutants in regard to flowering time or Rc inhibition of hypocotyl elongation. The authors did note that *PIL1* transcript levels are high in etiolated seedlings, but disappear rapidly upon exposure to WLc. Work by Gary Whitelam's lab showed that *PIL1* transcript levels are very sensitive to changes in R/FR, being upregulated rapidly in response to low R/FR [36]. They show that in seedlings grown in light/dark cycles the magnitude of the response to transient low R/FR is gated by the circadian clock.

Further, they show that in seedlings grown in light/dark cycles, *PIL1* transcript levels are low during the day and do not increase in the dark unless exposed to FR. This finding suggests that *PIL1* is actively repressed in the night by a light stable phytochrome and is bolstered by data showing elevated *PIL1* expression in *phyB* mutants. The authors show that the shade avoidance growth responses, similar to *PIL1* derepression, are also under circadian control. Seedlings exposed to low R/FR at dusk exhibit hypocotyl elongation as part of the shade avoidance response, while seedlings exposed to low R/FR at dawn exhibit inhibition of hypocotyl elongation. *PIL1* and *APRR1/TOC1* are required for normal hypocotyl elongation as part of the shade avoidance response to low R/FR. The authors also show that *pil1* mutants (like *toc1-2* mutants) exhibit a hyposensitive phenotype in both Rc and FRc, in contrast to work by Yamashino et al. [35].

Sessa et al. [20] demonstrated that *HFR1* negatively regulates *PIL1* transcript levels, but not *PIL1* induction under low R/FR conditions. This data was the basis for the so-called gas-and-brake model for controlling the shade avoidance response. In this model, low R/FR induces both positive (*PIL1*) and negative regulators (*HFR1*) of shade avoidance to ensure that plants do not overcommit to the shade avoidance strategy.

Roig-Villanova et al. [37] uncovered a role for *PIL1* in response to long-term shade, with *pil1* mutants slightly longer in extended shade conditions. They also extended the findings of Salter et al. [36] by showing that phytochrome overexpressors show reduced *PIL1* accumulation. Further, they show that upregulation of *PIL1* in response to shade does not require protein synthesis, suggesting that *PIL1* is a direct

target of phytochrome action. A recent paper by Hwang and Quail continued the study of *PIL1* regulation by phytochromes [38]. They show that *PIL1* transcripts in dark grown seedlings are reduced when moved to Rc, but can reaccumulate if given a FRp prior to incubation in the dark. *phy* mutants are impaired in the reduction of *PIL1* mRNA in response to Rc, and exhibit more rapid reaccumulation of *PIL1* mRNA in the dark. Further, *PIL1* reaccumulates more rapidly in the dark in seedlings that have been treated with six hours of Rc compared to those treated with one hour Rc. It is interesting to note that despite its regulation by phytochromes at the transcriptional level PIL1, like HFR1, does not interact physically with phyB [13].

Work by Khanna et al. [39] identified genes that are rapidly induced by phytochrome signals and then queried their role in the de-etiolation process. Included in their analysis was *PIL1*. They observed reduced hypocotyl inhibition and reduced cotyledon expansion in Rc and FRc in *pil1* seedlings, and longer petioles under low-intensity WL and delayed flowering in SD in adult *pil1* plants. While *PIL1* functions in multiple phyB-mediated response, there was no effect on phyB levels in *pil1* mutants. In contrast to published work, they also observed a reduced light induction of *APRR9/TOC1* in *pil1* mutants.

PIF1/PIL5

PIF1/PIL5 was first identified by Yamashino et al. [35] in a paper studying the interaction between members of the PIF family and APRRI/TOC1. This group showed previously that APRR1/TOC1 interacts with PIF3 and PIL1 [34], and in this follow up paper they identify three uncharacterized members of the PIF family: *PIL2/PIF6*,

PIL5/PIF1, and *PIL6/PIF5*. They test these newly identified members, along with HFR1 and PIF4, in yeast two-hybrid assays with APRR1/TOC1 and show that all except HFR1 interact with APRR1/TOC1. All members tested, with the exception of HFR1, contain a so-called PIL motif at their NH2-termini. The PIL motif is contained in what would later be defined as the active phytochrome binding motif (APB) [13]. *PIF1*/*PIL5* transcript levels were extremely low in both dark grown seedlings and in dark grown seedlings treated with six hours WLc [35]. Khanna et al. demonstrated that PIF1/PIL5 binds specifically to phyB in the Pfr form [13].

A role for PIF1 as a negative regulator of chlorophyll biosynthesis was established in a reverse genetics approach by the Quail lab [40]. Huq et al. observed bleaching in *pif1* seedlings grown in the dark and then transferred to WLc, with photooxidative damage the result of high levels of free protochlorophyllide [40]. This suggests that PIF1 functions to prevent accumulation of excess protochlorophyllide in darkness, thus providing a protective function to seedlings growing underground prior to emergence from the soil. In fact, seedling mortality in *pif1* mutants was increased by longer incubations in dark prior to WLc exposure. The authors also show that PIF1 interacts specifically with the Pfr forms of both phyA and phyB, with a much higher (10-fold) affinity for phyA than PIF3. As expected, PIF1 localizes to the nucleus, binds G-box motifs in a sequence-specific fashion, and activates transcription in transient assays. However, PIF1 (like PIF4) is unable to bind DNA and phytochromes simultaneously. A paper by Giltsu Choi's lab showed the PIF1 is also a negative regulator of phytochrome-mediated seed germination, inhibition of hypocotyl elongation, and inhibition of hypocotyl negative gravitropism [41]. A role for PIF1 in

seed germination was most notable in *PIF1* overexpression lines where a much higher fluence rate of Rc was required for seed germination compared to wild-type. Interestingly, *pif1* seedlings germinate after irradiation with FRc, a treatment that inhibits seed germination in wild-type. And while *phyB* seedlings germinate only in WLc, *pif1 phyB* seedlings germinate in all light conditions. Overexpression of *PIF1* also resulted in longer seedlings in both Rc and FRc, while *pif1* seedlings exhibited hyposensitivity only under FRc. While no phenotypes were reported for *pif1* seedlings by the Quail lab, they showed that *PIF1* overexpression resulted in Rc hypersensitivity [40]. The reason for the discrepancy is unclear, but likely due to co-suppression of endogenous *PIF1* in their lines.

A series of papers by the Huq lab explored the regulated turnover of PIF1. They first showed that PIF1 is degraded rapidly in response to light, but reaccumulates in the dark in plants grown in light-dark cycles [42]. This suggests a role for PIF1 not only in seedling establishment, but in diurnal cycles as well. They showed later that PIF1 is phosphorylated and ubiquitinated in response to Rc and FRc prior to its degradation [43]. Further, using transgenic plants containing mutations in the APA and APB motifs, they demonstrate that interaction with phytochromes is necessary for degradation. Interestingly, overexpression of a light stable form of PIF1 results in constitutively photomorphogenic phenotypes in the dark. In terms of seed germination, the Choi lab proposed a model whereby degradation of PIF1 leads to increased gibberellin (GA) levels via derepression of GA biosynthetic genes and repression of a GA catabolic gene [44]. This model provides a mechanistic explanation for how phytochromes regulate GA biosynthesis.

PIF5/PIL6

PIF5 was first characterized by Fujimori et al. [45], though it had been shown to interact with APRR1/TOC1 previously [35]. Fujimori et al. isolated a *PIL6* loss-of-function allele (*pil6-1*) and generated a *PIL6* overexpression line. They used these tools to show that *PIL6* is a negative regulator of the phyB-mediated phytochrome signal transduction pathway, with *pil6-1* seedlings hypersensitive to Rc but not FRc or Bc. Accordingly, seedlings overexpessing *PIL6* exhibit a hyposensitive phenotype under Rc. And while *pil6-1* adult plants are indistinguishable from wild-type, adult plants overexpressing *PIL6* exhibit elongated petioles and early flowering under SD and LD, similar to *phyB* mutant plants. *PIL6* transcript exhibits a diurnal rhythm under 12 h light/12 h dark cycles, but *CCA1* and *APRR1/TOC1* circadian rhythms are unaffected in plants with altered *PIL6* levels. This suggests that while PIL6 can physically interact with APRR1/TOC1, *PIL6* is downstream of the circadian clock. The authors also show that PIL6 can interact with PIF3 in a yeast two-hybrid assay.

In a recent paper by the Quail lab the authors observe phenotypes reminiscent of elevated ethylene levels in dark grown seedlings overexpressing *PIF5/PIL6* [46]. Accordingly, *pif5* mutants fail to maintain a tight apical hook when grown in darkness. The authors demonstrate that seedlings overexpressing *PIF5* have elevated levels of ethylene biosynthetic enzymes *ACS4* and *ACS8*, and increased ethylene levels in etiolated seedlings. The triple response phenotype of seedlings overexpressing *PIF5* can be rescued by blocking the ethylene receptor with $AgNO_3$. And while *pif5* mutants contain wild-type ethylene levels, the authors argue that regulation of ethylene levels by endogenous PIF5 is masked by genetic redundancy. They point out that

overexpression of closely related family members (including PIF1, PIF3, and PIF4) does not result in the triple response phenotype seen in seedlings overexpressing *PIF5*, suggesting that this capacity is specific to PIF5. Interestingly, data show that PIF5 levels affect phy protein levels. The authors show that overexpression of PIF5 leads to decreased levels of phyB (and phyC) and increased levels of phyA, while *pif5* mutants have increased phyB and phyC levels. phyA degradation is also delayed in seedlings overexpressing *PIF5*. They show that hypocotyl lengths in Rc grown *pif5* mutants and seedlings overexpressing *PIF5* can be correlated to increased and decreased phyB levels, respectively. Interestingly, a *PIF5* overexpression line containing a mutation in the APB of PIF5 exhibits the triple response phenotype in dark grown seedlings but lacks the hyposensitive phenotype (and decrease in phyB levels) in Rc grown seedlings. The authors use the above data to suggest that PIF5 functions by distinct mechanisms in the dark and in Rc. Previously, the Quail lab had shown that phyA and phyB act redundantly to phosphorylate PIF5 upon exposure to light, leading to its degradation via the proteasome [47]. Together these papers suggest that the light-mediated interaction between PIF5 and phytochromes leads to the destruction of both.

PIL2/PIF6

PIL2 was identified by Yamashino et al., as discussed above [35]. In addition to its interaction with APRR1/TOC1, PIL2 transcript levels were reported to decrease slightly in etiolated seedlings moved to WLc compared to etiolated seedlings [35]. Khanna et al. demonstrate that PIL2/PIF6 binds specifically to phyB in the Pfr form, with a binding capacity similar to that of PIF3 [13]. The C-terminus of PIL2/PIF6 may

negatively regulate its interaction between with phyB Pfr as the APB of PIL2/PIF6 alone binds better than full-length PIL2/PIF6.

PIL2 was also identified in a microarray experiment that identified genes upregulated in response to low R/FR [36]. Like *PIL1*, expression of *PIL2* in response to low R/FR is gated by the circadian clock. However, the derepression of *PIL2* by low R/FR occurs more slowly than *PIL1*, suggesting that *PIL2* may be involved in a long term response to shade conditions.

Results

Using ClustalW (http://www.ebi.ac.uk/Tools/clustalw2/index.html) we performed an alignment using HFR1, PIF1, PIF3, PIF4, PIF5, PIL1 and PIL2/PIF6 protein sequences. The alignment clearly identified both the previously described bHLH domain [48] and, in some proteins, the active phytochrome binding (APB) domain [13] (Figure 4.1). As the intervening regions are not conserved between the family members, we reasoned that using these amino acids as antigens should increase the chance of producing specific antibodies. We expressed these regions as GST fusion proteins in *E. coli* (Figure 4.2, A-H) and, after screening for rabbits with low background against *Arabidopsis* protein extracts, used the GST fusion proteins excised from SDS PAGE gels to immunize these rabbits for antibody production.

We isolated homozygous T-DNA insertion alleles [49] in the corresponding gene for each protein for which we attempted to produce an antibody. These alleles served not only as controls to test for antibody specificity, but also as experimental reagents. We tested the homozygous alleles for the presence of mRNA by qPCR

(Figure 4.3, A-P). We isolated two T-DNA insertion alleles (Salk_037727 and Salk_049497) for At1g02340 (*HFR1*). Analysis of *HFR1* mRNA in Salk_037727 by qPCR shows that this allele is likely a null allele, as no *HFR1* mRNA was detected (Figure 4.3A). *HFR1* mRNA is reduced approximately two-fold in Salk_049497 compared to wild-type (WT) (Figure 4.3B). This moderate reduction is likely due to the 5' UTR insertion site of Salk_049497. For At2g20180 (*PIF1*) we isolated two T-DNA insertion alleles (Salk_072677 and Salk_131872). qPCR analysis indicates that *PIF1* mRNA is significantly reduced in Salk_072677 compared to WT (Figure 4.3C). In contrast, *PIF1* mRNA is higher than WT in Salk_131872 (Figure 4.3D and E). We verified this result using primer sets 5' and 3' of the insertion site (Figure 4.3D and E, respectively). As both insertions reside in the same exon, the reason for the discrepancy between the two alleles is unclear. We isolated two insertion alleles (Salk_081927 and Salk_030753) for At1g09530 (*PIF3*). Salk_081927 is likely a null allele as no *PIF3* mRNA was detected by qPCR (Figure 4.3F). However, Salk_030753 shows a slight increase in *PIF3* mRNA compared to WT (Figure 4.3G and H). We verified this result using primer sets 5' and 3' of the insertion site (Figure 4.3G and H, respectively). Interestingly, the insertion sites of both Salk_081927 and Salk_030753 are within the fourth intron of the *PIF3* gene. It is possible that, despite the T-DNA insertion, the *PIF3* mRNA is transcribed and the intron containing the T-DNA is spliced correctly in Salk_030753. However, as Salk_030753 is the *pif3-1* allele used by Giltsu Choi's lab [6], it is more likely that while *PIF3* mRNA is present no functional protein is produced. We isolated two T-DNA insertion alleles (Salk_087012 and Salk_072306) for At3g59060 (*PIF5*). qPCR analysis indicates that Salk_087012

is likely a null allele as no *PIF5* mRNA was detected (Figure 4.3I). The moderate three-fold reduction in *PIF5* mRNA observed in Salk_072306 (Figure 4.3J) is likely due to the 5' insertion site of the T-DNA. We isolated two T-DNA insertion alleles (Salk_043937 and Salk_025372) for At2g46970 (*PIL1*). *PIL1* mRNA in Salk_043937 was greatly reduced compared to WT, suggesting that this T-DNA insertion allele is likely a null (Figure 4.3K). However, qPCR analysis of Salk_025372 showed an increase in *PIL1* mRNA compared to WT (Figure 4.3L and M). We verified this result using primer sets 5' and 3' of the insertion site (Figure 4.3L and M, respectively). The insertion site of Salk_043937 is within the fourth exon of *PIL1*, while that of Salk_025372 is within the fifth intron. This difference in insertion site may explain the difference in mRNA level, similar to the situation for *PIF3*. We isolated three T-DNA insertion alleles (Salk_090239, Salk_147579, and Salk_040838) for At3g62090 (*PIL2/PIF6*). None of the three alleles displayed a reduction of *PIL2/PIF6* mRNA compared to WT (Figure 4.3N-P). We obtained a *PIF4* insertion allele from Dr. Christian Fankhauser (University of Lausanne). Thus, with the exception of At3g62090, we have at least one null T-DNA insertion allele for each member of this bHLH subfamily.

We tested the progress of antibody production using test bleeds from immunized rabbits. Based on published data regarding protein expression or regulation of mRNA, we devised a condition for each bHLH protein where the protein is expected to be present and a condition where the protein is expected to be absent (see Materials and Methods). Proteins were extracted from *Arabidopsis* seedlings grown

under the appropriate conditions, and western blots were performed using sera from the test bleeds (Figure 4.4 A-K).

PIF3 is regulated in a light-dependent manner, with accumulation in the dark and rapid degradation in response to light [7]. Using unpurified PIF3 sera we were able to detect a band of the correct molecular weight in dark grown seedlings that is absent from WLc grown seedlings (Figures 4A and B). In a time course experiment we observed the disappearance of a band that is present in dark grown seedlings but absent in seedlings exposed to 5 or 10 min Rc (Figure 4.4C). PIF3 antibodies have been published previously [7, 12]. The stability of PIF4 and PIF5 has also been shown to be light dependent, with accumulation of the proteins in the dark and disappearance in the light [30]. Lorrain et al. showed that under monochromatic light, only Rc is sufficient to cause a reduction in PIF4 and PIF5 protein levels [31]. Work from the Quail lab [47] showed that a Rp given to dark grown seedlings is sufficient to cause degradation of PIF5. We used this information to verify our PIF4 and PIF5 antibodies. Using unpurified PIF4 sera, we observe a band of the correct molecular weight (48.4 kDa) that is present in dark grown seedlings but absent in dark grown seedlings given a Rp and then returned to darkness for 30 min (Figure 4.4D). Further, in a time course experiment (Figure 4.4E) we observed the disappearance of a band that likely corresponds to PIF4 in seedlings given a Rp and then returned to darkness. Using unpurified PIF5 sera and tissue from the same conditions as above, we also observe the disappearance of a band that likely corresponds to PIF5 (Figure 4.4F). The observed band migrated at a slightly higher molecular weight than predicted, though PIF5 is phosphorylated prior to degradation [47]. While an antibody for PIF5 does

exist, the published data on regulation of PIF4 and PIF5 protein levels has relied largely on tagged PIF4 and PIF5 alleles expressed from a constitutive promoter.

No information is available regarding the post-transcriptional regulation of PIL1 or PIL2/PIF6. According to work by Yamashino et al., *PIL2* mRNA is present at highest levels in the dark, is decreased upon WLc exposure within one hour, but returns to near dark levels after seven hours in WLc [35]. In the same paper, *PIL1* mRNA was shown to be present in dark grown seedlings but rapidly downregulated in response to WLc. A recent paper confirmed and extended this finding by showing that *PIL1* mRNA is rapidly downregulated by Rc but can be derepressed by a subsequent FRp [38]. *PIL1* mRNA is also induced in response to low R/FR ratios [37]. Unpublished data from our lab shows that *PIL1* expression is low in dark grown seedlings, but upregulated in response to FRc (Lin Li and Joanne Chory, unpublished data). The reason for the discrepancy between findings in our lab and published data is unclear. Using unpurified PIL2/PIF6 sera we observed a band of approximately the correct molecular weight that is present in dark grown seedlings and absent in seedlings grown in WLc (Figure 4.4G and H). This finding is consistent with published *PIL2/PIF6* mRNA expression. We used tissue from seedlings grown in several conditions to test unpurified PIL1 sera. Using tissue from seedlings exposed to one hour of FRc we observe a band migrating slightly higher than the predicted molecular weight (Figure 4.4I). This band is absent in dark grown seedlings. This finding would lend support to the unpublished data from our lab (see above). Using tissue from seedlings grown in the dark we were able to detect a band migrating slightly lower than the predicted molecular weight. This band is absent in tissue from

WLc grown seedlings (Figure 4.4J and K). This finding would be consistent with the published reports on *PIL1* mRNA. Further experiments are necessary to determine which band corresponds to PIL1.

We were able to produce antibodies to PIF3, PIF4, PIF5, PIL1, and PIL2/PIF6. However, using unpurified sera, we were unable to detect either HFR1 or PIF1 protein under the conditions tested. The negative results may stem from a lack of antibody production in these rabbits, a low level of HFR1 or PIF1 protein, or a low antibody titer. An antibody for PIF1 has been recently published but was affinity purified prior to use [43]. Antibodies to HFR1 have been published [24, 28]. Interestingly, as part of a collaboration, we provided Dr. Meng Chen (Duke University) with unpurified sera from rabbits used to produce antibodies against PIF1, PIF3, PIF4, and PIF5. He has purified the sera and shown that the antibodies can be used to detect PIF1, PIF3 and PIF5 in *Arabidopsis* seedlings (Figure 4.5, A-C). Purification of PIF4 antibodies is still underway in his lab. This finding demonstrates that PIF1 antibodies are present and can be purified from sera, and suggests that HFR1 antibodies might also be recovered from unpurified sera.

Taken together, we have generated antibodies against PIF1, PIF3, PIF4, PIF5, PIL1, and PIL2/PIF6 (Table I). As stated above, it remains possible that HFR1 antibodies could be recovered by purification of sera. Antibodies against PIF4, PIL1, and PIL2/PIF6 have not been published, and as such represent unique tools to study the regulation of these proteins and their role in phytochrome signaling. Moreover, the collection of antibodies reported here provides a resource not available elsewhere. This panel can be used to quickly and easily evaluate new phytochrome signaling

candidates, and to begin to answer outstanding questions regarding the biological function of these important phytochrome signaling intermediates.

Future Directions

The reagents presented here provide the tools to answer many outstanding questions regarding the role of PIFs, PILs and HFR1 in phytochrome signaling. To begin, there are two "low hanging fruit" experiments easily performed with these antibodies. No information exists regarding the regulation of PIL1 or PIL2/PIF6 at the protein level. As discussed above, the stability of many of the bHLH family members is regulated at the protein level by light via phytochromes, and it is likely that a similar situation exists for PIL1 and PIL2/PIF6. *PIL1* and *PIL2/PIF6* are both upregulated in response to low R/FR, albeit with different kinetics. Based on this, it has been speculated that PIL1 mediates an immediate response to shade, while PIL2 is involved in a long term response to shade [36]. Information regarding the stability of these proteins under shade conditions would provide much insight as to their roles in the shade avoidance response. Using previous papers in the field as a guide, data regarding regulation of PIL1 and PIL2/PIF6 at the protein level should form the basis for two publications.

The successful outcome of additional experiments depends on the competency of the antibodies for immunoprecipitation (IP). Only with PIF3 and PIF4 have any direct transcriptional targets of the PIF/PILs been shown [32, 33]. Should the antibodies presented here prove useful in IPs, one could look at direct targets of the PIF/PILs using chromatin IP (chIP) in an effort to assemble the phytochrome signaling

transcriptional network. To date, little information has been published regarding PIF/PIL interactions in planta, with most physical interactions shown in vitro. Using GFP antibodies and seedlings expressing a GFP-tagged phyB, our lab has shown that immunoprecipitation in combination with mass spectrometry to identify interacting proteins is a powerful approach to understanding phytochrome signaling (Kazu Nito and Joanne Chory, unpublished data). These antibodies could potentially identify new partners as well as establish conditions under which known partners interact. An extension of this approach is the use of the antibodies to interrogate the heterodimerization status of the PIF/PILs in planta. Several family members have demonstrated the ability to heterodimerize in vitro, including PIF5 and PIF3 [45], HFR1 and PIF3 [16], and PIF4 and PIF3 [50]. None of these interactions have been verified in planta. Using various antibody combinations one could begin to identify the conditions under which dimerization occurs and the role that dimerization plays in phytochrome signaling.

Materials and Methods

Recombinant Protein Expression and Purification We used ClustalW (http://www.ebi.ac.uk/Tools/clustalw2/index.html) to perform an alignment of the following bHLH transcription factors: At1g02340, At3g62090, At2g46970, At2g20180.2, At2g43010.1, At3g59060.2, and At1g09530.1. Protein sequences were obtained from TAIR (http://www.arabidopsis.org). We designed primers to amplify the region between the APB (where applicable) and the bHLH domain of each protein and cloned these fragments into the pGEX-4T-1 GST fusion vector (GE Healthcare). PCR products were first cloned into pCR-Blunt II-TOPO (Invitrogen) according to manufacturer instructions, sequence verified, and subcloned into pGEX-4T-1 (GE Healthcare) as EcoRI/SalI fragments. DNA was amplified using the following primers: At1g02340: 10605 (5'-gaattcGGCATGATGTCAGAA-3') and 10606 (5'-gtcgactcaTCGAGTAACTGAAGG-3'); At3g62090: 10617 (5'-gaattcTCCAACGTTTCTCTG-3') and 10618 (5'-gtcgactcaGACCAAAGCTTTTCT-3'); At2g46970: 10613 (5'-gaattcCCAAAGAACAACGGT-3') and 10614 (5'-gtcgactcaAGTCACCGGCTTTCT-3'); At2g20180.2: 10609 (5'-gaattcAGACTTCACACCAAG-3') and 10610 (5'-gtcgactcaGGTAGATGTTGTTGA-3'); At2g43010.1: 10611 (5'-gaattcGAACAAACCCAAACC-3') and 10612 (5'-gtcgactcaGTTTGATCCTGATCG-3'); At3g59060.2: 10615 (5'-gaattcGAACCGTCAGTCCAA-3') and 10616 (5'-gtcgactcaAGTAGATCCTGACCG-3'); and At1g09530.1: 10607 (5'-gaattcTCGAGGAACATTCCT-3') and 10608 (5'-gtcgactcaTGAACCCAAACCCGT-3'). Plasmids were introduced into chemically competent *E. coli* strain BL21-CodonPlus (DE3)-RIPL (Stratagene) by heat shock

transformation. Individual colonies were used to inoculate 6 mL of Luria-Bertani (LB) broth containing 50 mg mL-1 carbenicillin. After overnight growth at 37∞C with shaking, the culture was diluted into 1 L of LB broth with carbenicillin and grown to an OD600 of approximately 1.0. Expression was induced by addition of isopropyl b-D-1-thiogalactopyranoside (IPTG) at a final concentration of 0.5 mM, and cells were grown for an additional 3-5 h. Cells were harvested by centrifugation for 10 min at 5,000 x g and stored at -70∞C until use. Frozen cells were resuspended in 10 mL of ice-cold PGE buffer (1x PBS, 10% [v/v] glycerol, 1 mM EDTA, 1 mM DTT, and one Complete Mini EDTA-free Protease Inhibitor Cocktail Tablet [Roche]), lysozyme was added at a final concentration of 0.5 mg mL-1 and the solution was stirred for 30 min at 4∞C. Cells were disrupted by sonication using a Sonic Dismembrator Model 500 (Fisher Scientific). DNase was added to the lysate at a final concentration of 75 mg mL-1 and the solution was stirred for 30 min at 4∞C. Lysate was clarified by centrifugation at 4∞C for 20 min at 20,000 x g. Supernatant was removed and centrifuged as above. Supernatant was then mixed with 500 mL of Glutathione Sepharose 4B (GE Healthcare) previously equilibrated in PGE buffer, and incubated overnight in an Econo-Pac Chromotography Column (Bio-Rad) at 4∞C on a rotisserie shaker. Column was washed twice with 10 mL ice-cold PGE buffer, and GST fusion proteins were eluted with 5 mL 50 mM Tris, pH 8.0 containing 15 mM glutathione.

Antibody Production GST fusion proteins were separated by SDS-PAGE using 10 % ClearPAGE gels (CBS Scientific). Bands of interest were excised and used as antigens for antibody production. Antibodies were produced in rabbits by Cocalico Biologicals,

Inc. (Reamstown, PA). Rabbits were pre-screened using protein from WLc grown *Arabidopsis* Col-0 seedlings. Two rabbits per antigen were used.

T-DNA Genotyping Genomic DNA was extracted using Edwards Buffer [51]. Salk T-DNA lines were genotyped using T-DNA primer LB18 (5'-GGCAATCAGCTGTTGCCCGTCTCACTGGTG-3') and the following gene-specific primers: Salk_037727: 10824 (5'-TTCGAATGATCAAAATGGGTAC-3') and 10825 (5'-ATGCGAAGGAGGATTTATTGG-3');

Salk_049497: 10826 (5'-AACGGAGACGTCATCTTTTTG-3') and 10827 (5'-TTGATTATTCGACCTGCCAAG-3');

Salk_081927: 10828 (5'-TATGTTCTTCTGTTGGCTCGG-3') and 10829 (5'-GAACTGTGGTCCGTGGTTAAC-3');

Salk_030753: 10830 (5'-AAGATAACCAAAAGGCTTGCC-3') and 10831 (5'-TTGCATAAGGCATTCCCATAC-3');

Salk_131872: 10834 (5'-GAAGCCTATCCAGTACCAACC-3') and 10835 (5'-TTCGATTTCGCTCTTTGACAC-3');

Salk_072677: 10836 (5'-TCCGTTTCTGTTACCAAATCC-3') and 10837 (5'-GGGTGAAGATGATGATCTTATGG-3');

Salk_140393: 10838 (5'-AATTCATCATCGGGGATTAGG-3') and 10839 (5'-CGTTTAATAAACACGGCTTCG-3');

Salk_043937: 10840 (5'-ACCCATGGGAGAGTAATGACC-3') and 10841 (5'-TGTTGTTCTTTAAAGAGGAAGTATGG-3');

Salk_025372: 10842 (5'-GCATCTTCTAAGTTTGAGGCG-3') and 10843 (5'-TGAAAATTAATGCTAATTAAGGATTTG-3');

Salk_025598: 12661 (5'- TTCATGCGAGAACAAGAAAGC-3') and 12662 (5'-GTCTGAGAAACACACGAAGGC-3');

Salk_087012: 10844 (5'-TGTTCCTTCCATAGCTGCAAC-3') and 10845 (5'-ATCTTCCATCCATTCAGAGGC-3');

Salk_072306: 10846 (5'-CATCTTCTGGTCTGTCCCAAC-3') and 10851 (5'-TGAAAGAGAAGCATAAGAGGGG-3');

Salk_090239: 10847 (5'-TTCGTTTTTGGAAACGACATC-3') and 10848 (5'-ACTCTGCGTTGAGACAAAACC-3');

Salk_147579: 10849 (5'-GGCAATCTGATATTCTGACGG-3') and 10850 (5'-CGATCCTTCACTGTCTTCAGTG-3');

Salk_040838: 12107 (5'-ACAGGAAATTCATTGCACCTG-3') and 12108 (5'-TCGTTTTCTTTTGACCAAAGC-3').

Seed Sterilization *Arabidopsis* seeds were sterilized by washing 10 min with 1 mL 70% EtOH containing 0.05% [v/v] Triton X-100, followed by washing 5 min with 1 mL 95% EtOH. Seeds were dried on Whatman filter paper, plated on 1/2 x Linsmaier and Skoog (Caisson Laboratories, Inc.) plates containing 0.8% agar and stratified in the dark for 3 d at 4∞C.

qPCR Analysis qPCR was performed using RNA extracted from seedlings sterilized and stratified as above, and grown for one week in (95mE) continuous white light (WLc). Total RNA was isolated from 100 mg of tissue using the Spectrum Plant Total RNA Kit (Sigma) according to manufacturer instructions. cDNA was synthesized from 5 mg total RNA using the Superscript III First Strand cDNA Synthesis Kit (Invitrogen) according to manufacturer instructions. qPCR was performed using

SYBR Green and the iCycler iQ Real-Time PCR Detection System (Bio-Rad). A standard curve was constructed for each primer using an equal mixture of all cDNAs. PCR reactions were performed in triplicate. Primers were as follows:

At1g02340: 11270 (5'-TAATAAGATGCGTAAGCTACAGCAACT-3') and 5147 (5'-CGAAACCTTGTCCGTCTTGTG-3');

At1g09530: 11271 (5'-TCAAGTGCAGATCATGTCAATGG-3') and 11272 (5'-ACCGCCGGTGGCAGATA-3');

At2g20180: 11273 (5'-CACCTCAGTTTCAGAATCAAGCAA-3') and 11274 (5'-TCACCCTGCTCGAACTTGG-3');

At2g43010: 11275 (5'-GTTACCTCGATTTCCGGTTATGG-3') and 11276 (5'-CCGGGATTGTTCTGAATTGC-3');

At2g46970: 11277 (5'-CAAATTGTTACAAGGATGATAAGGCTT-3') and 11278 (5'-ATTTGATAGCCTCATCCAACAATG-3');

At3g59060: 11279 (5'-AATGAAAGCTCTTCAAGAACTCATACC-3') and 11280 (5'-GCTTTATCTGTTCTGCTGCAGTGA-3');

At3g62090: 11281 (5'-TCTCACAAGGACGACAACGAAT-3') and 11282 (5'-CATATAATTGATTGCTTCATCCAACA-3').

At5g15400 (U-Box) was used to normalize values: 3652 (5'-TGCGCTGCCAGATAATACACTATT-3') and 3653 (5'-TGCTGCCCAACATCAGGTT-3').

Antibody Testing Seeds were sterilized and stratified as above, and germination was broken with a 3 h WLc treatment. Based on published reports regarding conditions where proteins (or mRNA, if no protein data was available) were predicted to be

present and absent, seedlings were grown in the appropriate light conditions for one week. For HFR1, seedlings were grown in the dark (absent) and in the dark but given a 2 h WLc treatment (present) [23]. For PIF1, seedlings were grown in the dark but given a 1h Rc treatment (absent) and grown in the dark (present) [42]. For PIL1, seedlings were grown in the dark but given a 1 h FRc treatment (present) and grown in the dark (absent) [37]. For PIL2/PIF6, seedlings were grown in the dark (present) and grown in WLc (absent) [35]. For PIF3, seedlings were grown in the dark (present) and grown in WLc (absent) [7]. For PIF4 and PIF5, seedlings were grown in the dark (present) and grown in the dark but given a 5 m Rp (25.6 mE) followed by a 30 m incubation in dark [31]. Seedlings for the PIF4 time course were grown in the dark for 1 week, exposed to a 5 min Rp (25.6 mE), then incubated in the dark. Samples were taken at 2, 5, 10, and 30 min after transfer to dark. Total protein was extracted using the Urea/SDS/Salt extraction buffer (see below). Seedlings for the PIF3 time course were grown in the dark for 1 week, then exposed to Rc (20 mE). Samples were taken at 5, 10, 30, and 60 min. Total protein was extracted using the Urea/SDS/Salt extraction (see below). All tissue was collected in 2 mL tubes containing 3 metal beads, frozen in liquid nitrogen, and disrupted using a MM300 bead disruptor (Retsch). Five different protein extraction protocols were used. For the Boiling SDS extraction, disrupted tissue was resuspended in Boiling SDS Buffer (100 mM MOPS, pH 7.6, 40 mM BME, 5% SDS, 10% glycerol, 4 mM EDTA, and Complete Protease Inhibitor Cocktail [Roche]) heated to 95∞C. The resuspended tissue was clarified by centrifugation at room temperature for 5 min at 5000 x g. 5x Laemmli dye was added to the supernatant. For the Urea extraction, disrupted tissue was resuspended in Urea

Extraction Buffer (20 mM Tris-HCl, pH 8.0, 0.33 M Sucrose, 10 mM EDTA, 5 mM DTT, and Complete Protease Inhibitor Cocktail [Roche]). The resuspended tissue was clarified by centrifugation at 4∞C for 7 min at 2000 x g and the resulting supernatant was centrifuged as above. The resulting supernatant was then centrifuged at 4∞C for 30 min at 20,000 x g. The supernatant was removed to a new tube and 5x Laemmli dye was added to both the supernatant and pellet. For the Salt extraction, disrupted tissue was resuspended in Salt Extraction Buffer (100 mM Tris-HCl, pH 8.0, 50 mM EDTA, 0.25 M NaCl, 0.7% SDS, and 1 mM DTT). Resuspended tissue was heated for 10 min at 65∞C then centrifuged for 10 min at 20,000 x g. 5x Laemmli was added to the supernatant. For the Urea/SDS/Salt extraction, disrupted tissue was resuspended in USS Buffer (100 mM Tris-HCl, pH 7.8, 4 M urea, 5% SDS, 15% Glycerol, 10 mM BME, and Complete Protease Inhibitor Cocktail [Roche]). The resuspended tissue was heated for 5 min at 95∞C then centrifuged at room temperature for 15 min at 15,000 x g. To the supernatant, 0.05% bromophenol blue was added. The Bio-Rad RC DC Protein Assay was used to determine total protein concentration. 100 mg of total protein was separated on 10 % ClearPAGE gels (CBS Scientific) and transferred to nitrocellulose. Western blots were performed using sera at concentrations indicated. Goat Anti-Rabbit HRP (Bio-Rad) was used as the secondary antibody at a dilution of 1:15000. Proteins were visualized using SuperSignal West Pico Chemiluminescent Substrate (Thermo Scientific).

Table 4.1. Summary of Results

Name	Gene	T-DNA Line	RNA null (qPCR)	Antibody
HFR1	At1g02340	Salk_037737	Y	N*
		Salk_049497	N	
PIF3	At1g09530	Salk_081927	Y	Y*
		Salk_030753	N	
PIL5/PIF1	At2g20180	Salk_131872	N	Y*
		Salk_072677	Y*	
PIF4	At2g43010	Salk_140393	n.d.	Y
		SAIL_1288_E07	n.d.	
PIL1	At2g46970	Salk_043937	Y	Y
		Salk_025372	N	
		Salk_025598	n.d.	
PIL6/PIF5	At3g59060	Salk_087012	Y	Y*
		Salk_072306	N	
PIL2/PIF6	At3g62090	Salk_090239	N	Y
		Salk_147579	N	
		Salk_040838	N	

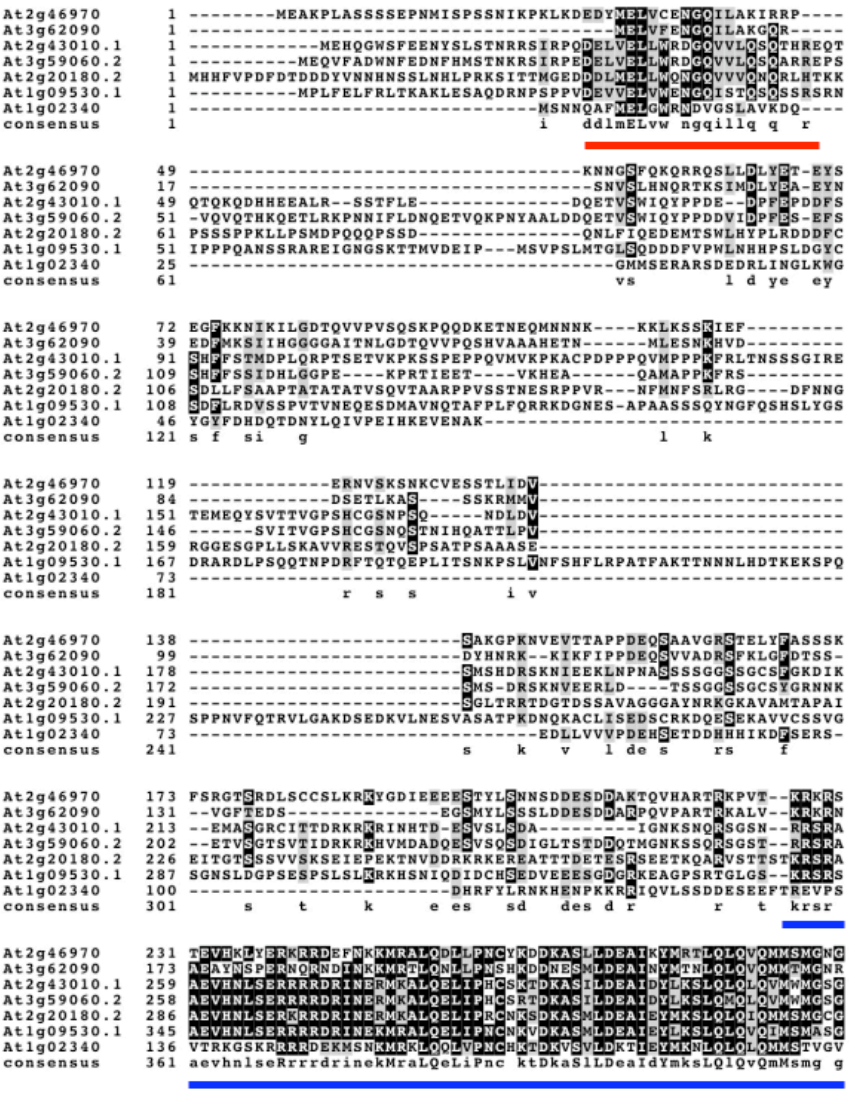

Figure 4.1. An alignment of the seven bHLH proteins. Alignment of HFR1 (At1g02340), PIF1 (At2g20180), PIF3 (At1g09530), PIF4 (At2g43010), PIF5 (At3g59060), PIL1 (At2g46970) and PIL2/PIF6 (At3g62090) was performed with ClustalW using protein sequences obtained from TAIR. Shown is the alignment of the NH-termini of the proteins up to, and including, the bHLH domain (underlined in blue). Active phytochrome binding domain (APB) is underlined in red. Intervening sequences were used as antigens.

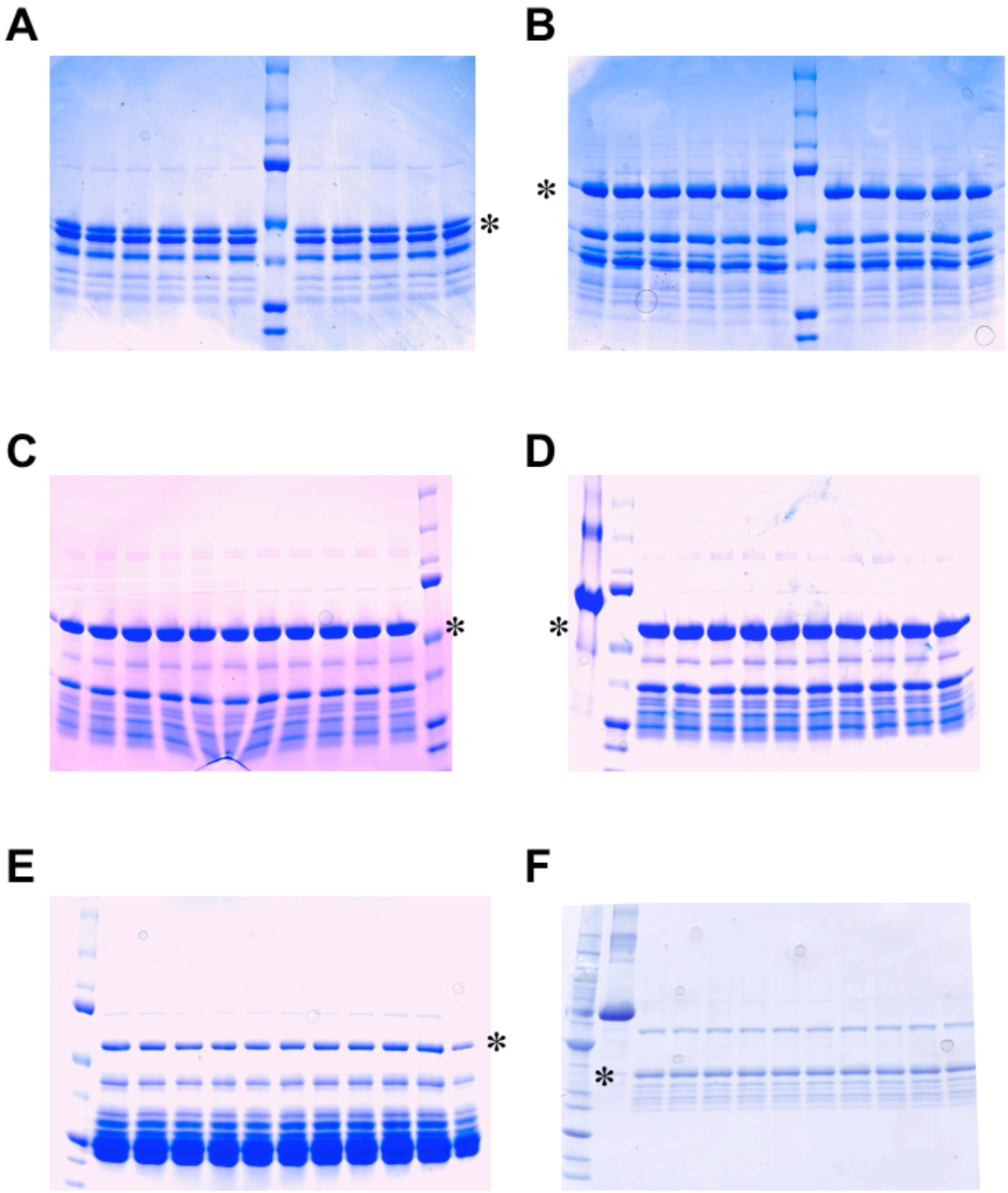

Figure 4.2. Expression of the truncated bHLH proteins as GST fusions. SDS PAGE gels showing the eluted GST fusion proteins. Asterisks (*) indicate protein bands excised from gels to be used as antigens. (**A**) PIL2/PIF6:GST (**B**) PIF3:GST (**C**) PIF5/PIL6:GST (**D**) HFR1:GST (**E**) PIF4:GST (**F**) PIF1/PIL5:GST (**G**) PIL1:GST.

G

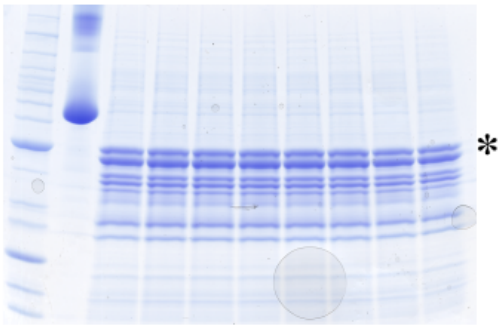

Figure 4.2. continued.

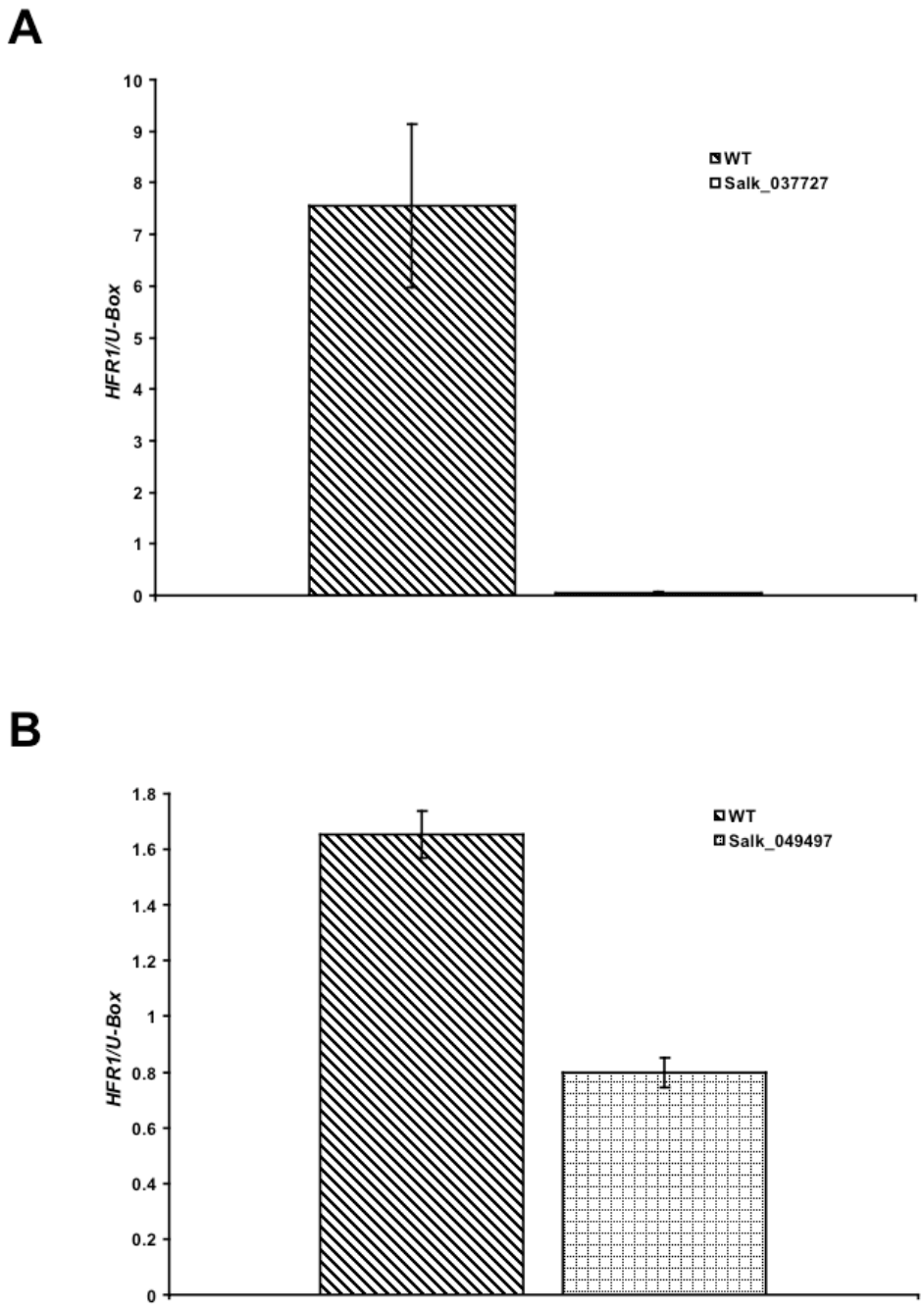

Figure 4.3. qPCR analysis of the T-DNA insertion alleles. Relative transcript levels in WLc grown seedlings. HFR1 (**A**) and (**B**); PIF1 (**C**), (**D**) and (**E**); PIF3 (**F**), (**G**) and (**H**); PIF5 (**I**) and (**J**); PIL1 (**K**), (**L**) and (**M**); PIL2 (**N**), (**O**), (**P**) and (**Q**).

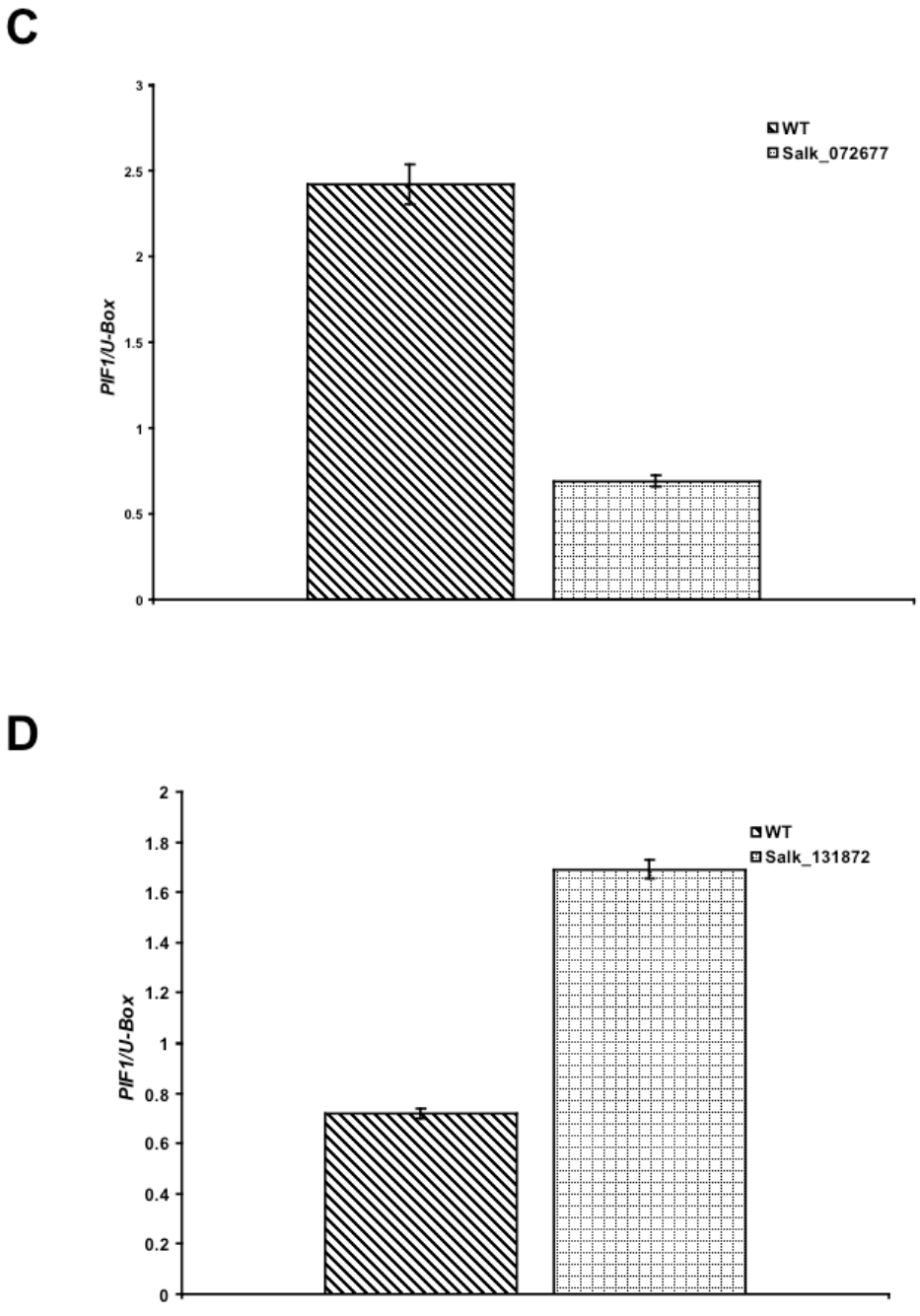

Figure 4.3. continued.

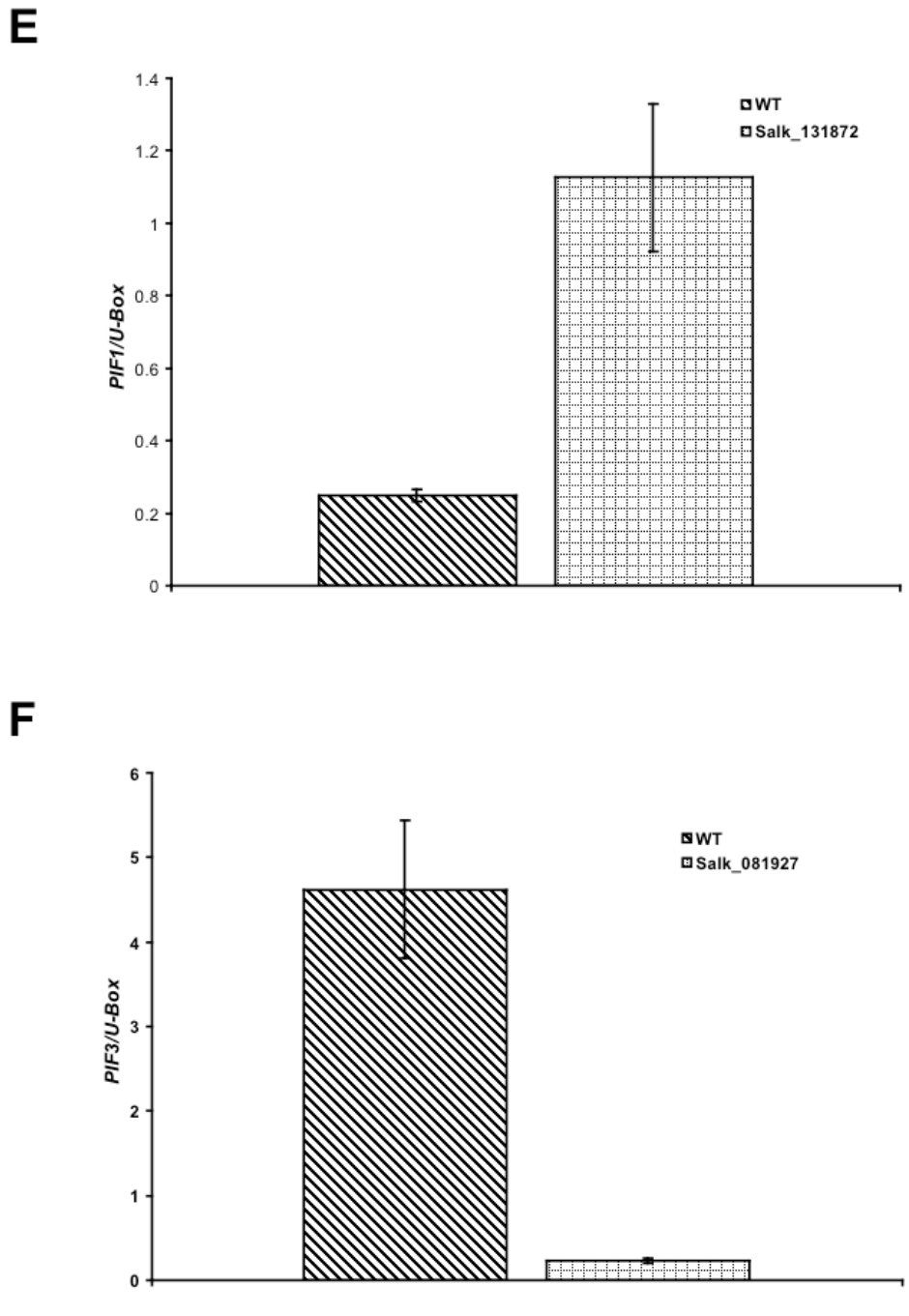

Figure 4.3. continued.

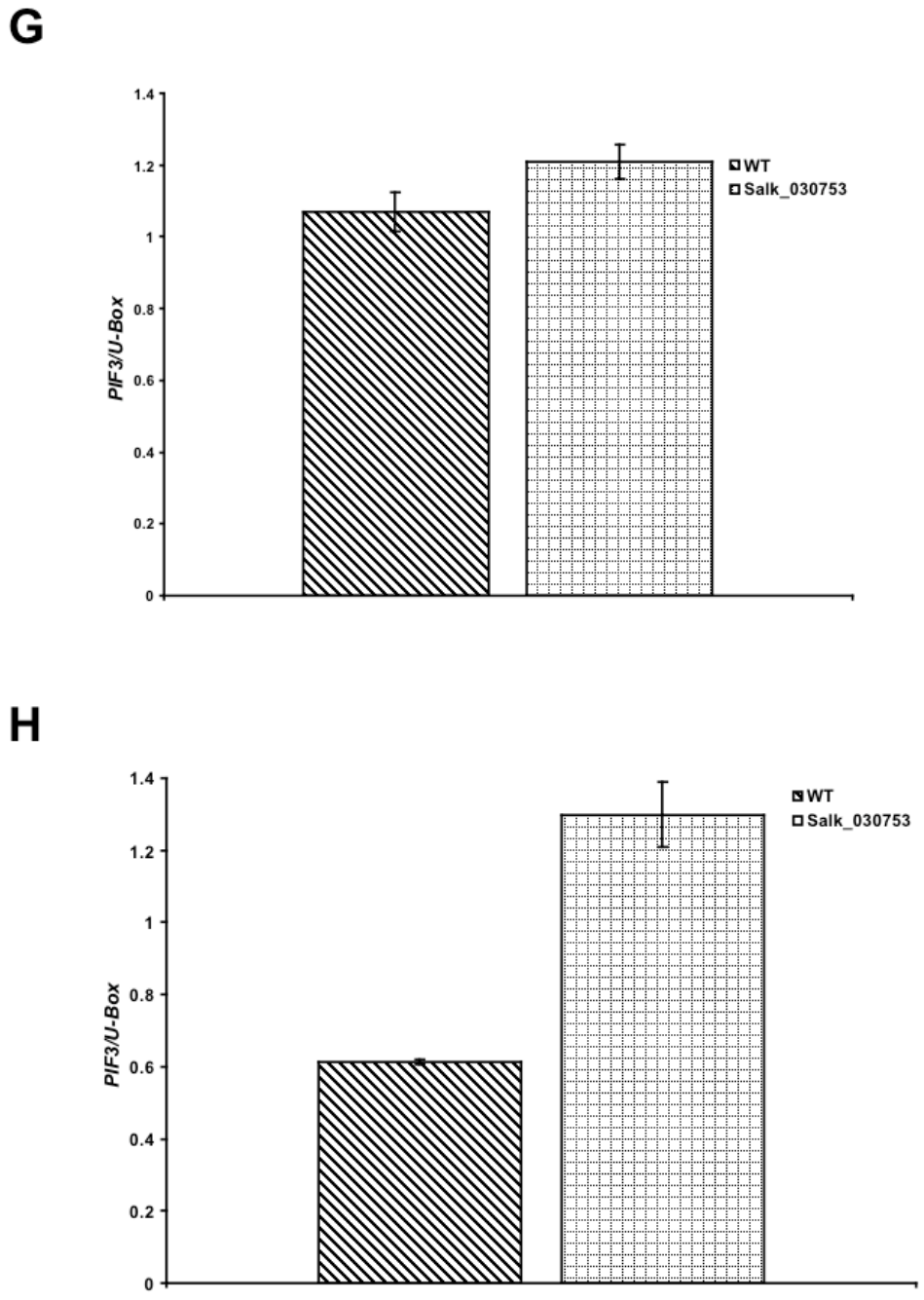

Figure 4.3. continued.

I

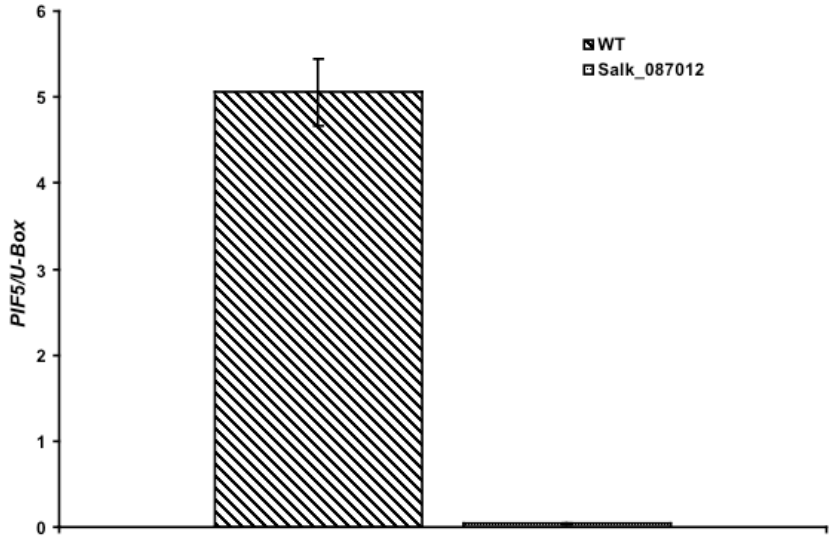

J

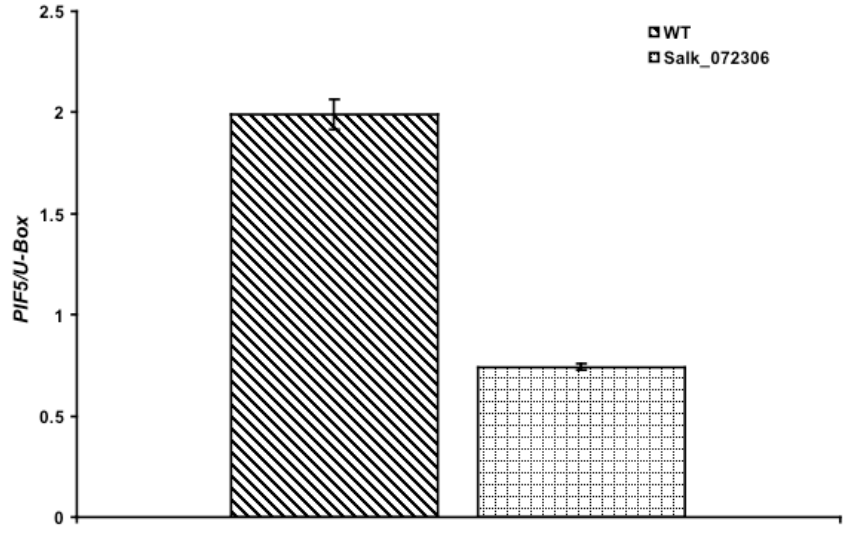

Figure 4.3. continued.

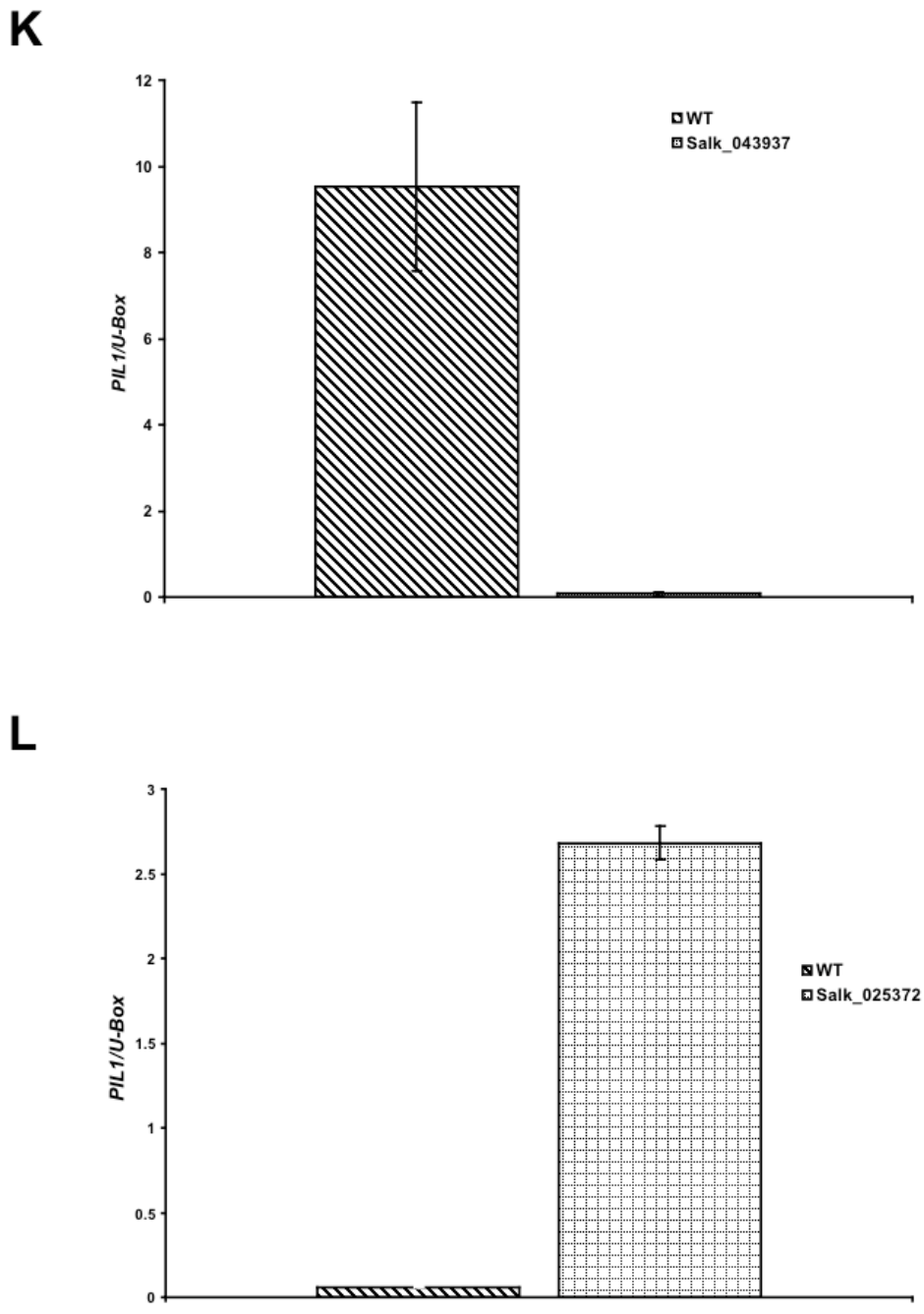

Figure 4.3. continued.

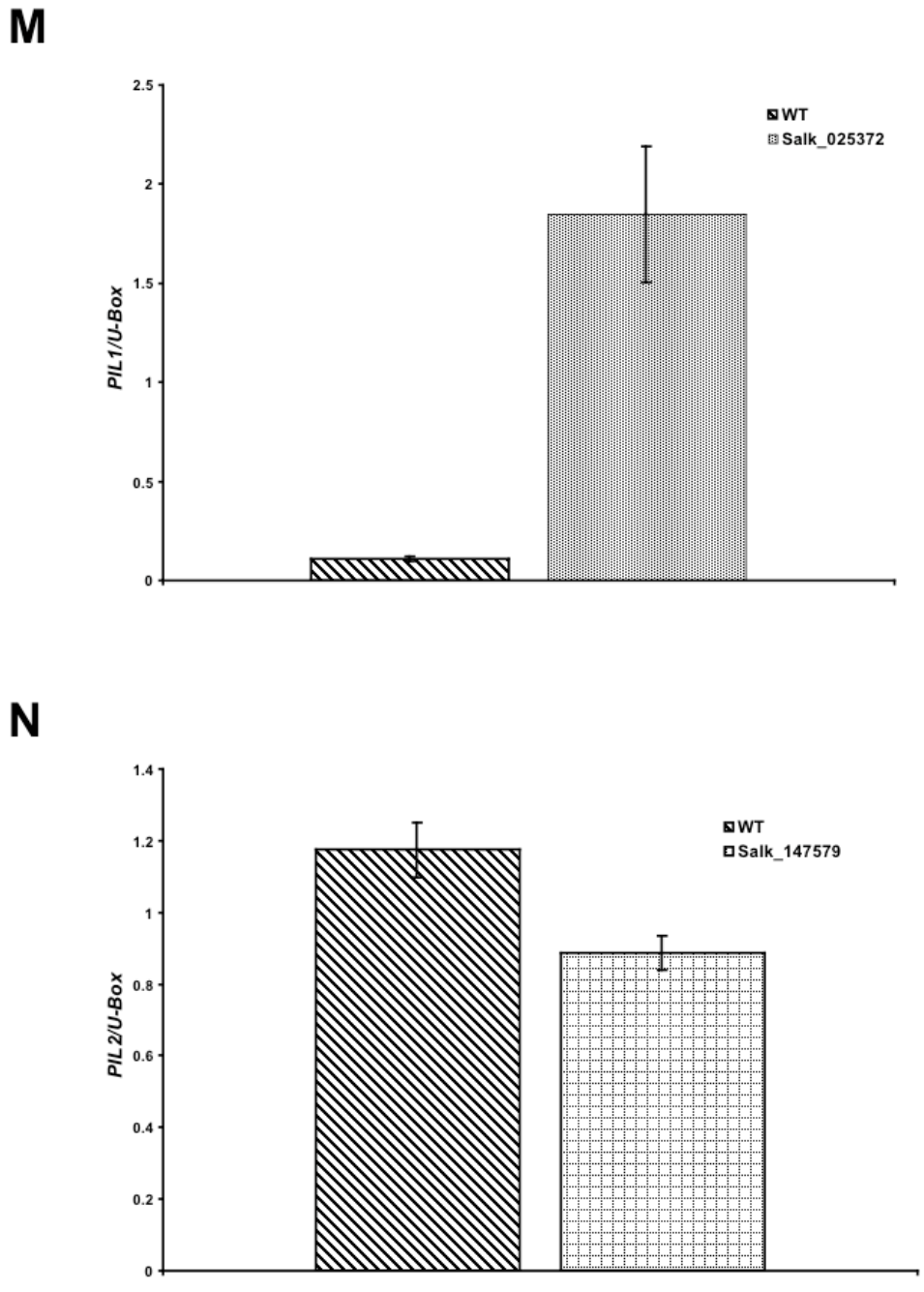

Figure 4.3. continued.

O

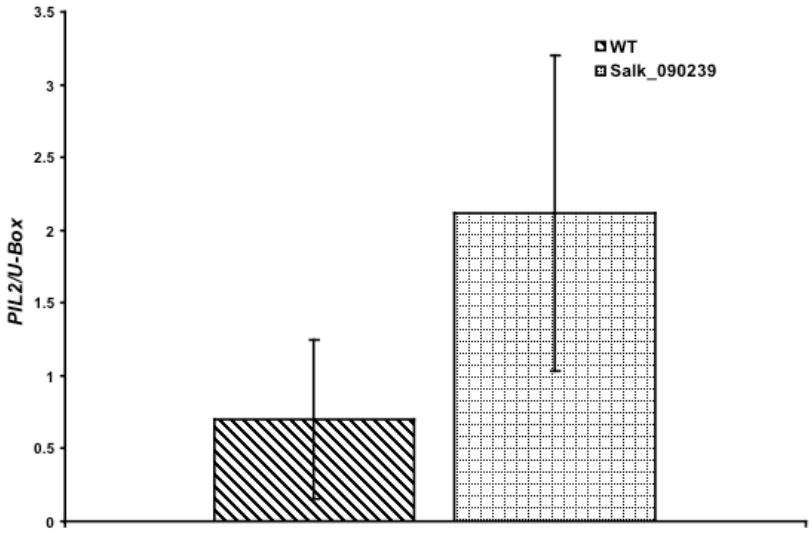

P

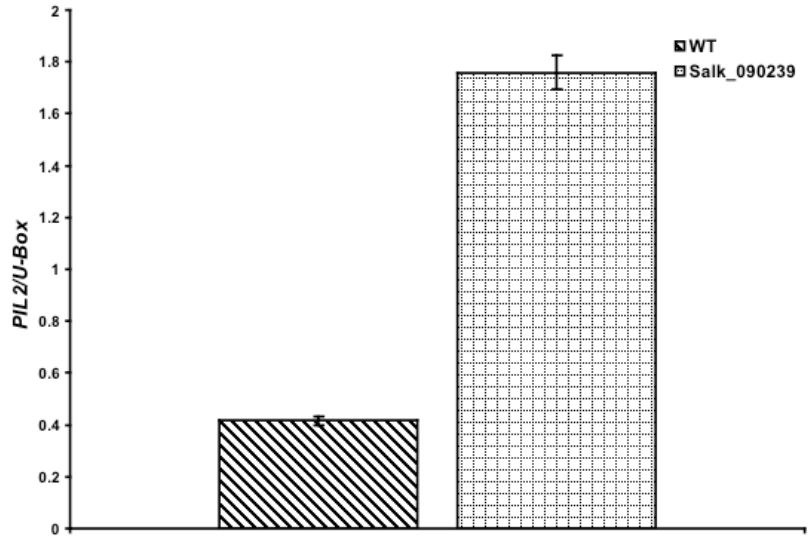

Figure 4.3. continued.

Q

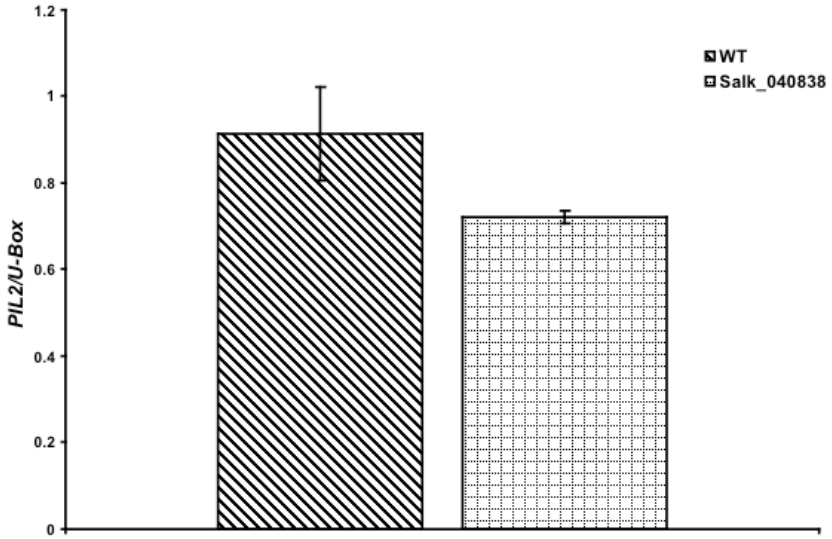

Figure 4.3. continued.

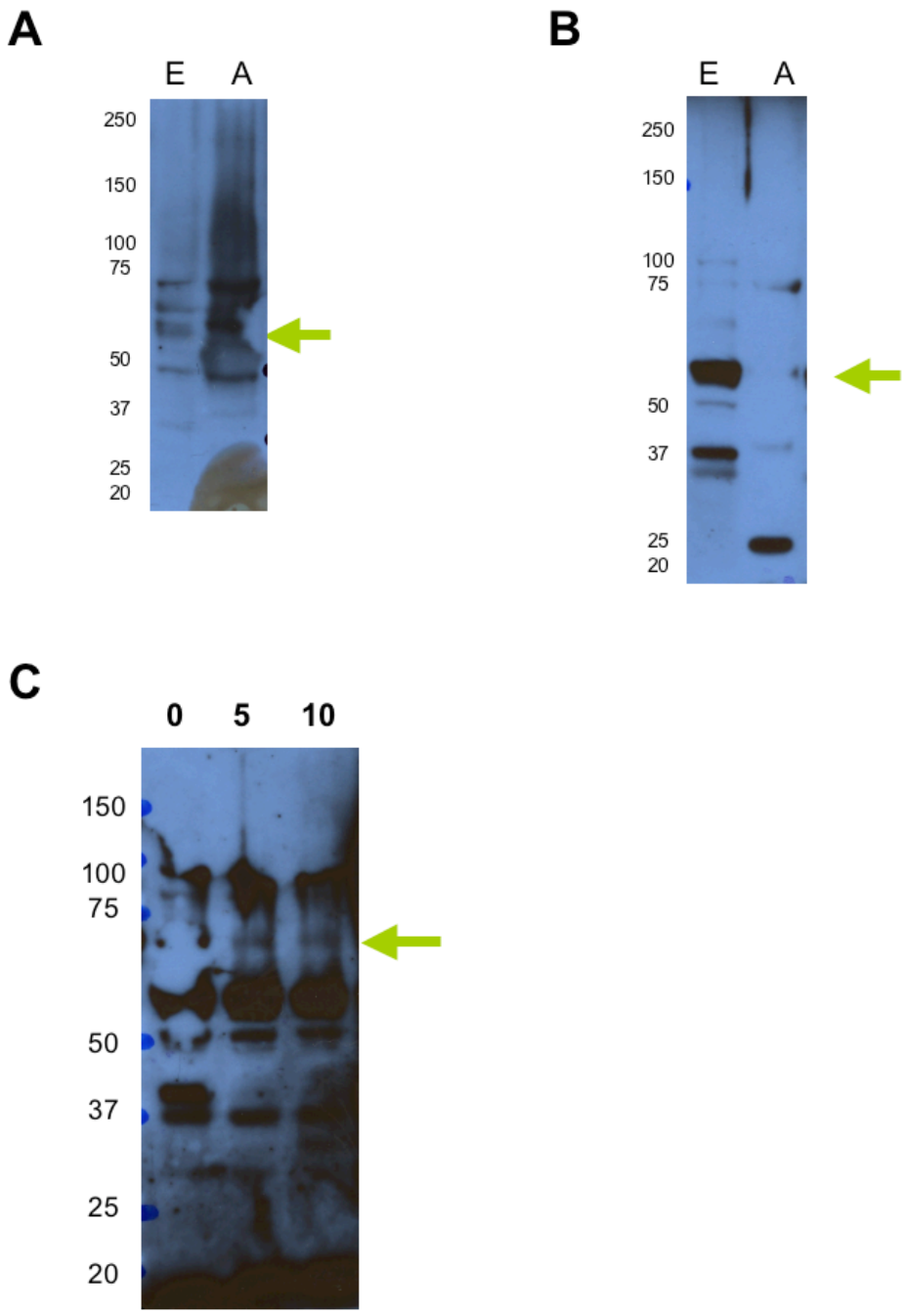

Figure 4.4. Antibody testing. Western blots with PIF3 (**A**) ,(**B**) and (**C**); PIF4 (**D**) and (**E**); PIF5 (**F**); PIL2/PIF6 (**G**) and (**H**); PIL1 (**I**), (**J**) and (**K**). E, expressed. A, absent.

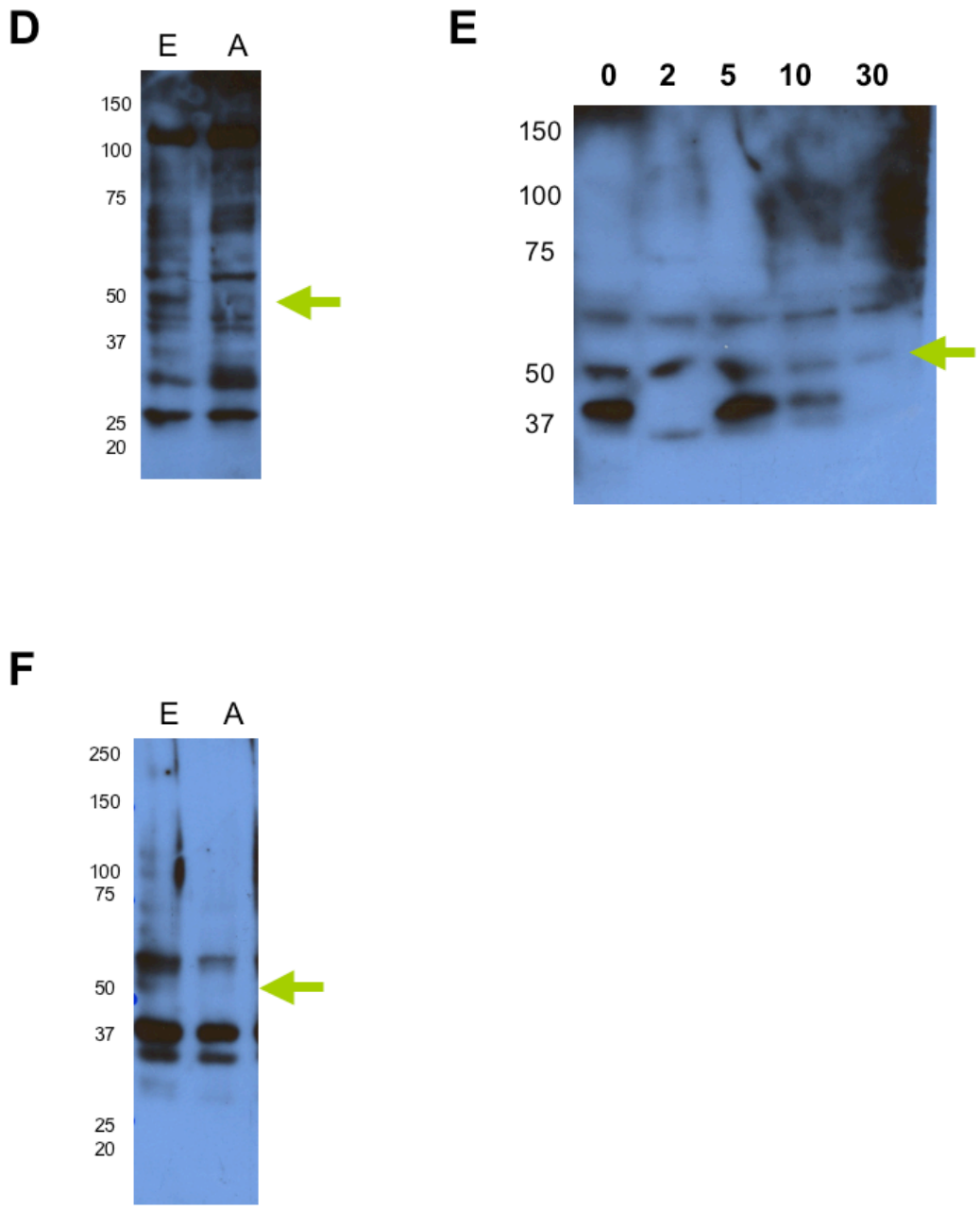

Figure 4.4. continued.

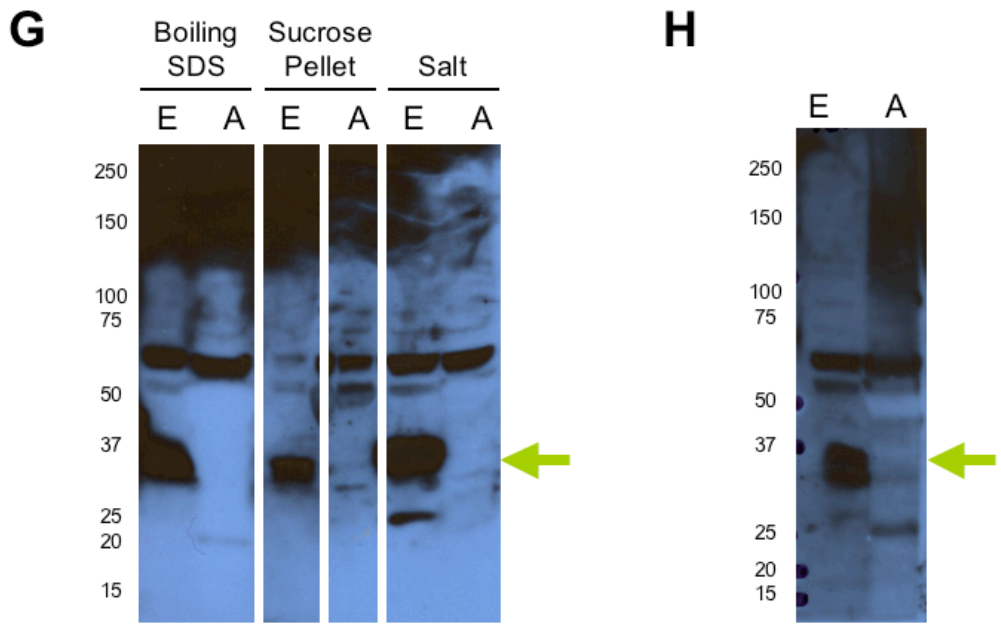

Figure 4.4. continued.

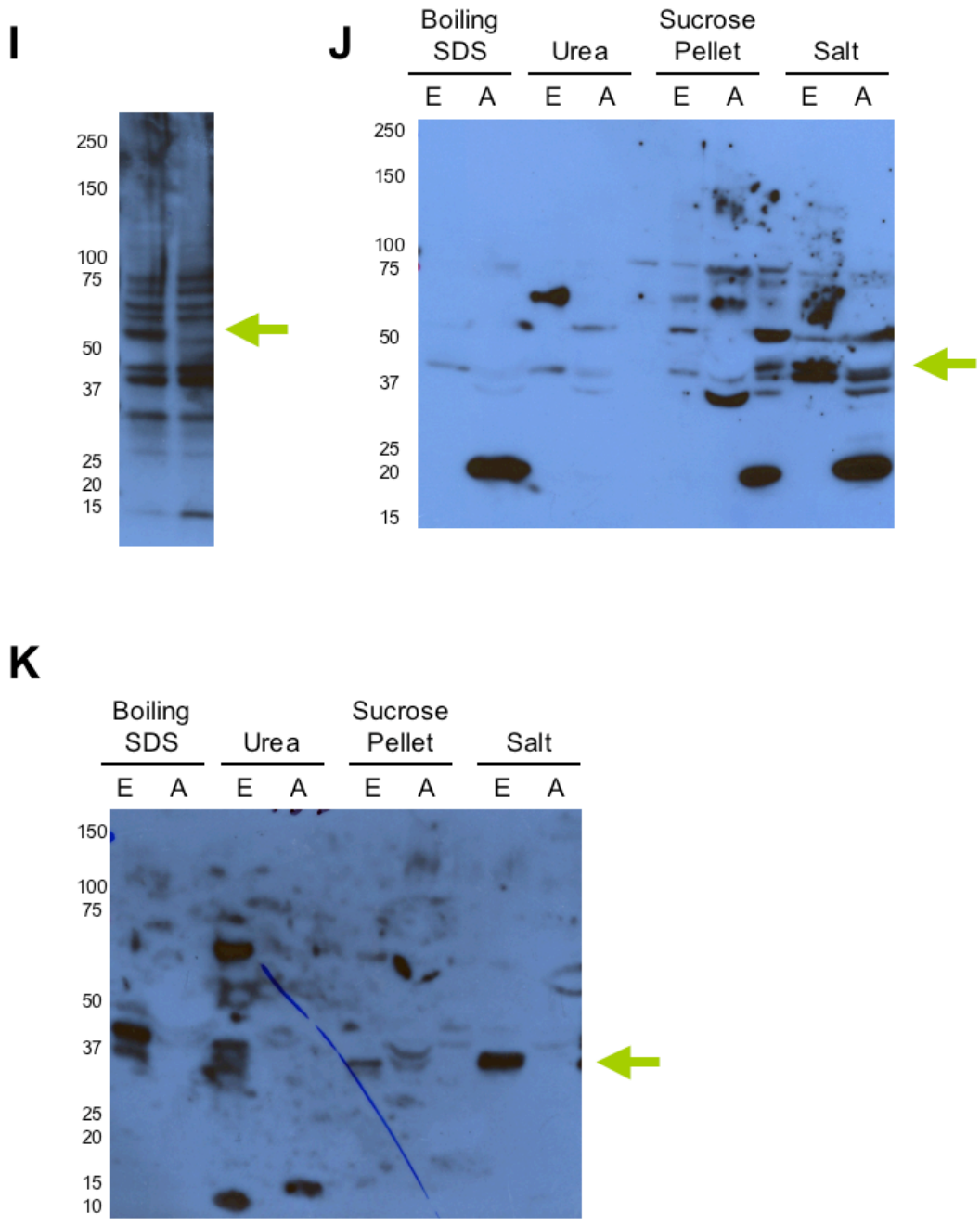

Figure 4.4. continued.

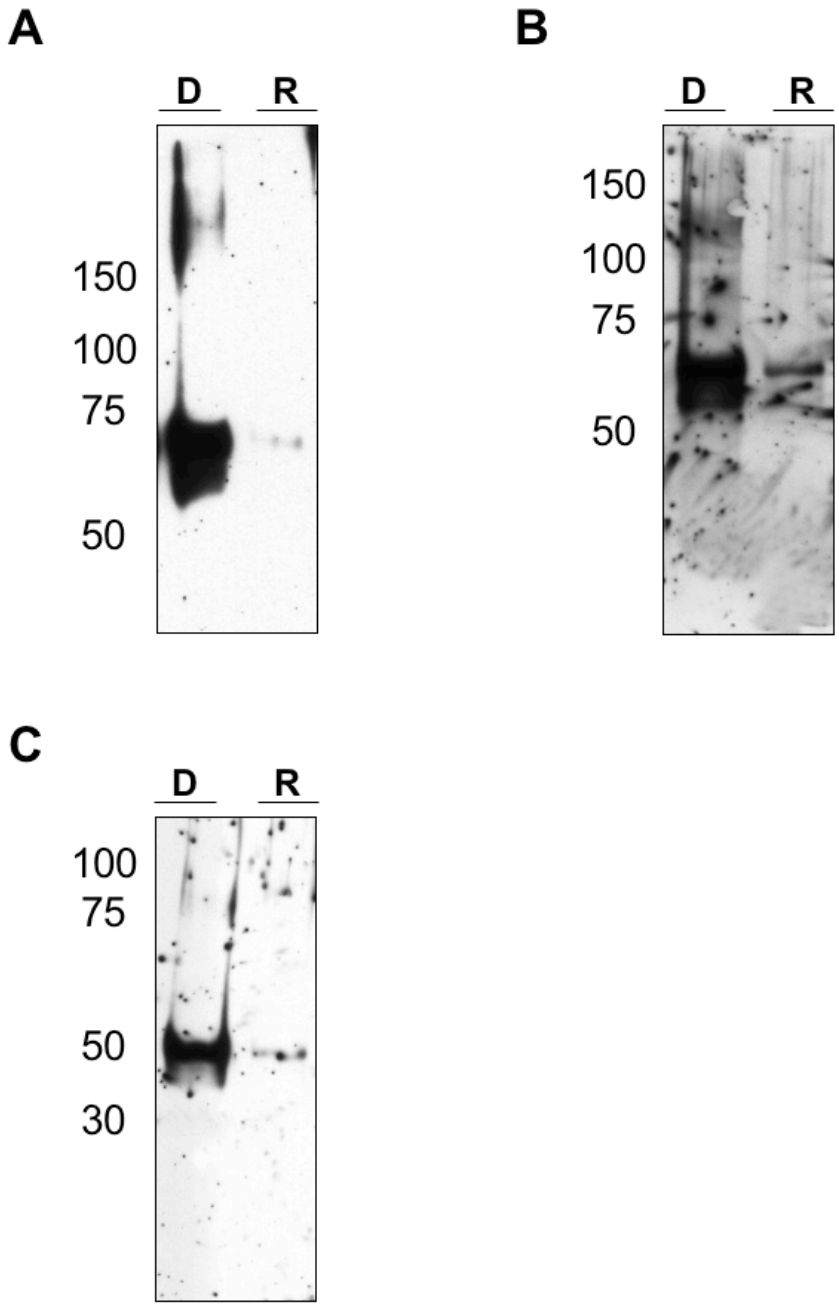

Figure 4.5. PIF1, PIF3, and PIF5 western blots. Protein was extracted from *Arabidopsis* (Col-0) seedlings and subjected to western blots with antibodies to PIF1 (**A**), PIF3 (**B**), and PIF5 (**C**). Western blots provided by Drs. Meng Chen and Meina Li (Duke University). D, 4 d continuous dark. R, 4 d continuous dark with 30 min R treatment.

References

1. Ni, M., Tepperman, J.M., and Quail, P.H. (1998). PIF3, a phytochrome-interacting factor necessary for normal photoinduced signal transduction, is a novel basic helix-loop-helix protein. Cell *95*, 657-667.

2. Halliday, K.J., Hudson, M., Ni, M., Qin, M., and Quail, P.H. (1999). poc1: An arabidopsis mutant perturbed in phytochrome signaling because of a T DNA insertion in the promoter of PIF3, a gene encoding a phytochrome-interacting bHLH protein. Proceedings of the National Academy of Sciences of the United States of America *96*, 5832-5837.

3. Ni, M., Tepperman, J.M., and Quail, P.H. (1999). Binding of phytochrome B to its nuclear signalling partner PIF3 is reversibly induced by light. Nature *400*, 781-784.

4. Martínez-García, J.F., Huq, E., and Quail, P.H. (2000). Direct targeting of light signals to a promoter element-bound transcription factor. Science (New York, N.Y *288*, 859-863.

5. Zhu, Y., Tepperman, J.M., Fairchild, C.D., and Quail, P.H. (2000). Phytochrome B binds with greater apparent affinity than phytochrome A to the basic helix-loop-helix factor PIF3 in a reaction requiring the PAS domain of PIF3. Proceedings of the National Academy of Sciences of the United States of America *97*, 13419-13424.

6. Kim, J., Yi, H., Choi, G., Shin, B., and Song, P.S. (2003). Functional characterization of phytochrome interacting factor 3 in phytochrome-mediated light signal transduction. The Plant cell *15*, 2399-2407.

7. Bauer, D., Viczian, A., Kircher, S., Nobis, T., Nitschke, R., Kunkel, T., Panigrahi, K.C., Adam, E., Fejes, E., Schafer, E., et al. (2004). Constitutive photomorphogenesis 1 and multiple photoreceptors control degradation of phytochrome interacting factor 3, a transcription factor required for light signaling in Arabidopsis. The Plant cell *16*, 1433-1445.

8. Monte, E., Tepperman, J.M., Al-Sady, B., Kaczorowski, K.A., Alonso, J.M., Ecker, J.R., Li, X., Zhang, Y., and Quail, P.H. (2004). The phytochrome-interacting transcription factor, PIF3, acts early, selectively, and positively in light-induced chloroplast development. Proceedings of the National Academy of Sciences of the United States of America *101*, 16091-16098.

9. Oda, A., Fujiwara, S., Kamada, H., Coupland, G., and Mizoguchi, T. (2004). Antisense suppression of the Arabidopsis PIF3 gene does not affect circadian rhythms but causes early flowering and increases FT expression. FEBS letters *557*, 259-264.

10. Viczian, A., Kircher, S., Fejes, E., Millar, A.J., Schafer, E., Kozma-Bognar, L., and Nagy, F. (2005). Functional characterization of phytochrome interacting factor 3 for the Arabidopsis thaliana circadian clockwork. Plant & cell physiology *46*, 1591-1602.

11. Park, E., Kim, J., Lee, Y., Shin, J., Oh, E., Chung, W.I., Liu, J.R., and Choi, G. (2004). Degradation of phytochrome interacting factor 3 in phytochrome-mediated light signaling. Plant & cell physiology *45*, 968-975.

12. Al-Sady, B., Ni, W., Kircher, S., Schafer, E., and Quail, P.H. (2006). Photoactivated phytochrome induces rapid PIF3 phosphorylation prior to proteasome-mediated degradation. Molecular cell *23*, 439-446.

13. Khanna, R., Huq, E., Kikis, E.A., Al-Sady, B., Lanzatella, C., and Quail, P.H. (2004). A novel molecular recognition motif necessary for targeting photoactivated phytochrome signaling to specific basic helix-loop-helix transcription factors. The Plant cell *16*, 3033-3044.

14. Al-Sady, B., Kikis, E.A., Monte, E., and Quail, P.H. (2008). Mechanistic duality of transcription factor function in phytochrome signaling. Proceedings of the National Academy of Sciences of the United States of America *105*, 2232-2237.

15. Leivar, P., Monte, E., Al-Sady, B., Carle, C., Storer, A., Alonso, J.M., Ecker, J.R., and Quail, P.H. (2008). The Arabidopsis phytochrome-interacting factor PIF7, together with PIF3 and PIF4, regulates responses to prolonged red light by modulating phyB levels. The Plant cell *20*, 337-352.

16. Fairchild, C.D., Schumaker, M.A., and Quail, P.H. (2000). HFR1 encodes an atypical bHLH protein that acts in phytochrome A signal transduction. Genes & development *14*, 2377-2391.

17. Fankhauser, C., and Chory, J. (2000). RSF1, an Arabidopsis locus implicated in phytochrome A signaling. Plant physiology *124*, 39-45.

18. Soh, M.S., Kim, Y.M., Han, S.J., and Song, P.S. (2000). REP1, a basic helix-loop-helix protein, is required for a branch pathway of phytochrome A signaling in arabidopsis. The Plant cell *12*, 2061-2074.

19. Duek, P.D., and Fankhauser, C. (2003). HFR1, a putative bHLH transcription factor, mediates both phytochrome A and cryptochrome signalling. Plant J *34*, 827-836.

20. Sessa, G., Carabelli, M., Sassi, M., Ciolfi, A., Possenti, M., Mittempergher, F., Becker, J., Morelli, G., and Ruberti, I. (2005). A dynamic balance between

gene activation and repression regulates the shade avoidance response in Arabidopsis. Genes & development *19*, 2811-2815.

21. Spiegelman, J.I., Mindrinos, M.N., Fankhauser, C., Richards, D., Lutes, J., Chory, J., and Oefner, P.J. (2000). Cloning of the Arabidopsis RSF1 gene by using a mapping strategy based on high-density DNA arrays and denaturing high-performance liquid chromatography. The Plant cell *12*, 2485-2498.

22. Kim, Y.M., Woo, J.C., Song, P.S., and Soh, M.S. (2002). HFR1, a phytochrome A-signalling component, acts in a separate pathway from HY5, downstream of COP1 in Arabidopsis thaliana. Plant J *30*, 711-719.

23. Duek, P.D., Elmer, M.V., van Oosten, V.R., and Fankhauser, C. (2004). The degradation of HFR1, a putative bHLH class transcription factor involved in light signaling, is regulated by phosphorylation and requires COP1. Curr Biol *14*, 2296-2301.

24. Yang, J., Lin, R., Sullivan, J., Hoecker, U., Liu, B., Xu, L., Deng, X.W., and Wang, H. (2005). Light regulates COP1-mediated degradation of HFR1, a transcription factor essential for light signaling in Arabidopsis. The Plant cell *17*, 804-821.

25. Jang, I.C., Yang, J.Y., Seo, H.S., and Chua, N.H. (2005). HFR1 is targeted by COP1 E3 ligase for post-translational proteolysis during phytochrome A signaling. Genes & development *19*, 593-602.

26. Yang, K.Y., Kim, Y.M., Lee, S., Song, P.S., and Soh, M.S. (2003). Overexpression of a mutant basic helix-loop-helix protein HFR1, HFR1-deltaN105, activates a branch pathway of light signaling in Arabidopsis. Plant physiology *133*, 1630-1642.

27. Yang, J., Lin, R., Hoecker, U., Liu, B., Xu, L., and Wang, H. (2005). Repression of light signaling by Arabidopsis SPA1 involves post-translational regulation of HFR1 protein accumulation. Plant J *43*, 131-141.

28. Jang, I.C., Yang, S.W., Yang, J.Y., and Chua, N.H. (2007). Independent and interdependent functions of LAF1 and HFR1 in phytochrome A signaling. Genes & development *21*, 2100-2111.

29. Huq, E., and Quail, P.H. (2002). PIF4, a phytochrome-interacting bHLH factor, functions as a negative regulator of phytochrome B signaling in Arabidopsis. Embo J *21*, 2441-2450.

30. Nozue, K., Covington, M.F., Duek, P.D., Lorrain, S., Fankhauser, C., Harmer, S.L., and Maloof, J.N. (2007). Rhythmic growth explained by coincidence between internal and external cues. Nature *448*, 358-361.

31. Lorrain, S., Allen, T., Duek, P.D., Whitelam, G.C., and Fankhauser, C. (2008). Phytochrome-mediated inhibition of shade avoidance involves degradation of growth-promoting bHLH transcription factors. Plant J *53*, 312-323.

32. de Lucas, M., Daviere, J.M., Rodriguez-Falcon, M., Pontin, M., Iglesias-Pedraz, J.M., Lorrain, S., Fankhauser, C., Blazquez, M.A., Titarenko, E., and Prat, S. (2008). A molecular framework for light and gibberellin control of cell elongation. Nature *451*, 480-484.

33. Feng, S., Martinez, C., Gusmaroli, G., Wang, Y., Zhou, J., Wang, F., Chen, L., Yu, L., Iglesias-Pedraz, J.M., Kircher, S., et al. (2008). Coordinated regulation of Arabidopsis thaliana development by light and gibberellins. Nature *451*, 475-479.

34. Makino, S., Matsushika, A., Kojima, M., Yamashino, T., and Mizuno, T. (2002). The APRR1/TOC1 quintet implicated in circadian rhythms of Arabidopsis thaliana: I. Characterization with APRR1-overexpressing plants. Plant & cell physiology *43*, 58-69.

35. Yamashino, T., Matsushika, A., Fujimori, T., Sato, S., Kato, T., Tabata, S., and Mizuno, T. (2003). A Link between circadian-controlled bHLH factors and the APRR1/TOC1 quintet in Arabidopsis thaliana. Plant & cell physiology *44*, 619-629.

36. Salter, M.G., Franklin, K.A., and Whitelam, G.C. (2003). Gating of the rapid shade-avoidance response by the circadian clock in plants. Nature *426*, 680-683.

37. Roig-Villanova, I., Bou, J., Sorin, C., Devlin, P.F., and Martinez-Garcia, J.F. (2006). Identification of primary target genes of phytochrome signaling. Early transcriptional control during shade avoidance responses in Arabidopsis. Plant physiology *141*, 85-96.

38. Hwang, Y.S., and Quail, P.H. (2008). Phytochrome-regulated PIL1 derepression is developmentally modulated. Plant & cell physiology *49*, 501-511.

39. Khanna, R., Shen, Y., Toledo-Ortiz, G., Kikis, E.A., Johannesson, H., Hwang, Y.S., and Quail, P.H. (2006). Functional profiling reveals that only a small number of phytochrome-regulated early-response genes in Arabidopsis are necessary for optimal deetiolation. The Plant cell *18*, 2157-2171.

40. Huq, E., Al-Sady, B., Hudson, M., Kim, C., Apel, K., and Quail, P.H. (2004). Phytochrome-interacting factor 1 is a critical bHLH regulator of chlorophyll biosynthesis. Science (New York, N.Y *305*, 1937-1941.

41. Oh, E., Kim, J., Park, E., Kim, J.I., Kang, C., and Choi, G. (2004). PIL5, a phytochrome-interacting basic helix-loop-helix protein, is a key negative regulator of seed germination in Arabidopsis thaliana. The Plant cell *16*, 3045-3058.

42. Shen, H., Moon, J., and Huq, E. (2005). PIF1 is regulated by light-mediated degradation through the ubiquitin-26S proteasome pathway to optimize photomorphogenesis of seedlings in Arabidopsis. Plant J *44*, 1023-1035.

43. Shen, H., Zhu, L., Castillon, A., Majee, M., Downie, B., and Huq, E. (2008). Light-Induced Phosphorylation and Degradation of the Negative Regulator PHYTOCHROME-INTERACTING FACTOR1 from Arabidopsis Depend upon Its Direct Physical Interactions with Photoactivated Phytochromes. The Plant cell.

44. Oh, E., Yamaguchi, S., Kamiya, Y., Bae, G., Chung, W.I., and Choi, G. (2006). Light activates the degradation of PIL5 protein to promote seed germination through gibberellin in Arabidopsis. Plant J *47*, 124-139.

45. Fujimori, T., Yamashino, T., Kato, T., and Mizuno, T. (2004). Circadian-controlled basic/helix-loop-helix factor, PIL6, implicated in light-signal transduction in Arabidopsis thaliana. Plant & cell physiology *45*, 1078-1086.

46. Khanna, R., Shen, Y., Marion, C.M., Tsuchisaka, A., Theologis, A., Schafer, E., and Quail, P.H. (2007). The basic helix-loop-helix transcription factor PIF5 acts on ethylene biosynthesis and phytochrome signaling by distinct mechanisms. The Plant cell *19*, 3915-3929.

47. Shen, Y., Khanna, R., Carle, C.M., and Quail, P.H. (2007). Phytochrome induces rapid PIF5 phosphorylation and degradation in response to red-light activation. Plant physiology *145*, 1043-1051.

48. Heim, M.A., Jakoby, M., Werber, M., Martin, C., Weisshaar, B., and Bailey, P.C. (2003). The basic helix-loop-helix transcription factor family in plants: a genome-wide study of protein structure and functional diversity. Mol Biol Evol *20*, 735-747.

49. Alonso, J.M., Stepanova, A.N., Leisse, T.J., Kim, C.J., Chen, H., Shinn, P., Stevenson, D.K., Zimmerman, J., Barajas, P., Cheuk, R., et al. (2003). Genome-wide insertional mutagenesis of *Arabidopsis thaliana*. Science (New York, N.Y *301*, 653-657.

50. Toledo-Ortiz, G., Huq, E., and Quail, P.H. (2003). The Arabidopsis basic/helix-loop-helix transcription factor family. The Plant cell *15*, 1749-1770.

51. Edwards, K., Johnstone, C., and Thompson, C. (1991). A simple and rapid method for the preparation of plant genomic DNA for PCR analysis. Nucleic acids research *19*, 1349.

Chapter 5

A zinc knuckle protein that negatively controls morning-specific growth in *Arabidopsis thaliana*

Abstract

Growth in plants is modulated by a complex interplay between internal signals and external cues. While traditional mutagenesis has been a successful approach for the identification of growth regulatory genes, it is likely that many genes involved in growth control remain to be discovered. In this study, we utilized the phenotypic variation between Bay-0 and Shahdara, two natural strains (accessions) of *Arabidopsis thaliana*, to map quantitative trait loci (QTL) affecting light- and temperature-regulated growth of the embryonic stem (hypocotyl). Using heterogeneous inbred families (HIFs), the gene underlying one QTL, *LIGHT5*, was identified as a tandem zinc knuckle/PLUS3 domain encoding gene (At5g43630; *TZP*), which carries a premature stop codon in Bay-0. Hypocotyl growth assays in monochromatic light and microarray analysis demonstrate that *TZP* controls blue light associated growth in a time-of-day fashion by regulating genes involved in growth, such as peroxidase and cell wall synthesis genes. *TZP* expression is phased by the circadian clock and light/dark cycles to the beginning of the day, the time of maximal growth in *A. thaliana* in short-day conditions. Based on its domain structure and localization in the nucleus, we propose that TZP acts downstream of the circadian clock and photoreceptor signaling pathways to directly control genes responsible for growth. The identification of TZP thus provides new insight into how daily synchronization of growth pathways plays a critical role in growth regulation.

Introduction

The embryonic stem or hypocotyl is an excellent model for studying both internal and external factors controlling growth in plants [1]. Genetic screens in common laboratory accessions have yielded direct molecular insight into how light and hormone dependent signaling pathways interact with the circadian clock to regulate the final length of the hypocotyl [1]. The power of the hypocotyl assay is its simplicity, as well as its obvious meaningfulness. When germinating seeds are exposed to low levels of light, such as those caused by a covering layer of debris, the hypocotyl has to grow for a while. Only after the surface has been broken by the tip of the hypocotyls can the embryonic leaves, the cotyledons, unfold. Conversely, if a seed has fallen on open ground, there is no need for the hypocotyls to be particularly long. Because of the ease and reproducibility with which hypocotyl length can be measured in thousands of individuals, it has also been a powerful model in mapping genes with more subtle effects on light and hormone regulated growth, using methods of quantitative genetics [2]. Multiple light signaling genes controlling hypocotyl length have been characterized in quantitative trait locus (QTL) studies [3-6].

In this study, we utilize the hypocotyl assay to identify QTL controlling growth in two light and two temperature conditions. We identified a recessive large effect QTL on chromosome five controlling 40% of the growth variation segregating in Recombinant Inbred Lines (RILs) derived from the Bay-0 and Shahdara accessions of *A. thaliana*. The QTL was fine-mapped and the causal factor shown to be a mutation affecting a tandem zinc knuckle/PLUS3 protein (At5g43630; *TZP*), which is encoded by a single-copy gene in all completely sequenced plant genomes. We show

that TZP acts downstream of the circadian clock and light signaling, directly regulating blue light-dependent, morning (dawn)-specific growth, during seedling development and beyond. Based on its nuclear localization and its novel domain structure, we argue that TZP functions at the transcriptional level to control growth-promoting pathways. TZP represents a new component of the growth pathway that was not previously identified using traditional genetic screens.

Results and Discussion

Mapping QTL for hypocotyl elongation in the Bay-0 x Shahdara RIL population

Intraspecific variation provides a fertile source of genetic combinations that can be utilized to map new genes (or new alleles) involved in complex traits such as growth. To investigate natural variation for hypocotyl elongation response to light and temperature, we phenotyped a core set of 164 RILs from the Bay-0 x Shahdara cross in four different environments combining two white-light (17 µmol m-2 s-1 [L1] and 10 µmol m-2 s-1 [L2]) and two temperature (22°C and 26°C) conditions (Supplementary Figure 5.S1A). The parental phenotypes reveal that in our conditions Shahdara responds poorly to temperatures above 22°C or light below 17 µmol m-2 s-1, or a combination of both. In contrast, Bay-0 responds strongly to both temperature and light, with a synergistic interaction between both factors. Variation among the RILs seems to follow parental variation with signs of bimodality (especially at 26°C / L1 and 26°C / L2) suggesting the segregation of some large-effect QTL. Transgression was also prevalent in all conditions and in both directions. Overall, genotypic variation was significant in each environment and broad-sense heritability

of the trait was accordingly high, above 70% (Online Supplementary Material, Table 1). While RIL response to contrasted temperature and light treatments was significant (P<0.001), RIL x light interactions were not significant at either 22°C or 26°C, and the RIL x temperature interaction was only significant under L1 (data not shown). This indicates that most of the phenotypic variation between RILs is stable and conserved across environments.

The genetic architecture of variation in hypocotyl elongation under these environmental conditions is presented in Supplementary Figure 5.S1B (see also Online Supplementary Material). Two loci with major effects are detected across all environments and called *LIGHT1* and *LIGHT5*, whereas the remaining loci called *'HYP'* are specific to a single environment with more subtle phenotypic contributions (only 4% each). The identification of these two major effect QTL is in accordance with the meager RIL x environment interactions found. The *LIGHT5* locus explains over 40% of the variance, with no *LIGHT5* x environment interaction found in any condition (data not shown). Its negative allelic effect is predicted to represent a combined 2.1 to 2.5 mm increase in hypocotyl elongation contributed by Shahdara alleles (Sha) relative to the Bay-0 alleles (Bay). In contrast, Sha alleles at *LIGHT1* are responsible for a decrease in hypocotyl elongation compared to Bay alleles, but with a relatively smaller phenotypic contribution (explaining 25 to 30% of the variance). The opposite allelic effects of *LIGHT1* and *LIGHT5* are responsible for most of the transgression observed in each environment. *LIGHT1* interacts with temperature under either L1 or L2 conditions and with light at either 22°C or 26°C (data not shown).

There is no significant epistatic relationship between *LIGHT1* and *LIGHT5*, or among any other pair of loci.

Confirmation and fine-mapping of *LIGHT5* to three candidate genes

Identifying the Quantitative Trait Gene (QTG) underlying a QTL is a challenging task that requires several independent lines of proof that a gene is linked to a trait of interest and that variation in this gene explains the trait [7]. The most general approach is fine-mapping to a very small physical candidate interval, which in the best case allows immediate identification of candidate polymorphisms (Quantitative Trait Nucleotide, QTN) within the causal gene or regulatory regions [8]. For most QTL and situations in *A. thaliana*, phenotyping for a QTL effect remains much more limiting than genotyping many individuals. Therefore, an efficient strategy for fine-mapping is to first isolate recombinants within a segregating nearly-isogenic line based on genotype alone and then to phenotypically interrogate only the informative ones (in successive rounds) to reduce the candidate interval to the gene level [9].

We followed the HIF strategy to build nearly-isogenic lines from a RIL (RIL350) that was segregating solely for the *LIGHT5* region. Comparing plants homozygous for the Sha allele with plants homozygous for the Bay allele at the QTL region (in an otherwise identical genetic background) confirmed the phenotypic impact of *LIGHT5* on hypocotyl elongation (Figure 5.1A). HIF350-Sha hypocotyls are consistently 1.6 mm longer than those of HIF350-Bay (slightly less than predicted by the QTL analysis). The analysis of heterozygous plants showed that the Sha allele of

LIGHT5 is fully dominant over the Bay allele (Figure 5.1A). The phenotypic effect observed was identical when first fixing alternate genotypes at the QTL region and then comparing the phenotypes of the descendants produced by those homozygous plants ("fixed progeny") or when directly studying the segregating descendants of a heterozygous plant ("progeny testing"). This precludes any maternal phenotypic effect and demonstrates a direct control of the phenotype expressed in seedlings by the *LIGHT5* alleles.

Screening for recombinants by genotyping 600 plants descended from the initial RIL350 individual (heterozygous over the whole QTL region) allowed us to identify 80 recombinants (recombined HIF, or rHIF) over the ~1.9 Mb heterozygous region. Twenty-six of these rHIF were individually interrogated in successive rounds of progeny testing to score for the presence (or absence) of the QTL effect caused by the remaining interval. This first screen allowed us to narrow the candidate region to less than 300 kb between markers at 17.405 and 17.692 Mb (Figure 5.1B). Screening 4,000 descendants from one of the positive rHIFs found in the previous step allowed us to identify 73 new rHIFs within the 300 kb candidate interval; 25 of these were individually progeny tested to define a smaller interval containing the QTL (Figure 5.1B). Results were consistent among rHIFs, and the last five recombinants delimited a 7 kb interval, from 17.545 Mb (one recombinant) to 17.552 Mb (four independent recombinants; Figure 5.1C). Three predicted genes, At5g43630, At5g43640, and At5g43650, are at least partially included in the 7 kb candidate region. We crossed two independent rHIFs with appropriate genotypes (Supplementary Figure 5.S2) in order to generate a line that was segregating only for the candidate region (and fixed to

the north and south), following a strategy suggested by Kroymann and Mitchell-Olds [10] that we named 'advanced rHIF (arHIF) cross'. This approach confirmed that the 17.545 - 17.552 Mb interval was sufficient to recapitulate the *LIGHT5* phenotype (Supplementary Figure 5.S2).

Sequencing the 7 kb interval in Bay-0 and Shahdara revealed dozens of SNPs and several indels, many of which resulted in non-silent changes in the coding regions of the three candidate genes. Eight, one and five SNPs caused amino-acid changed in At5g43630, At5g43640 and At5g43650, respectively. Two single amino-acid deletions and one larger deletion were discovered in At5g43630. Finally, an 8 bp insertion in Bay-0 caused a frameshift and a premature stop within the coding region for the predicted PLUS3 domain of At5g43630 (Figure 5.1C and D).

Identification of the *LIGHT5* causal gene as *TANDEM ZINC KNUCKLE/PLUS3 (TZP)*

The three genes in the *LIGHT5* interval are annotated as encoding a tandem zinc knuckle/PLUS3 (*TZP*, At5g43630), a 40S ribosomal protein (*RPS15E*, At5g43640), and a basic helix-loop-helix protein (*bHLH092*, At5g43650). *TZP* has no close homologs, but does share similarity with other *Arabidopsis* proteins that only have the zinc knuckle or PLUS3 domains. *bHLH092* is part of the large bHLH family of transcription factors [11], and a close homolog is *TRANSPARENT TESTA 8 (TT8;* At4g09820). There are four closely related *RPS15E* genes (At1g04270, At5g09500, At5g09510, and At5g09490) [12]. The transcript/expression of all three annotated genes in the Columbia background was confirmed by tiling array data and full length

cDNAs. Quantitative RT-PCR (qPCR) revealed that all three genes are expressed in Bay-0 and Shahdara (data not shown).

T-DNA-insertions in *RPS15E* or *bHLH092* did not result in hypocotyl elongation phenotypes (data not shown). No insertion mutants were available for *TZP* (an insertion GABI-KAT line could not be recovered). To determine the association of the stop codon in *TZP* with the hypocotyl phenotype, we sequenced the PLUS3 domain in other *A. thaliana* accessions. Although we identified 10 synonymous changes and 13 nonsynonymous changes (including two changes affecting residues at least partially conserved in other species), we could not detect the Bay-0 premature stop codon polymorphism in a panel of ~300 additional accessions (data not shown). We discovered that a Bay-0 single seed descent (SSD) line (Bay-0[41AV]), which was derived independently of the parent for the RIL set, did not have the 8 bp-insertion in *TZP*. Sequencing the entire 7 kb-candidate region revealed that this was the only sequence difference between Bay-0 and Bay-0[41AV] at LIGHT5. Genotyping additional markers in Bay-0[41AV] (as well as a careful phenotypic observation of the lines) showed that it is from the same genetic background as Bay-0 (data not shown). We crossed the two lines, with and without the *TZP* stop codon, to determine whether the mutation was responsible for the *LIGHT5* phenotype. As shown in Supplementary Figure 5.S2, phenotypes of F2 plants homozygous for either allele were very similar to the phenotypes of the arHIF fixed for either the Bay (stop) or Sha allele, respectively. This demonstrates that the 8 bp insertion in *TZP* is sufficient to explain the *LIGHT5* phenotype, and allows us to conclude that *TZP* controls hypocotyl growth. Bay-0 [41AV] is the only Bay-0 stock we have which does not carry the 8 bp-insertion. The

question remains as to when this causative polymorphism appeared in the Bay-0 lineage (before or after collection) and whether it really exists in nature. Unfortunately, indications about the exact collection site of Bay-0 are very poor and make it nearly impossible to locate the original natural population and answer this question.

Additionally, we employed a transgenic approach to confirm the role of *TZP* in hypocotyl growth. The Sha alleles of all three genes were overexpressed in the rHIF containing the Bay allele (rHIF138-8). Overexpression of *TZP* (*TZP-OX*) caused plants to have very long hypocotyls (Figure 5.2B and C), with increased growth throughout development and extended duration of the reproductive phase (Figure 5.2D and E). All linearly-elongating organs were more extended, including petioles, internodes and peduncles and the main floral stem of *TZP-OX* plants was usually twice as long as in its background. In contrast, *RPS15E* or *bHLH092* overexpressing plants were indistinguishable from the parental line in terms of growth (data not shown). Overexpression of *bHLH092* resulted in white seeds, similar to a phenotype found in mutants of its closest homolog *TT8* [13]. From these data we conclude that *TZP* is the QTG explaining the *LIGHT5* QTL, and that the 8 bp indel leading to a premature stop codon in the Bay-0 allele is the causative polymorphism.

TZP is a large, nuclear-localized protein encoded by a single copy gene

TZP is a single copy gene in *A. thaliana*. *TZP* orthologs are also single copy in the fully sequenced plant genomes (Supplementary Figure 5.S3). Interestingly, *TZP* is

not found in the moss *Physcomitrella patens*, or in *Chlamydomonas reinhardtii* or any earlier algal lineages queried, suggesting that it is specific to vascular plants.

The zinc knuckle (znkn; CX2CX4HX4C) domain has been shown to be important for protein-protein interactions, as well as for binding single-stranded DNA [14]. There are at least 24 znkn-containing proteins in *Arabidopsis*, five of which are closely related to each other, but not to *TZP* (Online Supplementary Material, Table 2). Mutations in one of them, *SWELLMAP* 1 (*SMP1*), result in small plants with small cells because of a dysfunction in the commitment to the cell cycle [15]. Another znkn protein, RSZ33, regulates interactions between splicing factors [16, 17]. In yeast, the znkn of MPE1 has been found to control 3' end processing of pre-mRNA, and its human ortholog RBBP6 has been shown to interact with tumor suppressor pRB1 [14]. Znkn domains are also found in retroviral gag proteins (nucleocapsid), including that of HIV [18].

The PLUS3 domain is thought to play a role in nucleic acid binding through three conserved positive amino acids [19]. There are five proteins in *Arabidopsis* with the PLUS3 domain (Supplementary Figure 5.S3; see also Online Supplementary Material). Three of these also have a SWIB domain, two have either a CCCH or a C3H3C4 zinc finger, and VERNALIZATION INDEPENDENT 5 (VIP5) contains only the PLUS3 domain [20]. VIP5 is a homolog of the yeast RTF1 protein, which is part of the yeast Paf1 complex that regulates histone H2B ubiquitination, histone H3 methylation, RNA polymerase II carboxy-terminal Ser2 phosphorylation and RNA 3' end processing [19]. The SWIB domain-containing proteins are part of the SWI/SNF chromatin-remodeling complex [21]. The combination of tandem zinc knuckles and a

PLUS3 domain is unique to *TZP*-type genes in plants. Based on GFP fusions, TZP is localized to the nucleus in small punctate structures (Figure 5.2F). Considering the domain structure and the localization, it seems most likely that TZP has a role in transcriptional control, perhaps at the level of chromatin remodeling.

TZP regulates light quality-dependent growth

Our initial QTL study suggested that *LIGHT5* is involved in light-regulated hypocotyl growth. To determine whether the growth defects in *LIGHT5* are specific to certain light environments, we measured hypocotyl lengths for both the rHIF and *TZP-OX* lines under different fluence rates of monochromatic red, blue and far-red light, and in continuous dark. We found that both loss and gain of *TZP* activity had a significant effect on hypocotyl length under a range of blue or white fluence rates, but not in red or far-red light, or in the dark (Figure 5.2A and B; data not shown). These results are consistent with *TZP* playing a role in light-dependent hypocotyl elongation, and suggest that TZP is involved in blue-light signaling.

We measured transcript abundance in Shahdara, Bay-0, rHIF138-8, rHIF138-13, arHIF47-2, arHIF47-5, and *TZP-OX* line #3 seedlings grown in constant blue light (15 μmol m-2 s-1) for five days and then harvested at subjective dawn (relative to the time when they were moved from stratification to light). The extent of growth paralleled *TZP* expression levels (Supplementary Figure 5.S4), consistent with *TZP* having a direct effect on growth. To identify potential downstream transcriptional targets of TZP, we analyzed genome wide expression patterns of five genotypes (rHIF138-8 and rHIF138-13; arHIF47-2 and arHIF47-5; *TZP-OX* line#3) using

Affymetrix *Arabidopsis* ATH1 GeneChip arrays. In pairwise comparisons, we found 135, 12 and 769 genes to be differentially expressed between lines with contrasting alleles, rHIF138-8 vs. rHIF138-13, arHIF47-2 vs. arHIF47- 5, and *TZP-OX* vs. rHIF138-8, respectively ($P < 0.01$; Online Supplementary Material, Table 3-6; Materials and Methods in SI Text). The top four significant gene ontology categories in the comparison of *TZP-OX* and rHIF138-8 (769 genes) are cytosol, ribosome, structural molecule activity, and cell wall (Online Supplementary Material, Table 7), consistent with TZP playing a specific role in modulating growth. We found similar results with the rHIF138-8 vs. rHIF138-13 comparison (data not shown).

TZP controls morning-specific growth through an auxin-related pathway

It is well established that hypocotyl elongation is controlled by the circadian clock [1, 22]. Therefore, we tested whether *TZP* is clock regulated and if the circadian clock is altered in *TZP-OX* plants and the rHIF carrying the Bay-0 allele. We found that *TZP* cycles under both diurnal and circadian conditions with peak expression at dawn (transition from dark to light; Figure 5.3A; Supplementary Figure 5.S5). Hypocotyl growth is maximal at dawn and many genes that regulate growth, such as cell wall and phytohormone genes, have dawn-specific transcript abundance [1, 23]. The dawn-specific *TZP* transcript peak suggests that it may be part of a circadian-controlled growth mechanism. To confirm that the clock controls *TZP*, we asked if circadian mutants disrupt expression of *TZP*. Indeed, *TZP* expression was changed in both *early flowering3* (*elf3*) and *late elongated hypocotyl* (*lhy*) mutants (Supplementary Figure 5.S6). However, the circadian clock is not disrupted in either

the rHIF or *TZP-OX* under light/dark cycles (Supplementary Figure 5.S7), consistent with no feedback of *TZP* into the circadian clock. Based on these results we propose that TZP functions to control growth downstream of the circadian clock.

Since *TZP* is regulated by light/dark cycles and the circadian clock, we asked if the genes disrupted by *TZP-OX* were time-of-day specific. We used the PHASER time-of day analysis tool (http://phaser.cgrb.oregonstate.edu/), which determines if there is a pattern of time-of-day co-expression in a given gene list compared to a background model. The peak expression of genes that were disrupted in *TZP-OX,* and differentially expressed in rHIF138-8 vs. rHIF138-13 is biased towards dawn (Figure 5.3C). This is consistent with the dawn-specific expression of *TZP*. In addition, morning-specific response elements such as the morning element (CCACA), G-box (CACGTG) and HUD (CACATG) (Online Supplementary Material, Table 8; [23, 24]) were overrepresented in the promoters (500 bp) of these genes as determined using the ELEMENT motif-searching tool ([25]; http://element.cgrb.oregonstate.edu/). These results support a role of *TZP* in the transcriptional activity of dawn-specific genes.

In an effort to capture the entire effect of *TZP-OX*, we carried out a time course under light/dark cycles (12 hr white light/12 hr dark) in seven day-old seedlings, sampling every four hours over one day in the same genotypes as above. We validated the overexpression of *TZP* using qPCR, which revealed that *TZP* continued to cycle despite overexpression (Figure 5.3B), suggesting that *TZP* is also controlled posttranscriptionally. Global expression changes were assessed using Affymetrix ATH1 GeneChip arrays in *TZP-OX*, rHIF138-8 and rHIF138-13. The resulting time courses were analyzed for differentially expressed genes and for cycling genes [[24];

Online Supplementary Material, Table 9-12; Materials and Methods in SI text]. Using the time points as replicates, we identified 117 upregulated and 40 downregulated genes in *TZP-OX* ($P < 0.01$).

Similar to the results in blue light, the genes that were upregulated in *TZP-OX* were dawn-specific (Supplementary Figure 5.S8) and cell wall genes were overrepresented (Online Supplementary Material, Table 13). *IRX1* is one example of the eight cell wall genes that were upregulated in *TZP-OX* (Figure 5.3D). Like *IRX1*, many of the upregulated genes were specifically overexpressed at dawn, similar to the overexpression pattern of *TZP* itself (Figure 5.3A; Supplementary Figure 5.S9). Peroxidases, which can function to polymerize cell wall compounds, were also upregulated in *TZP-OX*, consistent with their role in growth and cell wall expansion [26]. Peroxidases *PER27*, *PER30*, and *PER64* have been shown to be part of the cell wall proteome [27](6 PER genes total; Supplementary Figure 5.S9A). However, *CATALASE 3* (*CAT3; SEN2*) was one of the most downregulated genes (Supplementary Figure 5.S9D). *CAT3* cycles under all diurnal and circadian conditions and may play a role in senescence and stress responses [28, 29]. Two additional genes of note were downregulated in *TZP-OX*: *PW9* (encoding a MATH/TRAF domain protein) and one of the PLUS3 homologs that encodes also a SWI/SNF domain (Supplementary Figure 5.S9E and F). In general, the genes that were misregulated in *TZPOX* are involved in cell expansion, consistent with TZP being intimately related to regulation of hypocotyl elongation and downstream of the circadian clock.

Auxin-response genes, including *WES1* (GH3.5; [30]), *DFL1* (GH3.6; [31]) (Supplementary Figure 5.S9B), and *AXR5* (IAA1; [32]), all of which have been shown to control hypocotyl growth, were also upregulated upon *TZP* overexpression. It has been shown recently that auxin controls growth in a time-of-day fashion [33], which fits with TZP controlling morning-specific growth through these genes. In addition, two homeobox-leucine zipper genes induced in *TZP-OX* (*HAT4* and *HAT52*) are upregulated under low light conditions and in response to auxin (Supplementary Figure 5.S9C). Mutations in these genes lead to growth defects [34, 35]. Together, these results support the notion that TZP plays a broad role in the regulation of phytohormone-dependent gene transcription [23].

A similar number of genes were found to cycle across all three genotypes as reported for this condition previously ([24]; ~7,700 genes), and there was no significant difference between the number of genes cycling in rHIF lines and *TZP-OX*, although there were genes specific to each genotype. However, the peak transcript abundance of 362 genes was shifted by six hours or more in *TZP-OX* compared to rHIF138-8 (only genes that cycled in both genotypes were considered). Phytohormone-related (*SIR1*, *ETO1, GH3.3, RGA1, ABF4*), homeobox-leucine zipper (*HAT2*, *HAT3*), chromatin remodeling (*HD2B*, *HDT4*, *SUVH9, CHR4, TAF1*), leaf polarity (*KAN3, AS1*) and ribosomal genes were mis-phased in *TZP-OX*. *PHYTOCHROME D* (*PHYD*) was also phased eight hours earlier in *TZP-OX* (Supplementary Figure 5.S9L). The first *phyD* mutant was originally identified as a natural allele, and subsequently was shown to affect shade-avoidance associated growth and flowering [3, 36].

Consistent with TZP controlling blue light dependent growth, *LONG HYPOCOTYL IN FARRED 1* (*HFR1*) is overexpressed at dawn more than 100 fold with the same pattern as *IRX1* (Supplementary Figure 5.S9I). *HFR1* encodes a bHLH transcription factor that is required for both phytochrome A-mediated far-red and cryptochrome 1-mediated blue light signaling [37]. *HFR1* expression is high under low light conditions such as shade and continuous dark conditions [35], and is elevated in circadian and light signaling mutants, much like in *TZP-OX* (Supplementary Figure 5.S9I; [23]). Recently it has been shown that two other transcription factor genes related to *HFR1 (PIF4* and *PIF5)* control morning-specific hypocotyl growth. Disruption of the circadian clock gene *CCA1* results in the overexpression of *PIF4* and *PIF5* leading to uncontrolled elongation [1]. However, *PIF4* and *PIF5* are expressed at control or slightly lower levels in *TZP-OX* (Supplementary Figure 5.S9G-H). These results support *TZP* acting in parallel with (or downstream of) *PIF4* and *PIF5* in growth control.

Online Supplementary Material is located at www.inra.fr/vast/Files/Loudet_PNAS_SITables.xls.

Conclusions

Despite extensive forward genetics screens in *A. thaliana*, natural variation has recently made important contributions to the identification of genes not previously known to impact several different traits (e.g., [38-41]). Apart from being able to exploit allelic variation (in multiple genetic backgrounds) that cannot be generated by

conventional mutagenesis, the success of these studies has often been due to the use of quantitative phenotyping, as opposed to the qualitative gauges employed in typical mutant screens. We have demonstrated here the power of QTL analysis to reveal a new component of the hypocotyl growth pathway in *A. thaliana*, TZP, a unique, tandem zinc knuckle/PLUS3 domain protein encoded by a single copy gene in the vascular plant lineage. TZP provides a direct link between light signaling and the pathways that control growth in an environmentally independent fashion.

Materials and Methods

Plant material and phenotyping. The Core-Population of 164 RILs from the Bay-0 x Shahdara set (http://dbsgap.versailles.inra.fr/vnat/) was phenotyped in four different light and temperature environments to map QTL affecting hypocotyl elongation. Complete phenotypic data from RILs is available in Online Supplementary Material, Table 14. HIF350 was developed from an F7 line (RIL350) that still segregated for a single and limited genomic region around *LIGHT5* locus. Plants still heterozygous for the QTL region were screened with adequate markers to isolate recombinants (rHIF) used in the fine-mapping process. Advanced rHIF crosses were generated from two different rHIFs recombined immediately to the north or immediately to the south of the *LIGHT5* interval giving rise to lines arHIF47. Distinct Bay-0 lines from the stock center were used to find variants at *LIGHT5*. rHIF138-8[Bay] was complemented by over-expressing each of the three positional candidate genes cloned from rHIF138-13[Sha].

QTL mapping. Analyses used hypocotyl length mean values of an average of 16 seedlings (from two distinct experiments) per genotype per environment. QTL analyses were performed using QTL Cartographer, with classical parameters for interval mapping and composite interval mapping.

Microarray analysis. Microarray experiments were carried out per Affymetrix protocols (ATH1 GeneChip), on seven day-old tissue harvested under either continuous blue at subjective dawn, or every four hours (starting at dawn) under 12 hr white light / 12 hr dark cycles over one day (six time points). Hybridization intensities from all microarrays were normalized together using gcRMA implemented in the R

statistical package. The blue dataset was then separated and differentially expressed genes were identified using linear modeling with the limma bioconductor package in R.

Materials and Methods Supplementary Information

Plant material The Bay-0 x Shahdara RIL set (http://dbsgap.versailles.inra.fr/vnat/; [1]) was initially phenotyped in four different environments to map QTL affecting hypocotyl elongation. We employed the core-pop164, a subset of 164 lines of the whole population designed to optimize QTL mapping while limiting the phenotyping effort. HIF350 was developed from an F7 line (RIL350) that still segregated for a single and limited genomic region around MSAT5.9, following a strategy described previously [2], which allowed for comparison of plants with alternative genotypes at *LIGHT5* in a common (though heterogeneous) background. Plants still heterozygous for the QTL region (thus segregating for the phenotype) were screened with adequate markers to isolate recombinants (rHIF) used in the fine-mapping process (see below).

Distinct Bay-0 lines from the stock center were used to find variants at *LIGHT5*, especially the single seed descent (SSD) lines issued from the initial plant used to generate the RIL set (CS57923) called 'Bay-0' throughout this paper and an SSD (41AV) from the Versailles resource center (http://dbsgap.versailles.inra.fr/vnat/) called 'Bay- 0[41AV]', progeny of CS954.

Hypocotyl measurements Seeds were sterilized in 70% EtOH with 0.1% Triton X-100 for 10 min, then rinsed in 95% EtOH for 10 min. They were then resuspended in 0.1% agar and stratified in darkness at 4°C for three days. Sixteen different genotypes

(RILs or parental line, 16 seeds each) were spotted onto a 90 mm square Petri plate containing 1/2 MS salts and 0.7% phytagar without sugar. Plates were then exposed to white light for six days under the following continuous light treatments: 17 µmol m-2 s-1 (L1) or 10 µmol m-2 s-1 (L2) at either 22 or 26°C. Each RIL was present once (16 seedlings) under L1 and once under L2 in each of the two distinct experiments performed at each temperature. Light treatments were always conducted side by side in a single chamber set to one temperature (two times eleven plates). Plates were rotated every day within each treatment. White light was provided by three 20-W Cool White fluorescent and two 25-W incandescent bulbs in Percival E30B chambers; the R/FR ratio (650-680nm/710-740nm) was 1.06. At harvest, hypocotyls were transferred to acetate sheets and scanned on a flatbed scanner. Length was measured with Scion Image for Windows. Complete phenotypic data from RILs in four environments is included in table 14 from our website's supplementary information at www.inra.fr/vast/Files/Loudet_PNAS_SITables.xls.

Statistical analysis and QTL mapping The complete set of data obtained using the RILs was included in different analyses of variance (ANOVA) models to determine the specific effects of the 'genotype', 'light', 'temperature' and 'residual' factors, and the interaction terms. Performed environment by environment, a similar ANOVA with the 'genotype' factor enabled us to quantify the broad-sense heritability (genetic variance/ total phenotypic variance). Subsequent analyses used hypocotyl length mean values of an average of 16 seedlings (from two distinct experiments) per genotype per environment. ANOVA estimations were obtained using the aov() function of the S-PLUS version 3.4 statistical package (Statistical Sciences, Seattle, Washington). The

original set of 38 microsatellite markers and the genetic map obtained with MAPMAKER 3.0, [1]; http://dbsgap.versailles.inra.fr/vnat/) were used to link phenotypic to genotypic variation. QTL analyses were performed using the Unix version of QTL CARTOGRAPHER 1.14 [3]. Standard methods for interval mapping (IM) and composite interval mapping (CIM) were used as previously [1]. Firstly, interval mapping [4] was carried out to determine putative QTL(s) involved in the variation of the trait. CIM model 6 of QTL CARTOGRAPHER was then performed on the same data: the closest marker to each local LOD score peak (putative QTL) was used as a cofactor to control the genetic background while testing at another genomic position. When a cofactor was also a flanking marker of the tested region, it was excluded from the model. The number of cofactors involved in our model reached a maximum of 4.

The walking speed chosen for QTL analyses was 0.1 centiMorgans. The LOD significance threshold (2.3 LOD) was estimated from several permutation test analyses, as suggested by [5]. Additive effects of detected QTL were estimated from CIM results, as representing the mean effect of the replacement of the Shahdara alleles by Bay-0 alleles at the studied locus. The contribution of each identified QTL to the total variance (R2) was estimated by variance component analysis, using phenotypic values for each RIL. The model used the genotype at the closest marker to the corresponding detected QTL as random factors in ANOVA. Only homozygous genotypes were included in the ANOVA analysis. QTL x QTL interactions were searched for in the ANOVA analysis, as well as using the 'Pair-Scan' function of the WebQTL tool (http://www.genenetwork.org/).

Fine-mapping Phenotyping during the fine-mapping process was performed in the same framework as described in "hypocotyl measurements" under 22°C / L1 conditions. Two sets of recombinants were isolated within the candidate region segregating in HIF350: the first one was screened from the initial HIF350 over the 16.173 – 18.050 Mb interval and the second one was screened from one of the positive recombined HIF (rHIF) obtained in the first round over the 17.405 – 17.692 Mb interval. Screens for recombinants involved respectively 600 and 4,000 individuals. Recombinant genotypes were determined using microsatellite or indel markers, then CAPS when previous types of markers were exhausted and finally direct sequencing of the SNPs to precisely localize recombination breakpoints. Once recombinants had been isolated they were tested for the segregation of the hypocotyl phenotype by progeny testing (96 seedlings individually phenotyped and genotyped per rHIF).

Following a strategy described by [6], advanced rHIF crosses were generated from two different rHIFs recombined immediately to the north or immediately to the south of the *LIGHT5* interval (and with adequate genotype elsewhere) that do segregate for the QTL phenotype, giving rise to lines arHIF47.

Transgenic complementation Genomic fragments spanning the predicted open reading frames of the three genes in the *LIGHT5* interval were amplified from rHIF138-13 and subcloned in a topoTA vector. The resulting insert was sequenced, and transferred using the GATEWAY system to a plant transformation vector containing the 35S promoter and a 3' YFP tag. rHIF138-8 plants were transformed to complement the short hypocotyl phenotype. T2 plants (*TZP- OX*) were used for all the described experiments.

Microarray analysis Microarray experiments were carried out per Affymetrix protocols and as described [7]. Briefly, seven day-old tissue was harvested under either continuous blue at subjective dawn, or every four hours (starting at dawn) under 12 hrs light (white, 30 μM)/ 12 hrs dark cycles (22°C) over one day (six time points). A total of 64 samples representing all genotypes under both conditions in quadruplicate were collected. Tissue was collected in 2 mL microcentrifuge tubes with three ball bearings, frozen immediately in liquid nitrogen and stored at -80°C. Tissue was disrupted using a Retsch shaker and extracted using RNAeasy (QIAGEN) with on column RNase-free DNase treatment. Resulting RNA was checked for quality and then labeled probe was made with 5 μg of RNA using the Affymetrix kit (Affymetrix). 33 samples were used for microarray analysis: blue, 5 genotypes (*TZP-OX*, rHIF138-8, rHIF138-13, arHIF47-2 and arHIF47-5), 3 replicates; 12 hrs light (white, 30 μM)/ 12 hrs dark cycles, 3 genotypes (*TZP-OX*, rHIF138-8, and rHIF138-13), 6 time points (0, 4, 8, 12, 16, 20 hrs after lights on). Probe was hybridized to Arabidopsis ATH1 GeneChip arrays overnight, washed and scanned using the standard Affymetrix protocol.

Hybridization intensities from all microarrays were normalized together using gcRMA implemented in the R statistical package. The blue dataset was then separated and differentially expressed genes were identified using linear modeling with the limma bioconductor package in R [8]. Time course data were analyzed for differentially expressed genes by using the time points as replicates. Cycling genes were identified as described [7].

Acknowledgments

We thank Justin Borevitz and Julin Maloof for helpful discussions on this work. We acknowledge funding from NIH Grant GM62932 (to J.C., and D.W.) and NSF Grant DBI0605240 (to T.C.M and J.C). T.P.M was supported by a Ruth L. Kirschstein NIH Postdoctoral Fellowship.

This chapter, in full, consists of the following manuscript in press at *Proceedings of the National Academy of Sciences*.

Loudet, Olivier; Michael, Todd P; Burger, Brian T; Le Metté, Claire, Mockler Todd C; Weigel, Detlef; Chory, Joanne. "A zinc knuckle protein that negatively controls morning-specific growth in *Arabidopsis thaliana*".

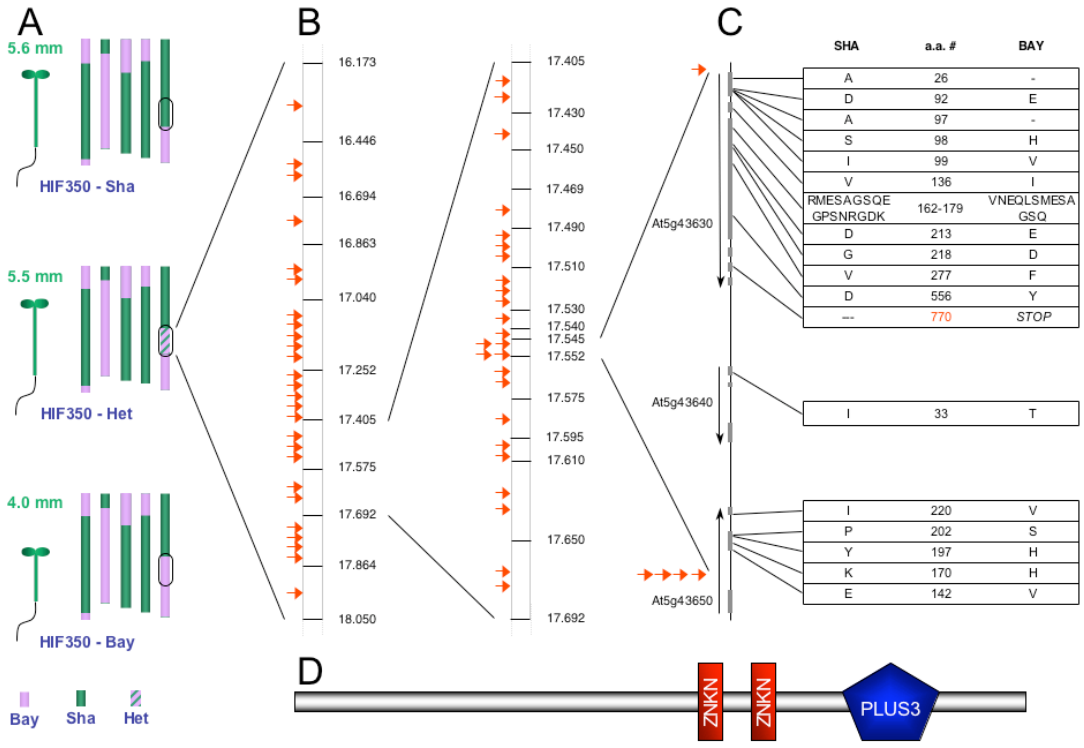

Figure 5.1. Confirmation and fine-mapping of the LIGHT5 QTL to three genes, among which At5g43630 is highly polymorphic between Bay-0 and Shahdara. (**A**) Confirmation of *LIGHT5* using HIFs. The Sha allele is fully dominant over the Bay allele. Two rounds of recombinant screening from HIF350 followed (**B**). Horizontal marks on the chromosomes are markers with physical position in Mb indicated to the right. Red arrows indicate the approximate position of different recombination events that were individually tested in rHIF to establish the QTL position. Fine-mapping identified a 7kb region containing three genes (**C**). Grey boxes along the vertical axes represent exons from three genes highlighted by vertical arrows. Horizontal red arrows indicate the exact physical position of the last 5 recombinants defining the QTL candidate region. Amino acid changes between Bay-0 and Shahdara within the interval are presented in the table and linked to their respective physical position along the gene model. (**D**) Model of the protein structure of TZP (At5g43630).

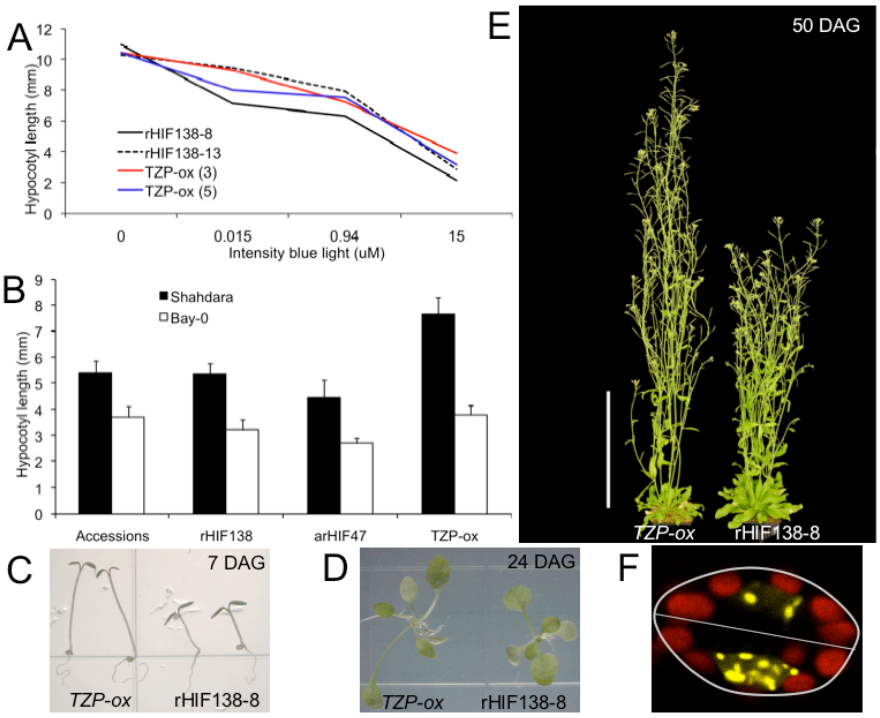

Figure 5.2. LIGHT5/TZP controls growth throughout development.
(**A**) Increased TZP activity results in longer hypocotyls under blue light. Seedlings were grown at the fluence rates indicated and measured on the sixth day. *TZP-OX(3)* and *TZPOX(5)* are two independent transgenic lines overexpressing *TZP* in rHIF138-8 background. rHIF138-8 contains the Bay allele with the premature STOP in *TZP* and rHIF138-13 contains the functional Sha allele. (**B**) Sha allele of *TZP* or overexpression result in longer hypocotyls. Plants were grown under light/dark cycles (12 hrs/12 hrs) at 22°C and hypocotyls were measured 7 DAG. Representative seedlings were used to make the images in (C). Measurements represent three independent experiments of twenty seedlings each. (**C**) *TZP-OX* plants have long hypocotyls 7 DAG under light/dark cycles (12 hrs/12 hrs) compared to its background (rHIF138-8). (**D**) *TZP-OX* petioles are elongated 24 DAG compared to rHIF138-8. (**E**) Mature *TZP-OX* plants are almost twice as tall as background plants 50 DAG. Plants were grown under long days (light/dark: 16 hrs/8 hrs) for 50 days. All plants pictured are representative of at least two independent transgenic lines (lines 3 and 5) and two independent experiments. The vertical bar represents 20 cm. (**F**) TZP::YFP is localized to speckles in the nucleus. T2 plants carrying the *35S::TZP:YFP* fusion were imaged to detect TZP localization. TZP:YFP localizes to the nucleus in guard cells of the stomata, in addition to all other tissues tested. Grey lines highlight the cell walls.

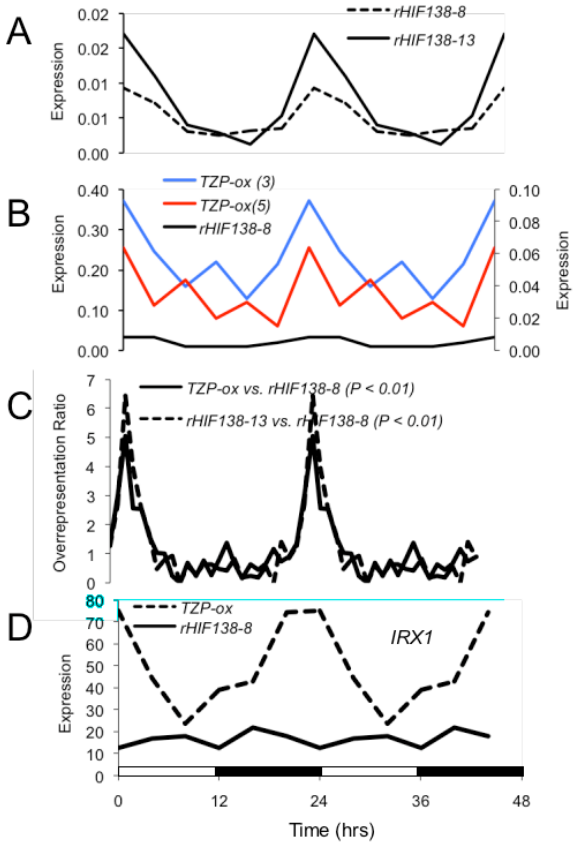

Figure 5.3. LIGHT5/*TZP* controls morning-specific growth pathways
(**A**) *TZP* displays dawn-specific transcript abundance under light/dark cycles (12 hrs/12 hrs) and constant 22°C (six time points). The second day of data is copied from the first (double plotted) for visualization purposes. Expression was determined by qPCR with primers specific to *TZP* and SyberGreen. (**B**) *TZP* transcript abundance is overexpressed in *TZP-OX*. Five independent lines overexpressing *TZP* were characterized. Two lines are shown here. Data were collected and plotted as in (A). (**C**) The genes that are misexpressed ($P < 0.01$) in long hypocotyl genotypes (*TZP-OX* or rHIF138-13 vs. rHIF138-8) under blue light short day photocycles are expressed at dawn as determined with PHASER. (**D**) Long hypocotyls of the *TZP-OX* mutant are due in part to overexpression of cell wall genes. As an example of the expression pattern of the cell wall genes that are overexpressed in the *TZP-OX* mutant, *IRX1* continues to cycle with peak expression at dawn, but its peak expression is 3 fold higher in *TZP-OX*. Other genes that are overexpressed in *TZP-OX* are listed in table 3 and 10 from our website data (7). Results are from array data.

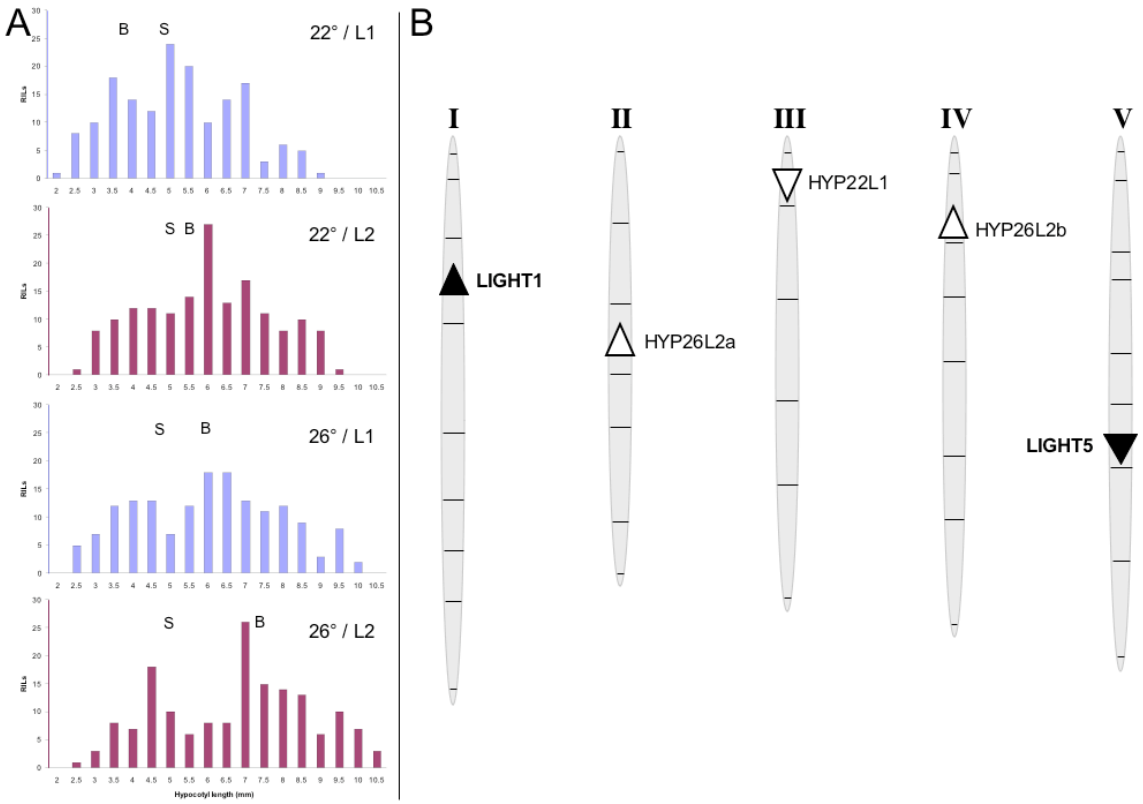

Supplementary Figure 5.S1. Phenotypic variation and significant QTL detected in the Bay-0 x Shahdara RIL set. Distribution of phenotypic values for hypocotyl elongation among 164 Bay-0 x Shahdara RILs across four different environments: two temperature x two white-light conditions (**A**). 'B' and 'S' above bars indicate phenotypic values obtained for the parents, Bay-0 and Shahdara respectively. Position and effect of the five significant QTL controlling this variation (**B**). Each QTL is depicted by a triangle located at the most probable QTL position on one of the 5 chromosomes. Upward- and downward-pointing triangles represent QTLs with a positive or negative allelic effect, respectively ('2a' in table S1 from www.inra.fr/vast/Files/Loudet_PNAS_SITables.xls, which represents the mean effect of the replacement of both Shahdara alleles by Bay-0 alleles at the QTL). The framework genetic map (horizontal marks indicate marker positions) is from Loudet *et al.* (2002). QTLs denoted as "LIGHT" were detected in all four environments. Other QTLs are named according to the specific environment in which they had a significant effect.

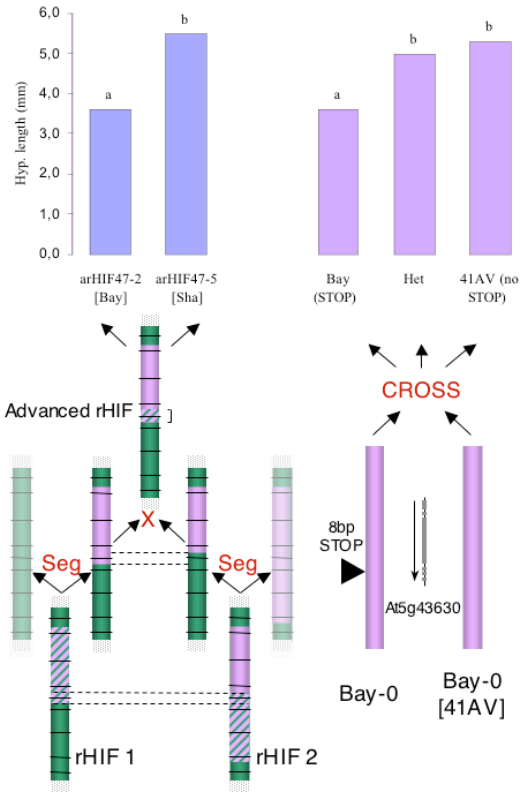

Supplementary Figure 5.S2. *LIGHT5* is At5g43630 and the causal polymorphism is the 8bp-insertion in Bay-0. Two rHIFs segregating for *LIGHT5* and defining the limits of the candidate interval were crossed to generate an advanced rHIF (arHIF47) segregating solely for the 7kb candidate region. Phenotypes are shown for the arHIF47 progeny fixed for either the Bay or Sha 7-kb region. Bay-0[41AV] lacks the 8 bp insertion causing the early stop in At5g43630, with the rest of the genome being the same as in Bay-0. Phenotypes are shown from F2 plants between the two isogenic parents. Different letters on bars indicate significantly different means ($P < 0.01$; least significant difference test).

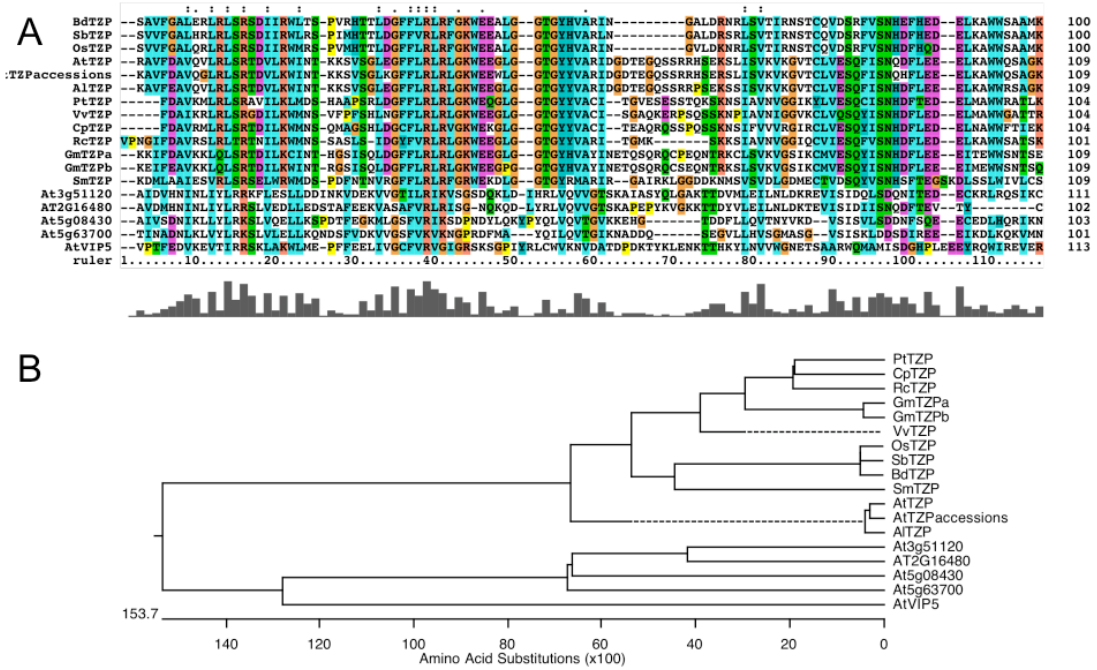

Supplementary Figure 5.S3. The PLUS3 domain is conserved across species. (A) Alignment of the PLUS3 domain in multiple species and the consensus of 96 *Arabidopsis thaliana* accessions. (B) Phylogenetic tree of the PLUS3 domain across species and with other PLUS3 domains of *Arabidopsis thaliana*. The *TZP* PLUS3 domain is more closely related to the PLUS3 domain from *TZP* orthologs in other species, than other PLUS3 domains in *Arabidopsis thaliana*. *Arabidopsis lyrata (Al)*, *Carica papaya (Cp)*, *Oryza sativa (Os)*, *Ricinus communis (Rc)*, *Populus trichocarpa*, *Sorghum bicolor (Sb)*, *Brachypodium distachyon (Bd)*, *Glycine max* (*Gm*), *Vitis vinifera* (Vv) and *Selaginella moellendorffii (Sm).*

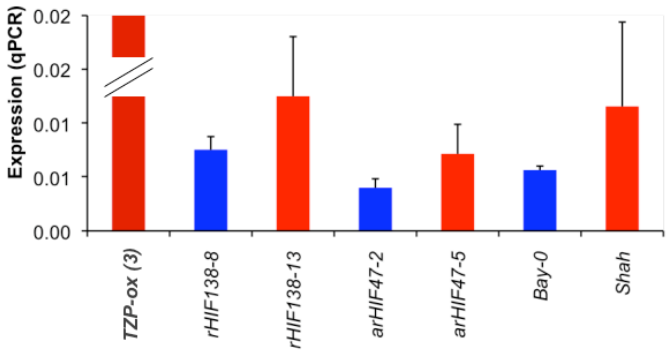

Supplementary Figure 5.S4. *TZP* expression is correlated with increased hypocotyl growth. Plants were grown under continuous blue light for five days and tissue was collected at dawn. Expression was measured by qPCR. Expression of TZP was higher in lines with longer hypocotyls, including *TZP-OX (3)*, *rHIF138-13*, *arHIF47-5* and Shahdara. The bar for *TZP-OX (3)* was truncated due to the expression being on a different scale than the rest of the lines.

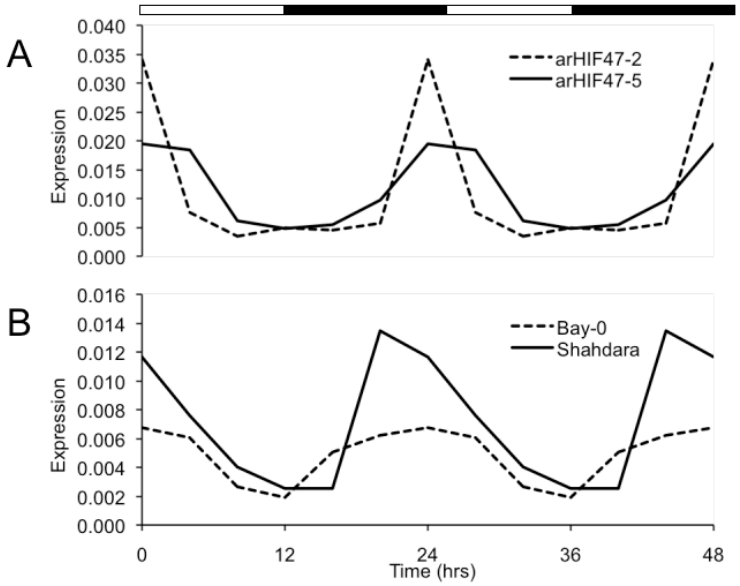

Supplementary Figure 5.S5. *TZP* transcript abundance peaks at dawn in the rHIF and the accession Bay-0 and Shahdara. Plants were grown for seven days under light/dark cycles and sampled over one day. Expression was measured using qPCR.

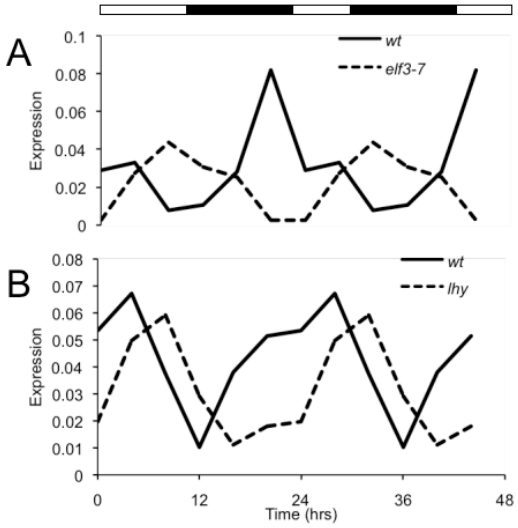

Supplementary Figure 5.S6. *TZP* expression is disrupted in core circadian clock mutants. The expression of *TZP* was measured in two circadian clock mutants, *late elongated hypocotyl* (*lhy*) and *early flowering 3* (*elf3-7*) under short day photocycles (8 hrs light/ 16 hrs dark at 22°C).

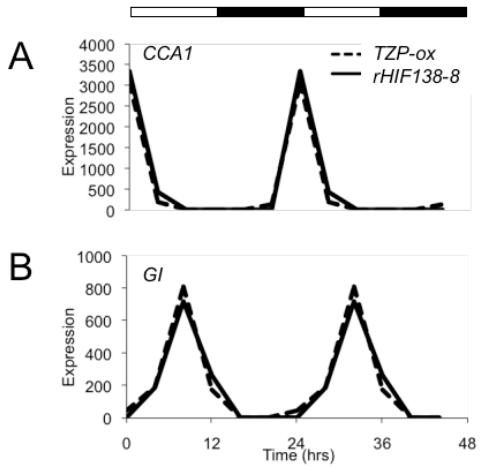

Supplementary Figure 5.S7. Core circadian clock gene expression is not disrupted in *TZP-OX*. Both *CIRCADIAN CLOCK ASSOCIATED 1* (*CCA1*) and *GIGANTEA* (*GI*) display completely wild type expression in *TZP-OX* as compared to HIF138-8.

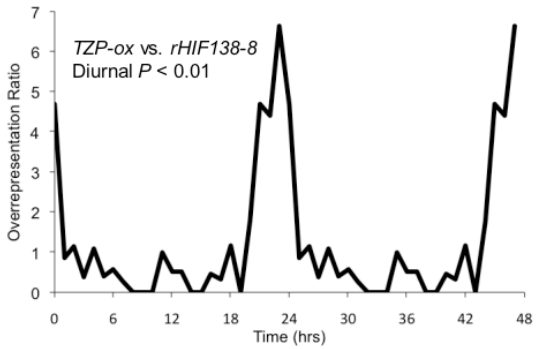

Supplementary Figure 5.S8. Genes upregulated under light/dark cycles in *TZP-OX* are expressed at dawn. Normally, the 117 genes that are upregulated by *TZP-OX* under light/dark cycles are phased to dawn. Overrepresentation plot created using the PHASER tool.

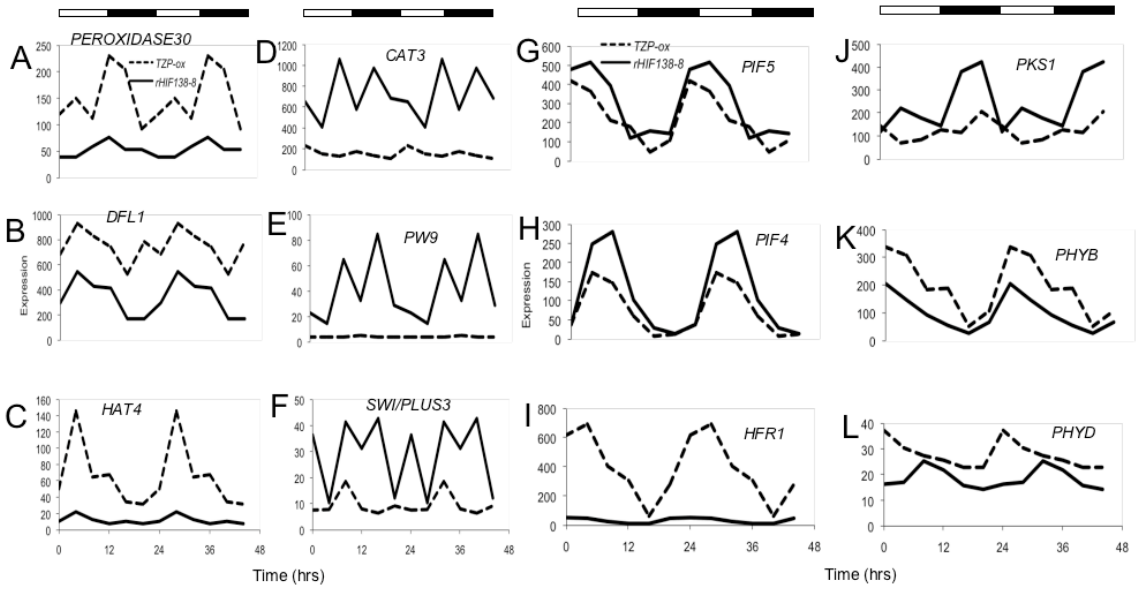

Supplementary Figure 5.S9. *TZP* overexpression specifically disrupts light-specific, time-of-day growth pathways. (A) *PEROXIDASE30* (B) *DFL1* (C) *HAT4* (D) *CATALASE3* (*CAT3*) (E) *PW9* (MATH/TRAF) (F*) SWI/PLUS3* (At2g16480) (G) *PIF5* (H) *PIF4* (I) *HFR1* (J) *PKS1* (K) *PHYB* (L*) PHYD*

References

1. Nozue, K., Covington, M.F., Duek, P.D., Lorrain, S., Fankhauser, C., Harmer, S.L., and Maloof, J.N. (2007). Rhythmic growth explained by coincidence between internal and external cues. Nature *448*, 358-361.

2. Borevitz, J.O., Maloof, J.N., Lutes, J., Dabi, T., Redfern, J.L., Trainer, G.T., Werner, J.D., Asami, T., Berry, C.C., Weigel, D., et al. (2002). Quantitative trait loci controlling light and hormone response in two accessions of Arabidopsis thaliana. Genetics *160*, 683-696.

3. Aukerman, M.J., Hirschfeld, M., Wester, L., Weaver, M., Clack, T., Amasino, R.M., and Sharrock, R.A. (1997). A deletion in the PHYD gene of the Arabidopsis Wassilewskija ecotype defines a role for phytochrome D in red/far-red light sensing. The Plant cell *9*, 1317-1326.

4. Balasubramanian, S., Sureshkumar, S., Agrawal, M., Michael, T.P., Wessinger, C., Maloof, J.N., Clark, R., Warthmann, N., Chory, J., and Weigel, D. (2006). The PHYTOCHROME C photoreceptor gene mediates natural variation in flowering and growth responses of Arabidopsis thaliana. Nat Genet *38*, 711-715.

5. Filiault, D.L., Wessinger, C.A., Dinneny, J.R., Lutes, J., Borevitz, J.O., Weigel, D., Chory, J., and Maloof, J.N. (2008). Amino acid polymorphisms in Arabidopsis phytochrome B cause differential responses to light. Proceedings of the National Academy of Sciences of the United States of America *105*, 3157-3162.

6. Maloof, J.N., Borevitz, J.O., Dabi, T., Lutes, J., Nehring, R.B., Redfern, J.L., Trainer, G.T., Wilson, J.M., Asami, T., Berry, C.C., et al. (2001). Natural variation in light sensitivity of Arabidopsis. Nat Genet *29*, 441-446.

7. Weigel, D., and Nordborg, M. (2005). Natural variation in Arabidopsis. How do we find the causal genes? Plant physiology *138*, 567-568.

8. Clark, R.M., Schweikert, G., Toomajian, C., Ossowski, S., Zeller, G., Shinn, P., Warthmann, N., Hu, T.T., Fu, G., Hinds, D.A., et al. (2007). Common sequence polymorphisms shaping genetic diversity in Arabidopsis thaliana. Science (New York, N.Y *317*, 338-342.

9. Peleman, J.D., Wye, C., Zethof, J., Sorensen, A.P., Verbakel, H., van Oeveren, J., Gerats, T., and van der Voort, J.R. (2005). Quantitative trait locus (QTL) isogenic recombinant analysis: a method for high-resolution mapping of QTL within a single population. Genetics *171*, 1341-1352.

10. Kroymann, J., and Mitchell-Olds, T. (2005). Epistasis and balanced polymorphism influencing complex trait variation. Nature *435*, 95-98.

11. Toledo-Ortiz, G., Huq, E., and Quail, P.H. (2003). The Arabidopsis basic/helix-loop-helix transcription factor family. The Plant cell *15*, 1749-1770.

12. Barakat, A., Szick-Miranda, K., Chang, I.F., Guyot, R., Blanc, G., Cooke, R., Delseny, M., and Bailey-Serres, J. (2001). The organization of cytoplasmic ribosomal protein genes in the Arabidopsis genome. Plant physiology *127*, 398-415.

13. Nesi, N., Debeaujon, I., Jond, C., Pelletier, G., Caboche, M., and Lepiniec, L. (2000). The TT8 gene encodes a basic helix-loop-helix domain protein required for expression of DFR and BAN genes in Arabidopsis siliques. The Plant cell *12*, 1863-1878.

14. Vo, L.T., Minet, M., Schmitter, J.M., Lacroute, F., and Wyers, F. (2001). Mpe1, a zinc knuckle protein, is an essential component of yeast cleavage and polyadenylation factor required for the cleavage and polyadenylation of mRNA. Molecular and cellular biology *21*, 8346-8356.

15. Clay, N.K., and Nelson, T. (2005). The recessive epigenetic swellmap mutation affects the expression of two step II splicing factors required for the transcription of the cell proliferation gene STRUWWELPETER and for the timing of cell cycle arrest in the Arabidopsis leaf. The Plant cell *17*, 1994-2008.

16. Kalyna, M., Lopato, S., and Barta, A. (2003). Ectopic expression of atRSZ33 reveals its function in splicing and causes pleiotropic changes in development. Molecular biology of the cell *14*, 3565-3577.

17. Lopato, S., Gattoni, R., Fabini, G., Stevenin, J., and Barta, A. (1999). A novel family of plant splicing factors with a Zn knuckle motif: examination of RNA binding and splicing activities. Plant molecular biology *39*, 761-773.

18. De Guzman, R.N., Wu, Z.R., Stalling, C.C., Pappalardo, L., Borer, P.N., and Summers, M.F. (1998). Structure of the HIV-1 nucleocapsid protein bound to the SL3 psi-RNA recognition element. Science (New York, N.Y *279*, 384-388.

19. de Jong, R.N., Truffault, V., Diercks, T., Ab, E., Daniels, M.A., Kaptein, R., and Folkers, G.E. (2008). Structure and DNA binding of the human Rtf1 Plus3 domain. Structure *16*, 149-159.

20. Oh, S., Zhang, H., Ludwig, P., and van Nocker, S. (2004). A mechanism related to the yeast transcriptional regulator Paf1c is required for expression of the Arabidopsis FLC/MAF MADS box gene family. The Plant cell *16*, 2940-2953.

21. Mlynarova, L., Nap, J.P., and Bisseling, T. (2007). The SWI/SNF chromatin-remodeling gene AtCHR12 mediates temporary growth arrest in Arabidopsis thaliana upon perceiving environmental stress. Plant J *51*, 874-885.

22. Dowson-Day, M.J., and Millar, A.J. (1999). Circadian dysfunction causes aberrant hypocotyl elongation patterns in Arabidopsis. Plant J *17*, 63-71.

23. Michael, T.P., Chory, J., and al., e. (2008). A morning specfic phytohormone gene expression program underlying rhythmic plant growth. PLoS Biology *in press*.

24. Michael, T.P., Mockler, T.C., Breton, G., McEntee, C., Byer, A., Trout, J.D., Hazen, S.P., Shen, R., Priest, H.D., Sullivan, C.M., et al. (2008). Network discovery pipeline elucidates conserved time-of-day-specific cis-regulatory modules. PLoS genetics *4*, e14.

25. Mockler, T.C., Michael, T.P., Priest, H.D., Shen, R., Sullivan, C.M., Givan, S.A., McEntee, C., Kay, S.A., and Chory, J. (2007). The DIURNAL project: DIURNAL and circadian expression profiling, model-based pattern matching, and promoter analysis. Cold Spring Harbor symposia on quantitative biology *72*, 353-363.

26. Passardi, F., Tognolli, M., De Meyer, M., Penel, C., and Dunand, C. (2006). Two cell wall associated peroxidases from Arabidopsis influence root elongation. Planta *223*, 965-974.

27. Bayer, E.M., Bottrill, A.R., Walshaw, J., Vigouroux, M., Naldrett, M.J., Thomas, C.L., and Maule, A.J. (2006). Arabidopsis cell wall proteome defined using multidimensional protein identification technology. Proteomics *6*, 301-311.

28. Zimmermann, P., Heinlein, C., Orendi, G., and Zentgraf, U. (2006). Senescence-specific regulation of catalases in Arabidopsis thaliana (L.) Heynh. Plant, cell & environment *29*, 1049-1060.

29. Michael, T.P., and McClung, C.R. (2002). Phase-specific circadian clock regulatory elements in Arabidopsis. Plant physiology *130*, 627-638.

30. Park, J.E., Seo, P.J., Lee, A.K., Jung, J.H., Kim, Y.S., and Park, C.M. (2007). An Arabidopsis GH3 gene, encoding an auxin-conjugating enzyme, mediates

phytochrome B-regulated light signals in hypocotyl growth. Plant & cell physiology *48*, 1236-1241.

31. Nakazawa, M., Yabe, N., Ichikawa, T., Yamamoto, Y.Y., Yoshizumi, T., Hasunuma, K., and Matsui, M. (2001). DFL1, an auxin-responsive GH3 gene homologue, negatively regulates shoot cell elongation and lateral root formation, and positively regulates the light response of hypocotyl length. Plant J *25*, 213-221.

32. Yang, X., Lee, S., So, J.H., Dharmasiri, S., Dharmasiri, N., Ge, L., Jensen, C., Hangarter, R., Hobbie, L., and Estelle, M. (2004). The IAA1 protein is encoded by AXR5 and is a substrate of SCF(TIR1). Plant J *40*, 772-782.

33. Covington, M.F., and Harmer, S.L. (2007). The circadian clock regulates auxin signaling and responses in Arabidopsis. PLoS Biol *5*, e222.

34. Sawa, S., Ohgishi, M., Goda, H., Higuchi, K., Shimada, Y., Yoshida, S., and Koshiba, T. (2002). The HAT2 gene, a member of the HD-Zip gene family, isolated as an auxin inducible gene by DNA microarray screening, affects auxin response in Arabidopsis. Plant J *32*, 1011-1022.

35. Sessa, G., Carabelli, M., Sassi, M., Ciolfi, A., Possenti, M., Mittempergher, F., Becker, J., Morelli, G., and Ruberti, I. (2005). A dynamic balance between gene activation and repression regulates the shade avoidance response in Arabidopsis. Genes & development *19*, 2811-2815.

36. Devlin, P.F., Robson, P.R., Patel, S.R., Goosey, L., Sharrock, R.A., and Whitelam, G.C. (1999). Phytochrome D acts in the shade-avoidance syndrome in Arabidopsis by controlling elongation growth and flowering time. Plant physiology *119*, 909-915.

37. Fairchild, C.D., Schumaker, M.A., and Quail, P.H. (2000). HFR1 encodes an atypical bHLH protein that acts in phytochrome A signal transduction. Genes & development *14*, 2377-2391.

38. Bentsink, L., Jowett, J., Hanhart, C.J., and Koornneef, M. (2006). Cloning of DOG1, a quantitative trait locus controlling seed dormancy in Arabidopsis. Proceedings of the National Academy of Sciences of the United States of America *103*, 17042-17047.

39. Mouchel, C.F., Briggs, G.C., and Hardtke, C.S. (2004). Natural genetic variation in *Arabidopsis* identifies *BREVIS RADIX*, a novel regulator of cell proliferation and elongation in the root. Genes Dev. *18*, 700-714.

40. Macquet, A., Ralet, M.C., Loudet, O., Kronenberger, J., Mouille, G., Marion-Poll, A., and North, H.M. (2007). A naturally occurring mutation in an Arabidopsis accession affects a beta-D-galactosidase that increases the hydrophilic potential of rhamnogalacturonan I in seed mucilage. The Plant cell *19*, 3990-4006.

41. Baxter, I., Muthukumar, B., Park, H.C., Buchner, P., Lahner, B., Danku, J., Zhao, K., Lee, J., Hawkesford, M.J., Guerinot, M.L., et al. (2008). Variation in molybdenum content across broadly distributed populations of Arabidopsis thaliana is controlled by a mitochondrial molybdenum transporter (MOT1). PLoS genetics *4*, e1000004.

References Supplementary Information

1. Loudet, O., Chaillou, S., Camilleri, C., Bouchez, D., and Daniel-Vedele, F. (2002). Bay-0 x Shahdara recombinant inbred line population: a powerful tool for the genetic dissection of complex traits in Arabidopsis. Theor. Appl. Genet. *104*, 1173-1184.

2. Tuinstra, M.R., Ejeta, G., and Goldsbrough, P.B. (1997). Heterogeneous inbred family (HIF) analysis: a method for developing near-isogenic lines that differ at quantitative trait loci. Theor. Appl. Genet. *95*, 1005 - 1011.

3. Basten, C., Weir, B., and Zhao-Bang, Z. (2004). QTL Cartographer. Volume 2004.

4. Lander, E.S., and Botstein, D. (1989). Mapping Mendelian factors underlying quantitative traits using RFLP linkage maps. Genetics *121*, 185-199.

5. Churchill, G.A., and Doerge, R.W. (1994). Empirical threshold values for quantitative trait mapping. Genetics *138*, 963-971.

6. Kroymann, J., and Mitchell-Olds, T. (2005). Epistasis and balanced polymorphism influencing complex trait variation. Nature *435*, 95-98.

7. Michael, T.P., Mockler, T.C., Breton, G., McEntee, C., Byer, A., Trout, J.D., Hazen, S.P., Shen, R., Priest, H.D., Sullivan, C.M., et al. (2008). Network discovery pipeline elucidates conserved time-of-day-specific cis-regulatory modules. PLoS genetics *4*, e14.

8. Smyth, G.K. (2005). In Bioinformatics and Computational Biology Solutions using R and Bioconductor, R. Gentleman, W. Huber, V.J. Carey, R.A. Irizarry and S. Dudoit, eds. (New York, NY: Springer), pp. 397-420.

Chapter 6

Conclusions and Perspectives

It has been nearly fifty years since the discovery of phytochrome and in that time much progress has been made on understanding the roles that phytochromes play in plant growth and development. Thanks to the recent structure of the chromophore-binding domain of *Deinococcus* phytochrome we have a better appreciation of phytochromes at the atomic level [1]. Genetic screens and biochemical experiments have added greatly to our understanding of the signal transduction pathway. Yet despite this accumulation of knowledge we are still a long ways from fully comprehending the pathway.

One of the outstanding questions lies with the photoreceptor itself. While the crystal structure of the chromophore-binding domain of *Deinococcus* phytochrome was extremely informative, it was but half the picture. As has been stated above, intramolecular interactions between the N- and C-termini of phytochrome play an important role in propagating the phytochrome signal. In the case of phyB, for example, this interaction is thought to prevent exposure of a cryptic NLS [2]. In the case of phyA, intramolecular interactions likely prevent the binding to FHY1 and FHL, which is required for nuclear accumulation [3]. Therefore, the field would be advanced by a crystal structure of a complete phytochrome molecule. As we know that Pr/Pfr photoconversion results in structural changes in the photoreceptor, a crystal structure of both forms would be even more enlightening. However, this latter goal may be technically challenging as complete conversion to either Pr or Pfr is not possible where, as in the case of plant phytochromes, Pr and Pfr spectra overlap. Nonetheless, such structures would provide the basis for countless experiments and

would allow the field to make sense of the many loss-of-function, and hypo- and hypersensitive phytochrome alleles available, including those presented here.

Another outstanding question in phytochrome signaling is the role of NBs in phytochrome signaling. As stated above, there is evidence for both a positive and negative role for NBs in phytochrome signaling. Further, there are published reports of mutants that affect NB formation, though the underlying genes have not been cloned [4]. Although some time has passed since the publication of these mutants, the field is still hopeful that the cloning of these mutants will shed light on NB formation or composition. Purification of these entities may prove difficult due to their dynamic nature, and the fact that phytochromes have many interacting partners may generate interactors not involved in NB formation. It seems, in this case, that genetics holds the key to understanding the NB.

Phytochrome is known to interact with many transcription factors, and genes that respond quickly to light are over-represented for transcription factors. This suggests that phytochromes play a central role in a large transcriptional network. Unraveling this transcriptional network should be a priority for the field. Microarray experiments using phytochrome null mutants and brief exposure to light have yielded many early targets. It is time now to ascertain the targets of these transcription factors so that a hierarchy can be established and the transcriptional program required for photomorphogenesis can be established. The work presented here has contributed to this question in many ways. First, PIK has been established as a new phytochrome interacting partner implicated in the control of phyA levels. Our model proposes that PIK mediates an interaction between phyA and one of the early, perhaps direct, targets

of the signaling pathway. Second, we have developed a set of tools that, in the best-case scenario, will allow for identification of direct targets of the PIF/PILs, and may also prove valuable in identifying interacting partners of the PIF/PILs. Lastly, we have identified TZP, a novel, plant-specific protein that controls the expression of growth genes in response to light, providing yet another entrée into light-regulated modulation of gene expression.

References

1. Wagner, J.R., Brunzelle, J.S., Forest, K.T., and Vierstra, R.D. (2005). A light-sensing knot revealed by the structure of the chromophore-binding domain of phytochrome. Nature *438*, 325-331.

2. Chen, M., Tao, Y., Lim, J., Shaw, A., and Chory, J. (2005). Regulation of phytochrome B nuclear localization through light-dependent unmasking of nuclear-localization signals. Curr Biol *15*, 637-642.

3. Kevei, E., Schafer, E., and Nagy, F. (2007). Light-regulated nucleo-cytoplasmic partitioning of phytochromes. Journal of experimental botany *58*, 3113-3124.

4. Chen, M., Schwab, R., and Chory, J. (2003). Characterization of the requirements for localization of phytochrome B to nuclear bodies. Proceedings of the National Academy of Sciences of the United States of America *100*, 14493-14498.